Study on Hydrochemical Dynamics of Groundwater and Streamwater in Forested Headwater Catchments

Masanori Katsuyama

Kyoto University
March 2002

'It's been a great run. Looking back, my career has gone by pretty fast.
I don't see this as an ending. I'm just moving on.'

- Cal Ripken, Jr. Announcing his retirement on June 19, 2001.

Study on Hydrochemical Dynamics of Groundwater and Streamwater in Forested Headwater Catchments

Contents

Abstract (in Japanese)

Study on hydrochemical dynamics of groundwater and streamwater in forested headwater catchments

(山地源頭部森林流域における地下水･渓流水の動態に関する水文化学的研究)

山地源頭部に位置する森林流域は下流域に対する水および各種の物質の供給源であり,例えば酸性降下物等が将来的に渓流水質に及ぼす影響が懸念されている.このような影響予測にも適用可能な水文化学モデルの構築には,流域内部の水文過程,すなわち流出発生機構を十分に考慮する必要がある.そこで本研究では山地源流域の地下水･渓流水質形成機構を,降雨から流出に至る水移動経路と,流出を構成する水の起源とに着目して考察した.観測は滋賀県南部に位置する桐生水文試験地内の 2 流域(マツ沢流域 0.68ha および赤壁流域 0.086ha),桐生水文試験地に近接する若女裸地谷流域(0.18ha)および京都大学芦生演習林内のトヒノ谷流域(0.64ha)で行なった.いずれの流域も源頭部に位置する 0 次谷流域である.各流域において雨量･流量･地下水位等の水文観測および降水･地下水･湧水･渓流水などの水質観測データを取得した.桐生水文試験地内の 2 流域では約 2 週間間隔の無降雨時の観測と,降雨時の集中的な観測とを並行した.若女裸地谷流域と芦生トヒノ谷流域では降雨時の観測を中心に行なった.

マツ沢流域および赤壁流域における観測から,流域面積の大部分を占める土層の薄い斜面部では,降雨の鉛直浸透によって土壌-基岩境界面上で地下水面が形成され,飽和側方流として流下する成分と,透水性を持つ基岩に浸透する成分とに配分される.斜面部の水収支を考えると年間降水量の約 50%は基岩に浸透していることが明らかになった.また,飽和側方流の発生は降雨中および降雨直後に限られるのに対し,基岩浸透水はほぼ年間を通じて存在した. マツ沢流域において,基岩面上を流下した飽和側方流は,流域末端部の土層が厚い部分に存在する恒常的地下水帯の表層を涵養した.一方基岩浸透水は恒常的地下水帯の深層を涵養した.流出解析のトレーサーとして用いる SiO_2 濃度に着目すると,飽和側方流の SiO_2 濃度は基岩浸透水の SiO_2 濃度よりも低い.そのため恒常的地下

水帯では表層で濃度が低く,下層で高い鉛直分布が生じた.無降雨時の渓流水の SiO_2 濃度は恒常的地下水帯の濃度分布の範囲内で変動した.そこで無降雨時の渓流水質は恒常的地下水帯の表層と深層の 2 層からの流出で形成されると仮定し,2 成分の混合モデルを用いて解析を行なったところ,渓流水質の季節変化は表層からの流出水量とその化学性が季節変化することによって生じることが明らかにされた.赤壁流域では渓流水の SiO_2 濃度が恒常的地下水の濃度と比べて高く,渓流水に対する基岩浸透水の直接的な寄与の大きさが示唆された.

マツ沢流域では降雨時には恒常的地下水に加え,河道上への直達降雨および湿潤期に恒常的飽和帯が拡大して発生する一時的地下水が流出に寄与した.一時的地下水は降雨時に斜面部の土壌-基岩境界面で発生した飽和側方流に由来し,特に降雨規模が大きい場合にはその流出によって渓流水質が大きく変動した.他流域の観測結果と比較すると,芦生トヒノ谷流域では流域下端の斜面土層内に存在する土中パイプからの流出によって渓流水質が大きく変動した.また,マツ沢流域と比べて恒常的飽和帯の規模が小さい若女裸地谷流域では比較的短時間で恒常的地下水の水質が変化し,その影響が渓流水質に現れたことから,恒常的地下水帯の規模が大きいほど水質の安定した地下水を供給することが可能となるバッファ作用が大きいことが示唆された.このように流域間の降雨流出特性の違いは降雨時の渓流水質の形成に大きな影響を与えることが明らかになった.また,マツ沢流域において,表層土壌中を通過して流出する一時的地下水の寄与をより明確に検出することが可能な溶存有機物の蛍光特性をトレーサーに用いて解析を行なったところ,流域面積に占める一時的地下水の流出寄与域は1%に満たず,流域末端部分のわずかな面積から大量の水および溶存物質が供給され,降雨時の渓流水質を規定していることが明らかになった.

従来,渓流水質形成に大きく影響する流域末端部と,流域面積の大部分を占める斜面部との関わりは不明な点が多く残されていた.本研究の結果,両者をつなぐ経路として基岩中を通過する地下水の役割の大きさが示されるとともに,この地下水は無降雨時の渓流水質を規定する重要な要素であることが明らかにされた.また,降雨時には無降雨時とは異なる流域内部の流出経路を考慮する必要があることが示された.

List of Tables and Figures

Tables

Chapter 1

Chapter 2

Chapter 4

Chapter 6

Figures

Chapter 1

Chapter 2

Chapter 1
Introduction

1.1 General Background

The need to address hydrochemical problems, such as the acidification of surface and subsurface waters and the transport of pollutants, at the drainage basin scale is well recognized. Solutions to hydrochemical problems in a stream often involve computer models of runoff generation in the catchment; unfortunately, coupled hydrological and biogeochemical models (hydrochemical models) have not been totally successful in explaining the hydrochemical behavior of streams, because they do not incorporate the correct mechanisms (or the correct mathematical formulation of these mechanisms) (Hooper et al., 1990; Sklash, 1990). For example, Hooper et al. (1988) demonstrated the overparameterization of simple six-parameter hydrological models (that is, the inclusion of parameters whose values cannot be uniquely determined by the calibration data), and pointed out that such overparameterization reduces the power of the models to assess the chemical mechanisms by making them more difficult to invalidate when faulty. Sklash (1990) demonstrated that one of the major reasons for these failures is that the models often incorrectly estimate the residence time of the water in the catchment; that is, the flow paths assumed in the models are often wrong. These facts emphasize the need for more accurate determination of the hydrological structure in hydrochemical models.

Tracer studies can improve the apportioning of runoff by tracing the movement of water through various pathways in a catchment. Indeed, tracer studies have been carried out in catchments in different areas of the world using a variety of tracers (both chemical and isotopic) (Table 1.1). Primarily, the use of chemical tracers by hydrologists has been limited to hydrograph separation, wherein the hydrograph is separated into pre-event (also known as "old") and event (or "new") water (Pinder and Jones, 1969; Sklash and Farvolden, 1979). The pre-event and event waters are called time-source components, because they provide a temporal separation of stream runoff (Genereux and Hooper, 1998).

Table 1.1 Recent "Geographic-Source" tracer studies

Authors	Year	Location	Nation	Area(ha)	Chemical Tracer	Isotope Tracer
Caine	1989	Martinelli	USA	8	EC,Na^+,SO_4^{2-},NO_3^-	
Christophersen et al.	1990	Birkenes	Norway	41	H^+,Ca^{2+},Si,inorganic monomeric Al	
		Afon Hafren	UK	347	H^+,Ca^{2+},Si,inorganic monomeric Al	
Hooper et al.	1990	Panola	USA	41	Alkalinity,SO_4^{2-},Na^+,Mg^{2+},Ca^{2+},SiO_2	
McDonnell et al.	1991	Maimai	New Zealand	3.8	EC,Cl^-	D
Hendershot et al.	1992	Hermine	Canada	6	SiO_2	
Easthouse et al.	1992	Birkenes	Norway	41	DOC fractions,H^+,Al,Ca^{2+}	
Ogunkoya and Jenkins	1993	Allt a' Mharcaidh	UK	998	ANC, Cl^-	D
Mulholland	1993	Walker Branch	USA	38.4	Ca^{2+},SO_4^{2-}	
Pionke et al.	1993	Mahantango Creek	USA	740	SiO_2,Na^+,Cl^-,Mg^{2+}	^{18}O
Hinton et al.	1994	Harp 4-21	Canada	3.7	SiO_2	^{18}O
Bazemore et al.	1994	Blue Ridge	USA	8.2	Cl^-	^{18}O
Elsenbeer et al.	1995	South Creek	Australia	25.7	K,ANC	
Elsenbeer and Lack	1996	La Cuenca	Peru	0.75	K/SiO_2 ratio	
Hensel and Elsenbeer	1997	South Creek	Australia	25.7	K/SiO_2 ratio,Ca	
		La Cuenca	Peru	0.75	K/SiO_2 ratio,Ca	
Hooper et al.	1998	Panola	USA	41	Ca^{2+},SO_4^{2-}	
Peters and Ratcliffe	1998	Panola	USA	41	Cl^-	
Rice and Hornberger	1998	Bear Branch	USA	98	Cl^-,Na^+,SiO_2	^{18}O,D
Ohrui and Mitchell	1999	Gunma	Japan	0.5-3.3	Ca^{2+},Na^+,NO_3^-,HCO_3^-	
Kendall et al.	1999	Sleepers River	USA	40.5	Ca^{2+},Mg^{2+},Na^+,SiO_2,DOC	
McGlynn et al.	1999	Sleepers River	USA	40.5	Ca^{2+}	^{18}O
Brown et al.	1999	Shelter Creek	USA	161	Cl^-,DOC	^{18}O
Hoeg et al.	2000	Zastler	Germany	1840	SiO_2	^{18}O
Hagedorn et al.	2000	Erlenbach	Switzerland	70	EC, Ca^{2+},SO_4^{2-},Cl^-	
Marc et al.	2001	Mont-Lozère	France	54	SiO_2	^{18}O
Ladouche et al.	2001	Strengbach	France	80	SiO_2,Na^+,Cl^-,DOC,Rb,Sr,Ba,U	^{18}O,D
Katsuyama et al.	2001	Kiryu	Japan	0.68	Na^+,SO_4^{2-}	
Burns et al.	2001	Panola	USA	10	Mg^{2+},Na^+,H_4SiO_4,Cl^-,SO_4^{2-}	

DeWalle et al. (1988) found that the traditional two-component model failed to explain the stormflow in the catchment that they studied, often producing old water percentages exceeding 100%. They also found that the inclusion of a third time-source component, soil water, was necessary. By using both isotopes and silica as tracers, three components of streamflow can be distinguished (Maulé and Stein, 1990; Rodhe, 1998) as illustrated in Figure 1.1:

- new surface water that has only been in contact with organic soils;
- new subsurface water that has infiltrated during the event; and
- old subsurface water, present in the ground before the event.

Although these classifications are primarily time-source separations, they also take into consideration which pathway each component has followed.

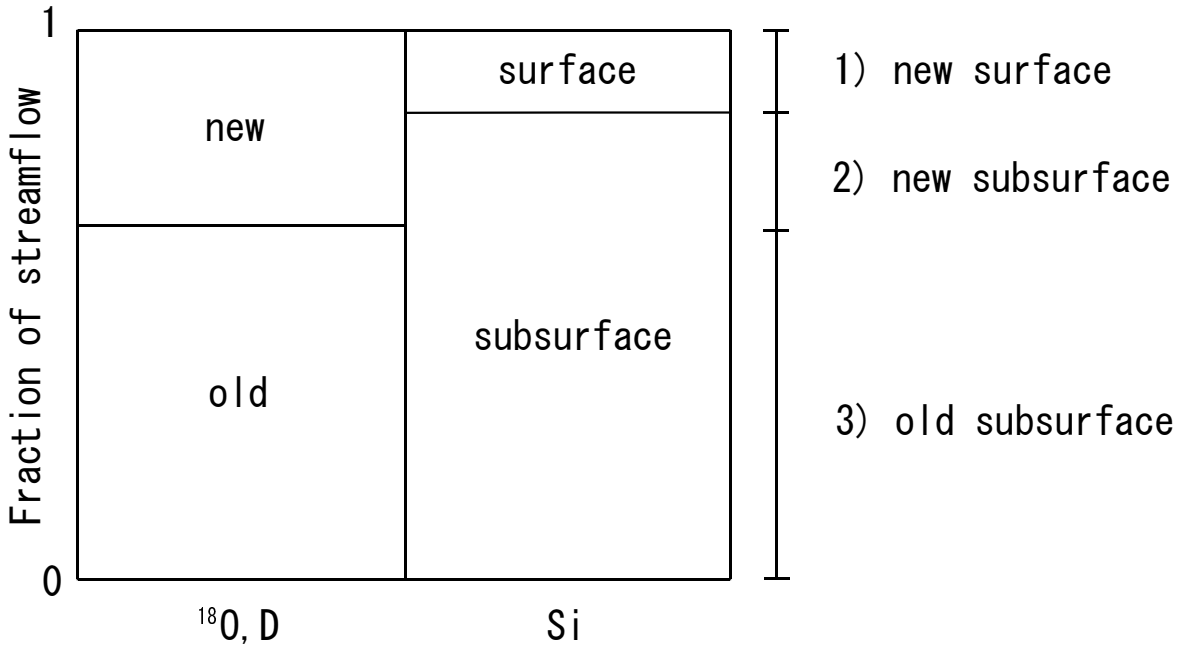

Figure 1.1 Separation of streamwater into three components by simultaneous use of ^{18}O or D and Si (from Rodhe, 1990)

Hooper et al. (1990) and Christophersen et al. (1990) proposed a technique "as a first step towards including soilwater quality in hydrochemical models" (Christophersen et al., 1990) that links the chemistry of each subsurface source (such as groundwater or soilwater) to the resulting streamwater chemistry, assuming that streamwater arises from a mixture of these sources. Because these sources form the chemical boundaries of possible streamwater components in the mixing diagram, they were called 'end-members' and the technique was referred to as "End-Member Mixing Analysis" (EMMA). The technique produces a geographic-source separation of streamwater into three runoff components. EMMA has been applied in many studies (*e.g.*, Mulholland, 1993; Ogunkoya and Jenkins, 1993; Elsenbeer et al., 1995; Ohrui and Mitchell, 1999; Hagedorn, et al., 2000; Burns et al., 2001). In general terms, geographic source components distinguish among different possible sources for the water arriving at a stream.

Strictly speaking, a two-component isotopic hydrograph separation (time-source separation) yields nothing more than the proportions of event and pre-event water in a stream (Genereux and Hooper, 1998). Genereux and Hemond (1990) observed, "not all old water is groundwater and, during and after storms, not all groundwater is old water". Because it is the mechanisms of runoff and, in some cases, their geographic sources that are of more fundamental significance in watershed hydrology, finding meaningful relationships between these components

and time-source components (event and pre-event water) has been and remains one of the fundamental priorities in extracting as much hydrologic information as possible from isotopic data (Genereux and Hooper, 1998).

Three-component models have been used in many studies to describe the components of streamwater through the mixing of throughfall, soilwater in the hillslope (or vadose) zone, and groundwater in the riparian zone (with some variations in terminology). However, the linkage between the hillslope and riparian zones is not well understood (Hooper et al., 1998). These authors found that the chemical signature of the hillslope, the largest component landform of the basin, was not apparent in the stream at the Panola Mountain Research Watershed, USA. Cirmo and McDonnell (1997) pointed out that riparian zones are thought to expand and contract on an event and seasonal basis, as described by the variable source-area concept (Hewllet and Hibbert, 1967). This implies that the riparian zone is important for both the hydrological processes (*e.g.*, McGlynn et al., 1999) and the hydrochemical processes (*e.g.*, Gilliam, 1994) involved in the production of streamwater. All hillslope water must pass through the riparian zone before reaching the stream. Therefore, as mentioned by McGlynn et al. (1999), further intensive studies of hillslope-riparian interactions, intra-riparian zone transport, and riparian-stream relationships are essential.

Streamwater chemistry in several catchments has been explained on the basis of geographic-source separations. Hooper (2001) emphasized the importance of the riparian zone to streamwater chemistry. He summarized recent and future problems in catchment hydrochemical studies based on observations at Panola Mountain Research Watershed (PMRW, 41 ha) as follows:

> *Much of the variation in stream chemistry, at least at PMRW, reflects differing proportions of water coming from the upper and lower portions of the riparian zone. From this point of view, we have learned what can be learned from frequent stream sampling during events. The largest part of the catchment, the hillslope area, is not chemically expressed in the stream during events, yet certainly this area supplies water (and solutes) to the stream. Perhaps there are chemical reactions that occur as the hillslope water enters the riparian zone that radically change the solution chemistry. Perhaps the hillslope water is volumetrically insignificant compared with water resident in the riparian zone. Perhaps there is a delay in the translation of water from hillslope to riparian zone,*

and the majority of transport occurs not during the storm, but between storms when there is also more opportunity for chemical transformations.

These results suggest that field studies shift their focus from the chemical dynamics that occur during storms to explore the connection between the hillslope and riparian portions of the catchment. How are they connected? How is water distributed between events? Does stream volume aggrade gradually with increasing upstream area or are there discrete points of large increase? Can the chemically distinct hillslope water be discerned in the alluvial aquifer?

Recently, on the other hand, the importance of subsurface flow through the bedrock in hydrological and hydrochemical processes has been pointed out (*e.g.*, Mulholland, 1993; Anderson et al., 1997; Montgomery et al., 1997; Onda et al., 2001; Tsujimura et al, 2001). For example, Mulholland (1993) used a three-component mixing model to demonstrate that bedrock-zone flow dominated baseflow prior to a storm in the Walker Branch Watershed, USA. Although the existence of subsurface flow through the bedrock had been previously pointed out (Chorley, 1978), the many uncertainties in the influence this component has on streams still remain. One of the important hydrological problems is to clarify the role of subsurface bedrock zone water as a pathway for runoff generation and a source of streamwater; another is to determine its effects on streamwater chemistry.

Concerning the riparian and bedrock pathways, Tsujimura et al. (2001) pointed out that the riparian zone is important in mountainous catchments with relatively low relief, and that bedrock flow is important in mountainous catchments with relatively high relief. However, the interactions of water in the hillslope zone, where infiltration into the bedrock and riparian zones occurs (that is, the hydrological and hydrochemical processes within the hillslope/riparian interface or the bedrock zone), are still not well understood and are therefore of continuing interest. This study addresses these processes, based on studies of hydrometric and hydrochemical observations in small headwater catchments.

1.2 Previous Hydrochemical Studies in the Kiryu Experimental Watershed

The Kiryu Experimental Watershed, a 5.99-ha forested catchment in Shiga prefecture, Japan, has been the site of many studies of hydrological processes since 1967 (*e.g.*, evapotranspiration by Suzuki, 1980; rainfall-runoff modeling by

Fukushima, 1988). Since 1989, hydrochemical and biogeochemical processes have been intensively studied in a 0.68-ha headwater subcatchment. The series of studies at the small headwater subcatchment scale are aimed at establishing an understanding of the hydrochemical processes in a temperate forest catchment, based on intensive observations of each hydrological element. The subcatchment has a large perennial groundwater zone, with deep soil in the downslope area. Shimada et al. (1993) demonstrated the processes of generation of SiO_2 concentrations in association with hydrological processes in the groundwater and streamwater. SiO_2 is supplied mainly from soil mineral weathering, and pH values may affect the process of chemical weathering. Ohte et al. (1995) showed that biologically supplied CO_2 in the soil controlled the pH. Hamada et al. (1996) presented the vertical profile of soil CO_2 gas. Ohte and Tokuchi (1997) determined the spatial distribution of the acid-buffering processes and emphasized the importance of the buffering potential in the lower layer, where hydrogen ions are produced mainly by dissolution and dissociation of soil CO_2 gas and are consumed in chemical weathering at the catchment scale. In addition, Asano et al. (1999) demonstrated that, as the soil depth of the catchment increases, the streamwater pH value after degassing (Ohte et al., 1995) also increases. These results indicate the importance of the perennial groundwater zone, which has considerable soil depth in this catchment, on the acid-buffering systems.

In a study of the dynamics of inorganic nitrogen, an *in situ* lysimeter was installed with controlled soil-moisture conditions in a situation representative of conditions at the downslope perennial groundwater zone (Ohte et al., 1997). Results showed that neither ammonium nor nitrate could be detected in the leachate. This demonstrated that reduction of NO_3^- by denitrification occurred under saturated conditions. Koba et al. (1997), using the ^{15}N natural abundance method, found intermittent occurrence of denitrification when the groundwater zone expanded upward in the perennial groundwater zone of this catchment. Hobara et al. (2001) estimated the effects of a natural disturbance (involving an outbreak of pine wilt disease in the upslope zone of the catchment) on the downslope perennial groundwater and streamwater, and concluded that even a small-scale natural disturbance drastically altered the nitrogen dynamics. Ohte et al. (submitted), using a two-source conceptual model, demonstrated that seasonality in the groundwater level of the perennial groundwater zone is the dominant factor controlling seasonal changes of streamwater NO_3^- concentration, and explained the changes of seasonal patterns in streamwater NO_3^- concentration

before and after the natural disturbance from the changes of shallow perennial groundwater chemistry. The responses of stormflow chemistry were explained by Katsuyama et al. (1998), who showed that the dominant factors were the distributions of the sources and the perennial groundwater levels around a spring outflow point (that is, riparian groundwater levels; see Paragraph 1.4, "Terminology") and developed a conceptual model of the processes involved. Perennial groundwater chemistry and groundwater level play an important role in the hydrochemistry of the streamwater in this catchment. However, the hydrological or hydrochemical linkage between the hillslope and the riparian groundwater, in other words, how the hillslope groundwater and its chemistry affect processes in the riparian zone, is still unclear.

1.3 Objective and Procedures of This Study

The objective of this study is to investigate the hydrochemical processes within the hillslope, hillslope/riparian interface, and riparian zones, considering the hydrologic pathways and the geographic sources. The application of mixing models to the streamwater and the hydrochemical processes in the streamwater are discussed. A characteristic of this study is intensive, biweekly- and event-based sampling of rainfall, throughfall, groundwater, and streamwater, with simultaneous intensive hydrometric observations in the two (or in some cases, four) catchments. The structure of this study is shown in Figure 1.2.

In **Chapter 2**, the characteristics of the study sites and the procedures for hydrometric observations, sampling, and chemical analyses are described.

The aim of **Chapter 3** is to clarify the hydrologic pathways in the catchments by using intensive hydrometric observations. The groundwater dynamics during a rainstorm, comprised of the saturated throughflow that occurs on the soil-bedrock interface, deep seepage and bedrock flow, and subsurface flow within the riparian groundwater body, are considered.

Chapter 4 describes the spatial and temporal distributions of groundwater chemistry, and the geographic sources of streamwater are allocated in each catchment, based on biweekly groundwater sampling. The hydrochemical processes within the hillslope, hillslope/riparian interface, and riparian zones are discussed. Specifically, the reasons why chemical variability is generated are examined, taking into account the relationship of flow pathways and their chemistry.

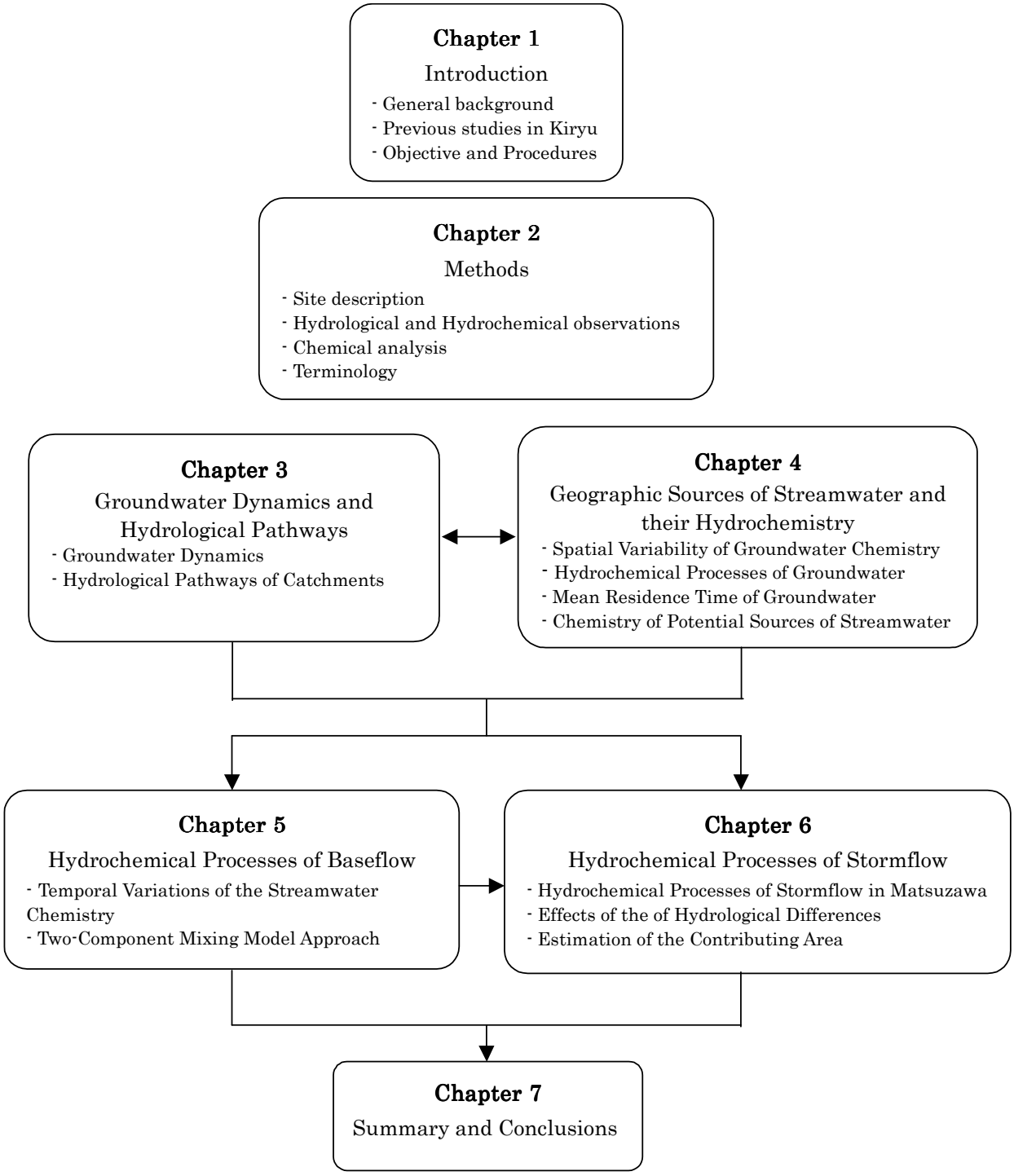

Figure 1.2 Structure of this study

The hydrochemical processes of baseflow are examined in **Chapter 5**. Mixing models are applied in each catchment, based on the hydrological pathways defined in **Chapter 3** and the geographic sources defined in **Chapter 4**, and the mechanisms producing seasonality of the streamwater chemistry are defined.

Chapter 6 discusses the hydrochemical processes of stormflow from various viewpoints, including rainfall duration and variable source area, the differences in the dominant hydrological processes between the catchments, and the estimation of the area contributing to stormflow. EMMA is applied to these analyses with some chemical tracers, including a new tracer--fluorescence of dissolved organic carbon--taking into consideration the hydrological pathways defined in **Chapter 3** and the geographic sources defined in **Chapter 4**.

Finally, **Chapter 7** summarizes the results from each of the preceding chapters. General conclusions from this study, "Hydrochemical dynamics of groundwater and streamwater in forested headwater catchments" are presented.

1.4 Terminology

Some of the terms used in this paper have special meanings that are defined herein:

- *bedrock*: The layer beneath the surface soil with N_4 values over 100, but which may be permeable (see **Chapters 2, 3**).
- *bedrock flow/bedrock groundwater*: The groundwater flow components that infiltrated to the bedrock (deep seepage), and flowed downward. In contrast, the groundwater flow component that does *not* infiltrate to the bedrock and flow *on* the soil-bedrock interface is called *saturated throughflow*.
- *riparian zone*: The definition of the riparian zone given by Hill (2000) is used: the riparian zone is composed of the area of land adjacent to streams and rivers and it can often be distinguished from upland areas of watersheds by vegetation, soils, and topography. In this study, it is defined as "the area around the spring outflow point containing a body of groundwater," because the observed catchment has gentle slopes that are clearly distinguished from those upslope.

References

Anderson, S. P., Dietrich, W. E., Torres, R., Montgomery, D. R. and Loague, K. (1997) Concentration-discharge relationships in runoff from a steep,

unchanneled catchment, Water Resour. Res., 33, pp. 211-225.

Asano, Y., Ohte, N., Uchida, T., Hamada, M. and Katsuyama, M. (1999) Various impacts of the forest growth on the acid buffering processes in small catchments － Effects of the vegetation and soil depth －, J. Jpn. For. Soc., 81, pp. 178-286 (in Japanese with English summary).

Bazemore, D. E., Eshleman, K. N. and Hollenbeck, K. J. (1994) The role of soil water in stormflow generation in a forested headwatar catchment: synthesis of natural tracer and hydrometric evidence, J. Hydrol., 162, pp. 47-75.

Brown, V. A., McDonnell, J. J., Burns, D. A. and Kendall, C. (1999) The role of event water, a rapid shallow flow component, and catchment size in summer stormflow, J. Hydrol., 217, pp. 171-190.

Burns, D. A., McDonnell, J. J., Hopper, R. P., Peters, N. E., Freer, J. E., Kendall, C. and Beven, K. (2001) Quantifying contributions to storm runoff through end-member mixing analysis and hydrologic measurements at the Panola Mountain Research Watershed (Georgia, USA), Hydrol. Process., 15, pp. 1903-1924.

Caine, N. (1989) Hydrograph separation in a small alpine basin based on inorganic solute concentrations, J. Hydrol., 112, pp. 89-101.

Chorley, R. J. (1978) The hillslope hydrological cycle, *In* Hillslope Hydrology, Kirkby, M. J. (Eds.), John Wiley and Sons, Chichester, pp. 1-42.

Christophersen, N., Neal, C., Hooper, R. P., Vogt, R. D. and Anderson, S. (1990) Modelling streamwater chemistry as a mixture of soilwater end-members - a step towards second-generation acidification models, J. Hydrol., 116, pp. 307-320.

Cirmo, C. P. and McDonnell, J. J. (1997) Linking the hydrologic and biogeochemical controls of nitrogen transport in near-stream zones of temperate-forested catchments: a review, J. Hydrol., 199, pp. 88-120.

DeWalle, D. R., Swistock, B. R. and Sharpe, W. E. (1988) Three-component tracer model for streamflow on a small Appalachian forested catchment, J. Hydrol., 104, pp. 301-310.

Easthouse, K. B., Mulder, J., Christopersen, N. and Seip, H. M. (1992) Dissolved organic carbon fractions in soil and stream water during variable hydrological conditions at Birkens, Southern Norway, Water Resour. Res., 28, pp. 1585-1596.

Elsenbeer, H., Lorieri, D. and Bonell, M. (1995) Mixing model approaches to estimate storm flow sources in an overland flow-dominated tropical rain forest

catchment, Water Resour. Res., 31, pp. 2267-2278.

Elsenbeer, H. and Lack, A. (1996) Hydrometric and hydrochemical evidence for fast flowpaths at La Cuenca, Western Amazonia, J. Hydrol., 180, pp. 237-250.

Fukushima, Y. (1988) A model of river flow forecasting for a small forested mountain catchment, Hydrol. Process., 2, pp. 167-185.

Genereux, D. P. and Hemond, H. F. (1990) Naturally occurring radon 222 as a tracer for streamflow generation: steady state methodology and field example, Water Resour. Res., 26, pp. 3065-3075.

Genereux, D. P. and Hooper, R. P. (1998) Oxygen and hydrogen isotopes in rainfall-runoff studies, Isotope tracers in catchment hydrology, Kendall, C. and McDonnell, J. J. (Eds.), Elsevier, Amsterdam, pp. 319-346.

Gilliam, J. W. (1994) Riparian wetlands and water quality, J. Environ. Qual., 23, pp. 896-900.

Hagedorn, F., Schleppi, P., Waldner, P. and Fluehler, H. (2000) Export of dissolved organic carbon and nitrogen from Gleysol dominated catchments - the significance of water flow paths, Biogeochemistry, 50, pp. 137-161.

Hamada, M., Ohte, N. and Kobashi, S. (1996) A measurement of soil CO_2 profile in a forest watershed, J. Jpn. For. Soc., 78, pp. 376-383 (in Japanese with English summary).

Hendershot, W. H., Savoie, S. and Courchesne, F. (1992) Simulation of stream-water chemistry with soil solution and groundwater flow contributions, J. Hydrol., 136, pp. 237-252.

Hensel, D. and Elsenbeer, H. (1997) Streamflow generation in tropical rainforest: a hydrochemical approach, *In* Hydrochemistry (Proceedings of the Rabat Symposium), Peters, N. E., Coudrain-Ribstein, A. (Eds.), IAHS Publ. 244, Wallingford, pp. 227-234.

Hewlett, J. D. and Hibbert, A. R. (1967) Factors affecting the response of small watersheds to precipitation in humid areas, International Symposium on Forest Hydrology, Sopper, W. E. and Lull, H. W. (Eds.), Pergamon Press, Oxford, pp. 275-290.

Hinton, M. J., Schiff, S. L. and English, M. C. (1994) Examining the contributions of glacial till water to storm runoff using two- and three-component hydrograph separations, Water Resour. Res., 30, pp. 983-993.

Hobara, S., Tokuchi, N., Ohte, N., Nakanishi, A. Katsuyama, M. and Koba, K. (2001) Mechanism of nitrate loss from a forested catchment following a small-scale, natural disturbance, Can. J. For. Res., 31, pp. 1326-1335.

Hoeg, S., Uhlenbrook, S. and Leibundgut, C. (2000) Hydrograph separation in a mountainous catchment - combining hydrochemical and isotopic tracers, Hydrol. Process., 14, pp. 1199-1216.

Hooper, R. P., Stone, A., Christophersen, N., Grosbois, E. D. and Seip, H. M. (1988) Assessing the Birkens Model of Stream Acidification Using Multisignal Calibration Methodology, Water Resour. Res., 24, pp. 1308-1316.

Hooper, R. P., Christophersen, N. and Peters, N. E. (1990) Modelling streamwater chemistry as a mixture of soilwater end-members - an application to the Panola Mountain catchment, Georgia, U.S.A, J. Hydrol., 116, pp. 321-343.

Hooper, R. P., Aulenbach, B. T., Burns, D. A., McDonnell, J., Freer, J., Kendall, C. and Beven, K. (1998) Riparian control of stream-water chemistry: implications for hydrochemical basin models, Hydrology, Water resources and Ecology in Headwaters (Proceeding of the HeadWater '98 Conference held at Merano, Italy, April 1998), Kovar, K. Tappeiner, U. Peters, N. E., Craig, R. G. (Eds.), IAHS Publ. 248, Wallingford, pp. 451-458.

Hooper, R. P. (2001) Applying the scientific methods to small catchment studies: A review of the Panola Mountain Experience, Hydrol. Process. 15. pp. 2039-2050.

Katsuyama, M, Ohte, N. and Kobashi, S. (1998) The influence of a rainfall event on the chemical changes of forest runoff water, Bull. Kyoto Univ. For., 69, pp. 26-37 (in Japanese with English summary).

Katsuyama, M., Ohte, N. and Kobashi, S. (2001) A three-component end-member analysis of streamwater hydrochemistry in a small Japanese forested headwater catchment, Hydrol. Process., 15, pp. 249-260.

Kendall, K. A., Shanley, J. B. and McDonnell, J. J. (1999) A hydrometric and geochemical approach to test the transmissivity feedback hypothesis during snowmelt, J. Hydrol., 219, pp. 188-205.

Koba, K., Tokuchi, N., Wada, E. Nakajima, T. and Iwatsubo, G. (1997) Intermittent denitrification: The application of a 15N natural abundance method to a forested ecosystem, Geochim. Cosmochim. Acta., 61, pp. 5043-5050.

Ladouche, B., Probst, A., Viville, D., Idir, S., Baqué, D. Loubet, M., Probst, J. -L. and Bariac, T. (2001) Hydrograph separation using isotope, chemical and hydrological approaches (Strengbach catchment, France), J. Hydrol., 242, pp. 255-274

Marc, V., Didon-Lescot, J. F. and Michael, C. (2001) Investigation of the hydrological processes using chemical and isotopic tracers in a small Mediterranean forested catchment during autumn recharge, J. Hydrol., 247,

pp. 215-229.

Maulé, C. P. and Stein, J. (1990) Hydrologic flow path definition and partitioning of spring meltwater, Water Resour. Res., 26, pp. 2959-2970.

McDonnell, J. J., Stewart, M. K. and Owens, I. F. (1991) Effect of catchment-scale subsurface mixing on stream isotopic response, Water Resour. Res., 27, pp. 3065-3073.

McGlynn, B. L., McDonnell, J. J., Shanley, J. B. and Kendall, C. (1999) Riparian zone flowpath dynamics during snowmelt in a small headwater catchment, J. Hydrol., 222, pp. 75-92.

Montgomery, D. R., Dietrich, W. E., Torres, R., Anderson, S. P., Heffner, J. T. and Loague, K. (1997) Hydrologic response of a steep, unchanneled valley to natural and applied rainfall, Water Resour. Res., 33, pp. 91-109.

Mulholland, P. J. (1993) Hydrometric and stream chemistry evidence of three storm flowpaths in Walker Branch Watershed, J. Hydrol., 151, pp. 291-316.

Ogunkoya, O. O. and Jenkins, A. (1993) Analysis of storm hydrograph and flow pathways using a three-component hydrograph separation model, J. Hydrol., 142, pp. 71-88.

Ohrui, K. and Mitchell, M. J. (1999) Hydrological flow paths controlling stream chemistry in Japanese forested watersheds, Hydrol. Process., 13, pp. 877-888.

Ohte, N., Tokuchi, N. and Suzuki, M. (1995) Biogeochemical influences on the determination of water chemistry in a temperate forest basin: Factors determining the pH value, Water Resour.Res., 31, pp. 2823-2834.

Ohte, N. and Tokuchi, N. (1997) Spatial variation on acid buffering mechanism in forest catchment: Vertical distribution of the buffering process in the weathered granitic catchment, J. Japan. Soc. Hydrol. & Water Resour., 10, pp. 463-473 (in Japanese with English summary).

Ohte, N., Tokuchi, N. and Suzuki, M. (1997) An in situ lysimeter experiment on soil moisture influence on inorganic nitrogen discharge from forest soil, J. Hydrol., 195, pp.78-98.

Ohte, N., Tokuchi, N., Katsuyama, M., Hobara, S. and Asano, Y., Episodic rising in nitrate concentration of streamwater by partial dieback of pine forest in Japan: Runoff generation processes as a controlling factor of the seasonality, Hydrol. Process. (in press).

Onda, Y., Komatsu, Y., Tsujimura, M. and Fujihara, J. (2001) The role of subsurface runoff through bedrock on storm flow generation, Hydrol. Process., 15, pp. 1693-1706.

Peters, N. E. and Ratcliffe, E. B. (1998) Tracing hydrologic pathways using chloride at the Panola Mountain Research Watershed, Georgia, USA, Water, Air, and Soil Pollution, 105, pp. 263-275.

Pinder, G. F. and Jones, J. F. (1969) Determination of the ground-water component of peak discharge from the chemistry of total runoff, Water Resour. Res., 5, pp. 438-445

Pionke, H. B., Gburek, W. J. and Folmar, G. J. (1993) Quantifying stormflow components in a Pennsylvania watershed when 18O input and storm conditions vary, J. Hydrol., 148, pp. 169-187.

Rice, K. C. and Hornberger, G. M. (1998) Comparison of hydrochemical tracers to estimate source contributions to peak flow in a small, forested, headwater catchment, Water Resour. Res., 34, pp. 1755-1766.

Rodhe, A. (1998) Snowmelt-dominated systems, Isotope tracers in catchment hydrology, Kendall, C. and McDonnell, J. J. (Eds.), Elsevier, Amsterdam, pp. 391-433.

Shimada, Y., Ohte, N., Tokuchi, N. and Suzuki, M. (1993) A dissolved silica budget for a temperate forested basin, *In* Tracers in Hydrology (Proceeding of Yokohama Symposium), Peters, N. E., Hoehn, E., Leibundgut, Ch., Tase, N. and Walling, D. E. (Eds.), IHAS publ., Wallingford, 215, pp. 79-88.

Sklash, M. G. and Farvolden, R. N. (1979) The role of groundwater in storm runoff, J. Hydrol., 43, pp. 45-65.

Sklash, M. G. (1990) Environmental isotope studies of storm and snowmelt runoff generation, *In* Process studies in hillslope hydrology, Anderson, M. G. and Burt, T. P. (Eds.), John Wiley and Sons, Chichester, pp. 401-436.

Suzuki, M. (1980) Evapotranspiration from a small catchment in hilly mountains (1) Seasonal variations in evapotranspiration, rainfall interception and transpiration, J. Jap. For. Soc., 62, pp. 46-53.

Tsujimura, M., Onda, Y. and Ito, J. (2001) Stream water chemistry in a steep headwater basin with high relief, Hydrol. Process., 15, pp. 1847-1851.

Chapter 2
Methods

2.1 Site Description

The experiments in this study were conducted in four small headwater catchments: Kiryu Matsuzawa catchment, Kiryu Akakabe catchment, Jakujo Rachidani catchment, and Ashiu Toinotani catchment. Figure 2.1 shows the locations of the four catchments. Results from the Matsuzawa and Akakabe catchments are detailed in the following chapters; results from the Rachidani and Toinotani catchments are discussed in **Chapter 6** and compared therein with those from the former two catchments.

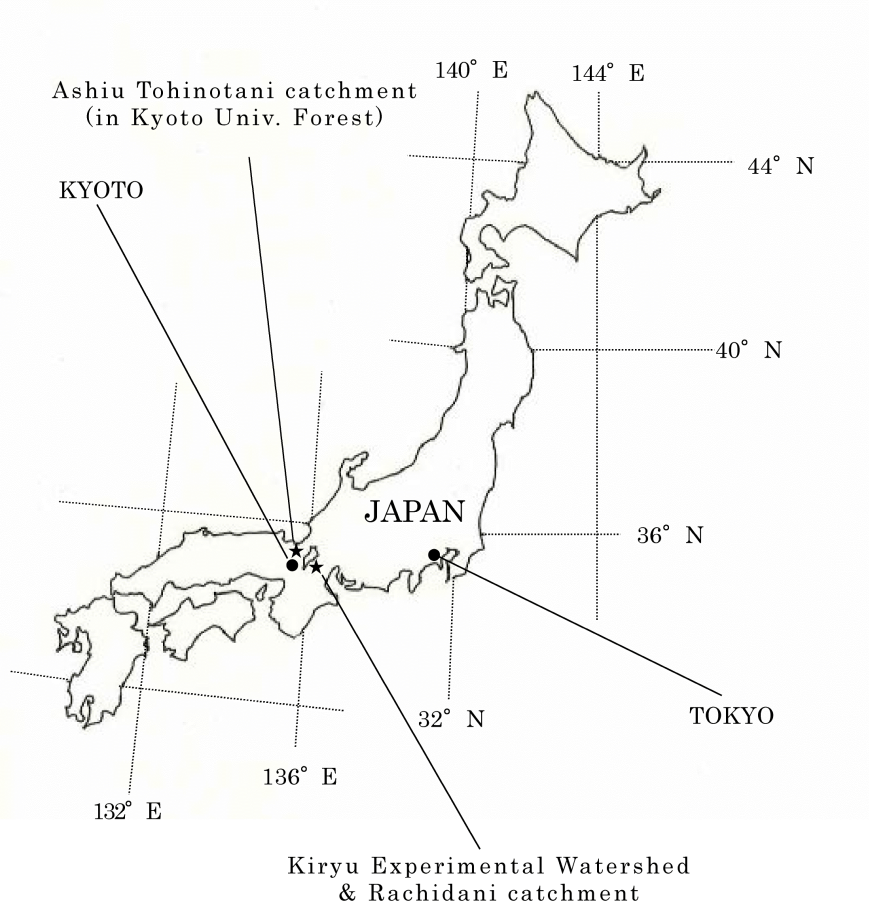

Figure 2.1 Locations of the study sites

2.1.1 Kiryu Matsuzawa Catchment

The Kiryu Experimental Watershed is southeast of Lake Biwa, in the

southern part of Shiga Prefecture, Central Japan. The Tanakami Mountains area, which includes this experimental catchment, was devastated about 1200 years ago by excessive timber use and remained denuded for a long period. Hillside restoration and reforestation works have been carried out over the last 100 years to prevent soil erosion. Most of this area has now been covered with plantation forest.

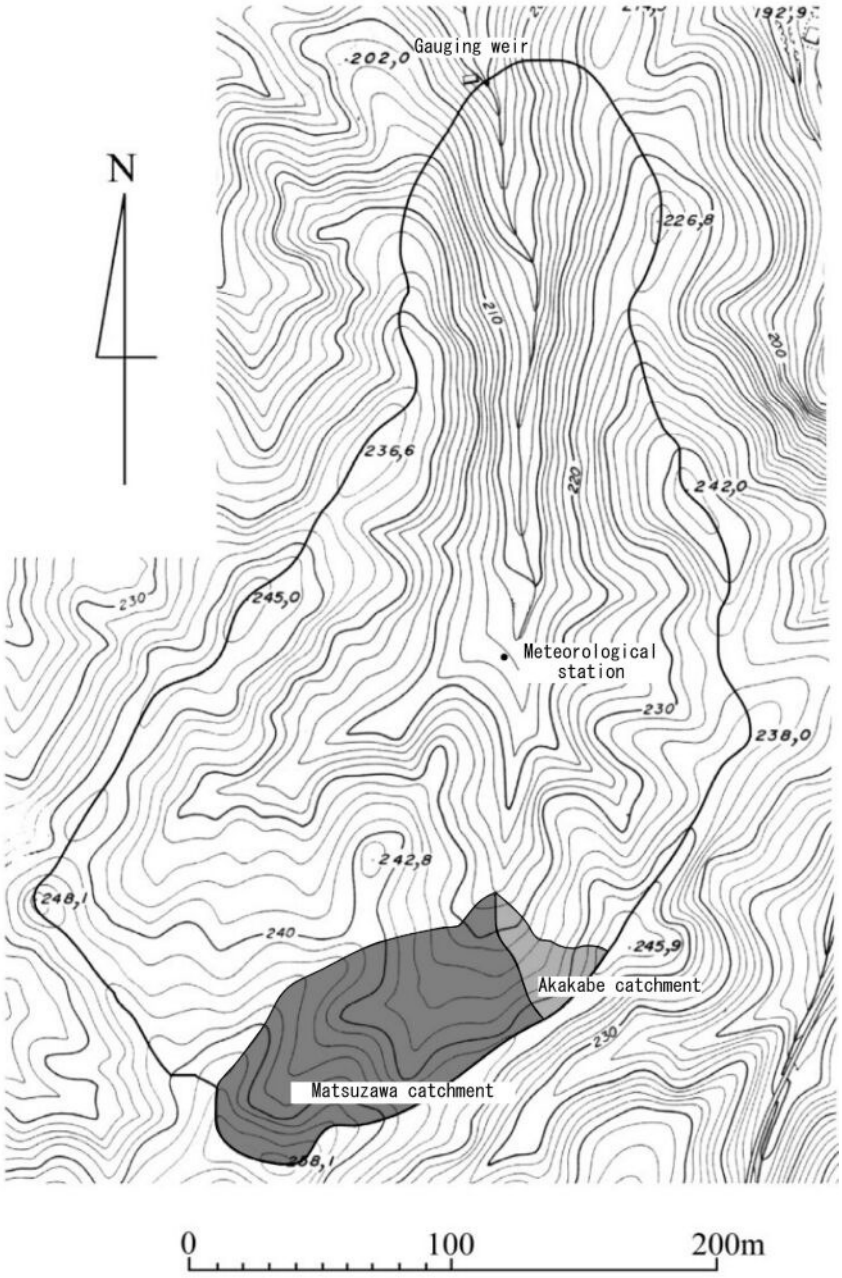

Figure 2.2 Topography of the Kiryu Experimental Watershed

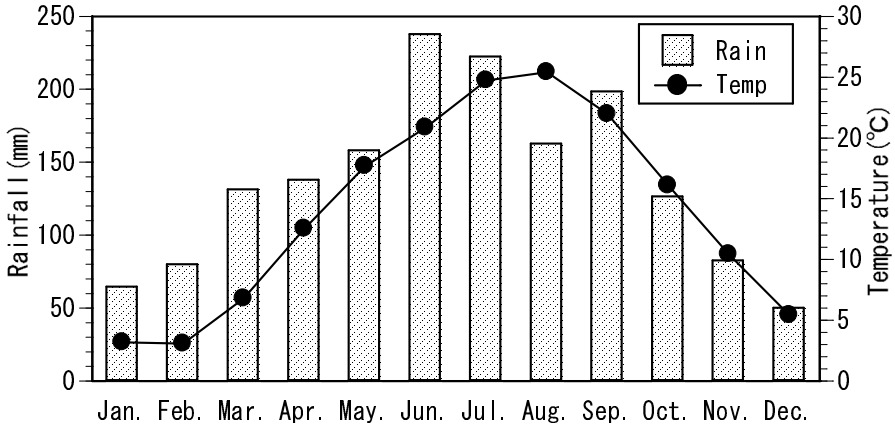

Figure 2.3 Monthly rainfall and air temperature in the Kiryu Experimental Watershed

note: Rainfall is averaged from 1972 to 2001.

Temperature is averaged from 1997 to 2001.

The Kiryu Experimental Watershed covers 5.99 ha; it is a forested watershed, located at 34°58'N, 136°00'E, with an elevation ranging from 190 m to 255 m. Topography is shown in Figure 2.2. Hydrological observations have continued since 1967. Monthly rainfall and air temperature are shown in Figure 2.3. The climate is warm temperate, with rainfall distributed throughout the year, peaking in summer but producing little snowfall in winter. The mean annual rainfall and runoff from 1972 to 2001 were 1645.0 mm and 888.5 mm, respectively. The mean annual air temperature from 1997 to 2001 was 14.0°C. Water budgets for the Kiryu Experimental Watershed and two subcatchments (the Matsuzawa and Akakabe catchments) are shown in Table 2.1.

Table 2.1 Water budgets for the Kiryu, Matsuzawa and Akakabe catchment

	Rainfall(mm)	Discharge(mm)		
		Kiryu	Matsuzawa	Akakabe
1996	1500.87	697.16	553.80	
1997	1703.94	872.23	830.38	
1998	2032.12	1300.12	1084.23	
1999	1590.96	831.54	526.70	841.30
2000	1402.60	551.14	335.25	467.64

The Kiryu Matsuzawa catchment is one of the small headwater subcatchments within the Kiryu Experimental Watershed, with an area of 0.68 ha. Vegetation consists of mixed stands of *Chamaecyparis obtusa* Sieb. et Zucc. planted in 1959 and *Pinus densiflora* Sieb. et Zucc., the natural regeneration of afforested

trees. In recent years, the *P. densiflora* stands have declined due to pine-wilt disease (Hobara et al., 2001). Some deciduous species are present on the ridge of the catchment. The leaf area index (LAI) measured on October 30 2000 was 4.91.

The entire area of the Matsuzawa catchment consists of weathered granitic rock with abundant amounts of albite. The soil profile has no apparent structure; organic matter is not mixed to any noticeable degree. The A_0 horizon has a moder humus form without any apparent H horizon, on both the upper and lower parts of the hillslope. The mineral soil on the upper part of the hillslope consists of an A and an AC horizon, which are thinner than 2 cm, and a B horizon that is not well established. At the lower part of the hillslope, although there is an A horizon of about 7 cm and a B horizon of about 30 cm, neither includes any apparent aggregates (Ohte et al., 1995). Detailed descriptions of the chemical characteristics of the soil were given by Ohte et al. (1997) and Asano et al. (1998).

The ground surface topography and the bedrock surface topography of the Matsuzawa catchment are shown in Figures 2.4 and 2.5, respectively. The size of the grid cell in each three-dimensional map is 2 m by 2 m. The Matsuzawa catchment is a headwater catchment, unchanneled, but the section from point SP (the spring outflow point) to point W (the weir) is channeled (about 12 m long, see Figure 2.4). Stream flow is perennial. Gentle slopes with deep soils adjoin steep slopes with shallow soils. The area with a gradient lower than 15° comprises 62.8% of the total area; the area steeper than 25° comprises 11.2% (Kim, 1990). The topography of the bedrock surface does not conform exactly to the ground surface. There are two hollows in the ground surface (lines G1-GE-GF-G15-G34 and GA-GB-GC-GD in Figure 2.4.), but only one hollow in the bedrock surface (line G1-GE-GF-G15-G34 in Figure 2.5).

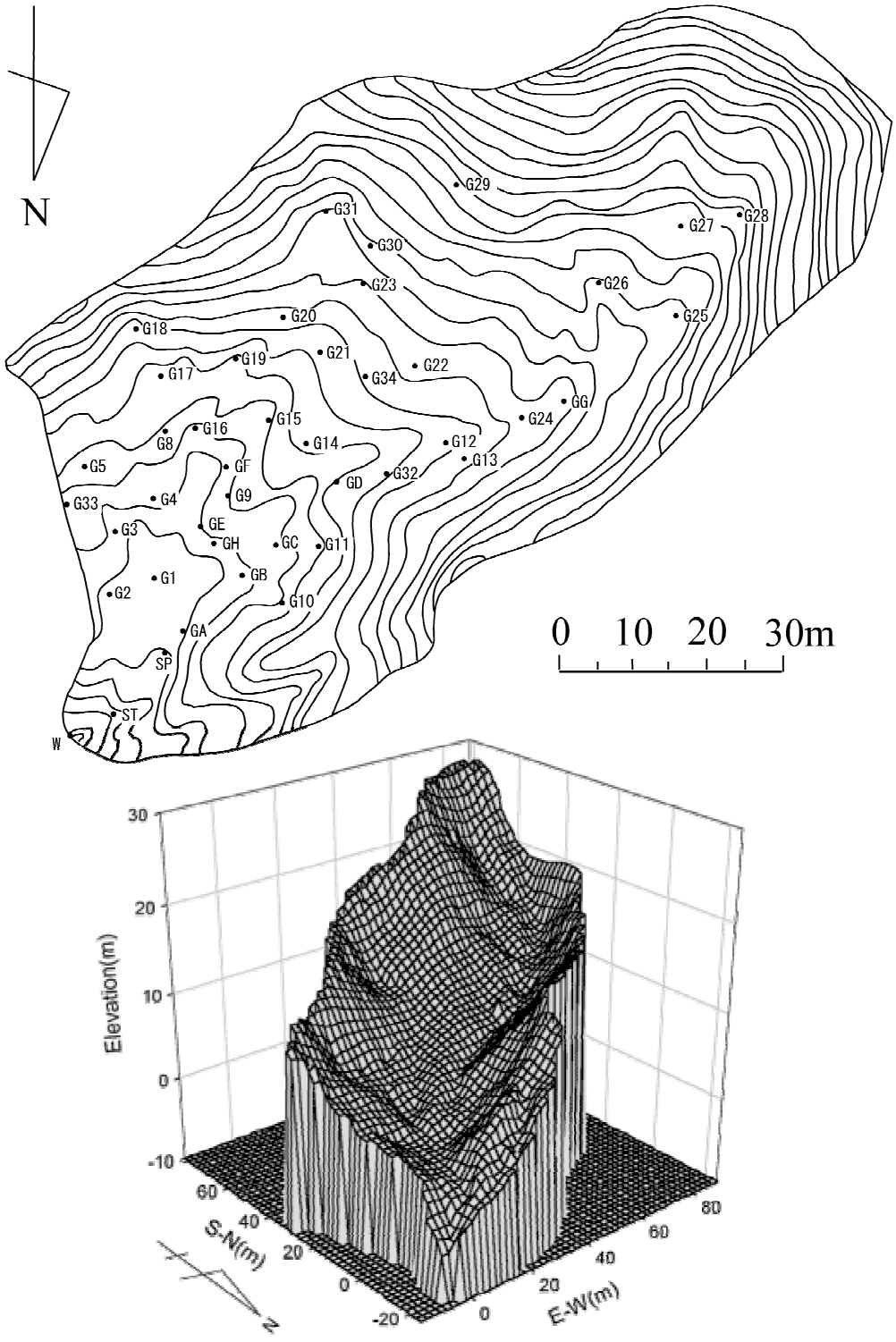

Figure 2.4 Ground surface topography of the Matsuzawa catchment

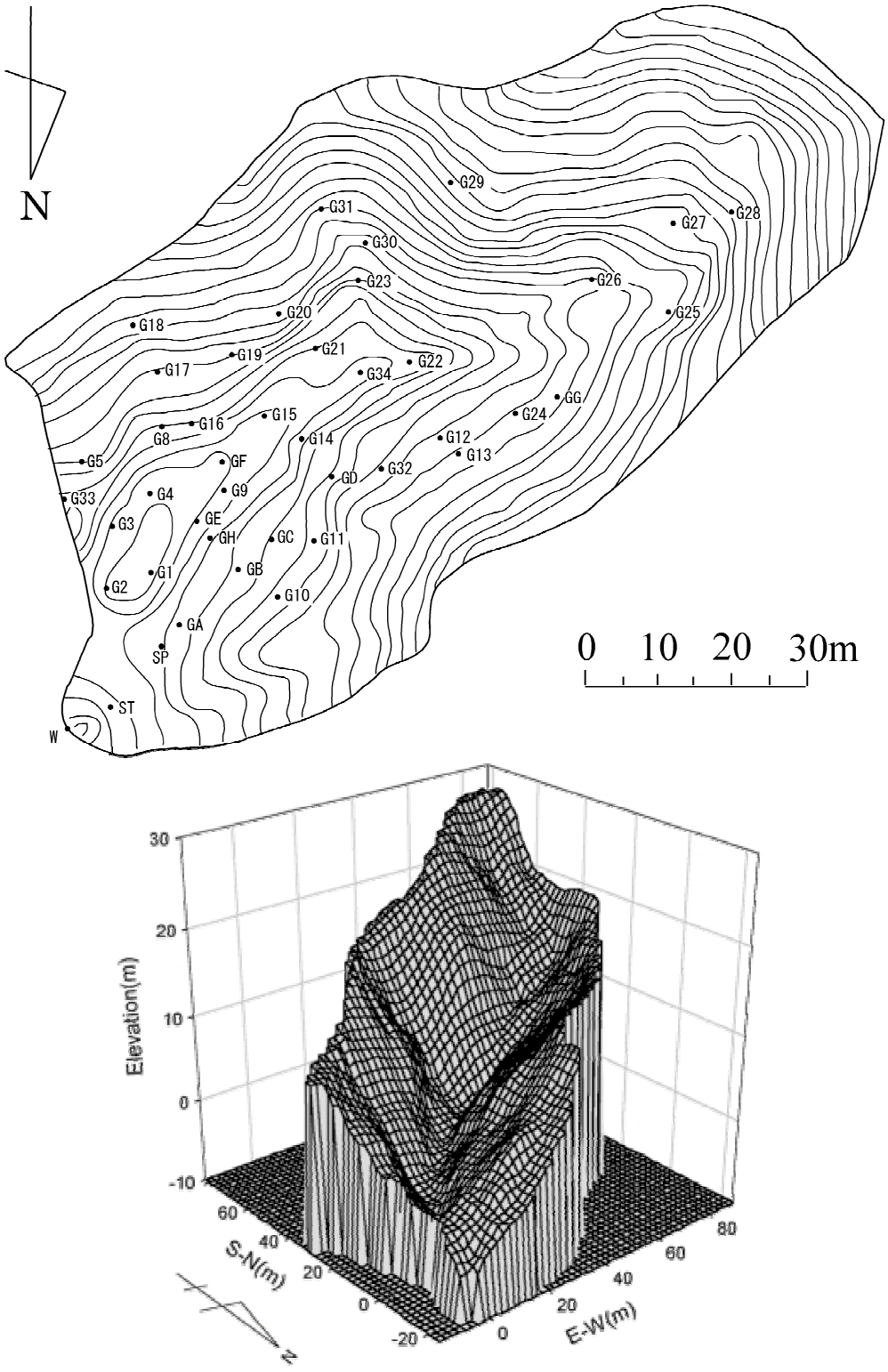

Figure 2.5 Bedrock surface topography of the Matsuzawa catchment

The spatial distributions of the topographic index (TPI, Beven and Kirkby, 1979) and their frequency distributions were calculated from the 2-m digital terrain models (DTMs) of the Matsuzawa catchment and are shown in Figure 2.6. The topographic index has the form

$$TPI = \ln(\alpha / \tan\beta)$$

where α is the upslope area per unit contour length contributing to a grid cell (derived from a raster DTM) and $\tan\beta$ is the local slope angle at the cell (Quinn et al., 1995). High-index-value areas will tend to saturate first and will therefore indicate potential subsurface or surface contributing areas (Beven, 1997). In the Matsuzawa catchment, cells with higher index values are distributed along the ground surface hollows, and the cells around G1 or SP have particularly high values; therefore, these areas are expected to saturate easily and to contribute to stream flow during rainstorms.

The spatial distribution of soil depths and their frequency distributions in the Matsuzawa catchment are shown in Figure 2.7. The mean soil depth of the area is 1.51 m; 62.4% of the area has a soil depth of less than 1 m (the area less than 0.5 m is 37.8%), and 25.8% has a soil depth greater than 2 m. The soil is especially deep in the area where the bedrock hollow is present.

The bedrock topography around the spring outflow of the Matsuzawa catchment was surveyed in detail using a cone penetrometer. A 20-m square plot was set up around the spring outflow point, and the soil depth was measured at each 2-m lattice point. Soil depth at each well was measured by a cone penetrometer with a cone diameter of 9.5 mm, a weight of 1.17 kg, and fall distance of 20 cm. The N_4 value is the number of blows required for a 4-cm penetration; in this study, N_4 values in excess of 100 were defined as constituting bedrock. Figure 2.8 shows the plot map and the distributions of the soil depth. Soil depth increases rapidly from the northwest to the southeast within the plot. The soil to the south or east of the spring outflow point is especially deep, indicating a bedrock depression around the spring.

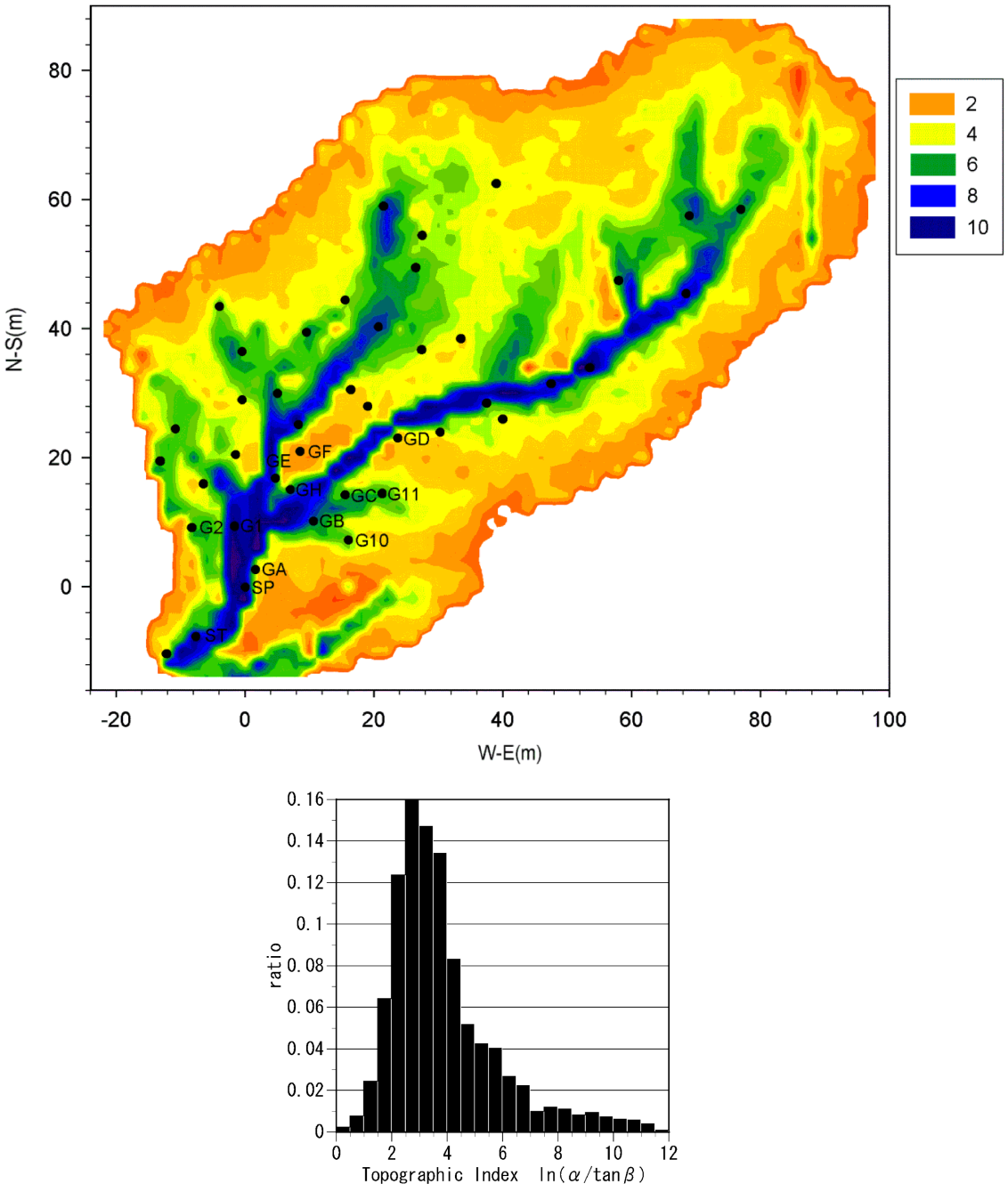

Figure 2.6 Spatial distributions of the topographic index and their frequency distributions of the Matsuzawa catchment

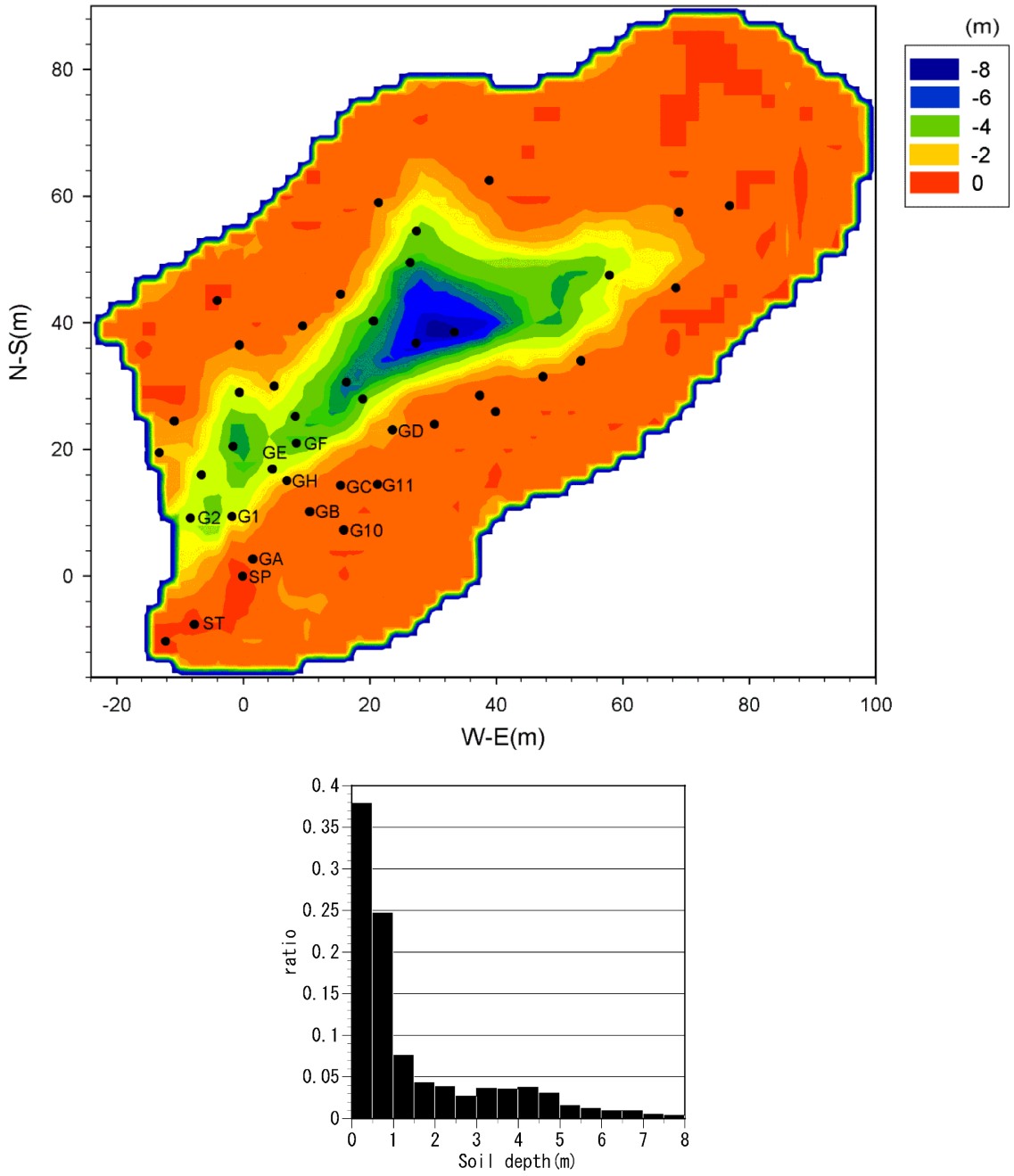

Figure 2.7 Spatial distribution of soil depths and their frequency distributions in the Matsuzawa catchment

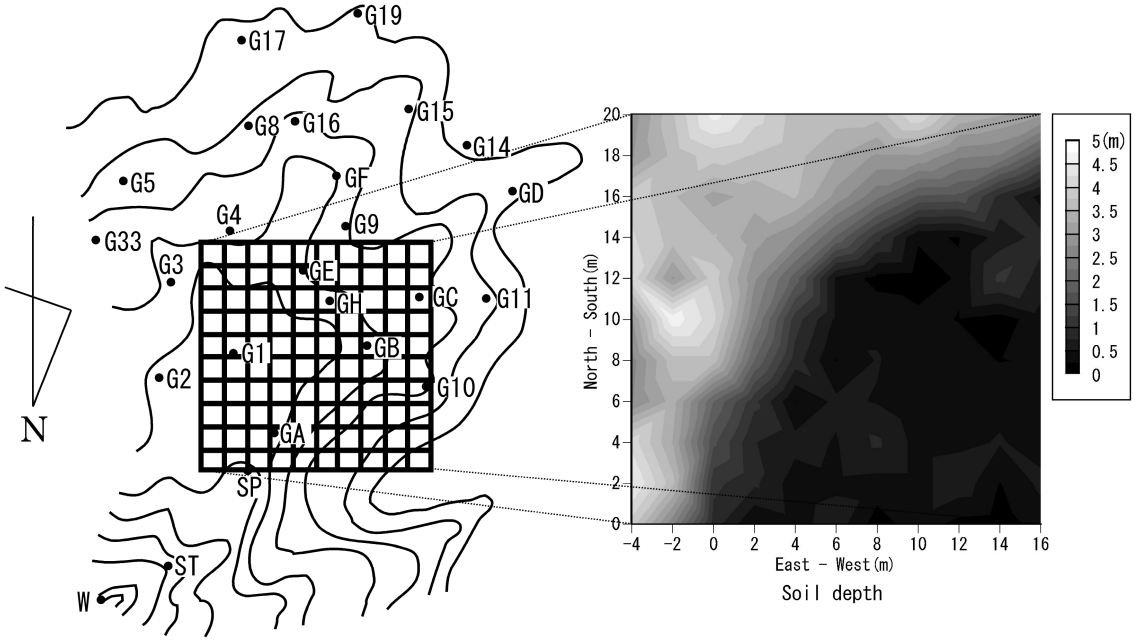

Figure 2.8 Bedrock topography around the spring outflow point of the Matsuzawa catchment

2.1.2 Kiryu Akakabe Catchment

The Kiryu Akakabe catchment is one of the small headwater subcatchments in the Kiryu Experimental Watershed and is adjacent to the Matsuzawa catchment (see Figure 2.2). The area of the Akakabe catchment is 0.086 ha and the vegetation consists of *Chamaecyparis obtusa* Sieb. et Zucc. planted in 1959. The geology and meteorology are the same as those of the Matsuzawa catchment. The ground surface topography and a longitudinal section of the Akakabe catchment are shown in Figure 2.9. A stonemasonry dam exists in the catchment, which was constructed to prevent soil erosion. The catchment is divided into three parts, the stream channel area downslope from the dam, the soil sedimentation area upslope from the dam, and the hillslope area connected to the soil sedimentation area. A spring outflow point exists below the dam, and the channel length between the spring and the weir is about 16 m. Streamflow is perennial, although the spring outflow moves downslope and the channel length becomes shorter during the dry season. Groundwater persists in the soil sediment zone all year. The gradients of the channel, and of the catchment as a whole, are 23.0° and 22.0°, respectively.

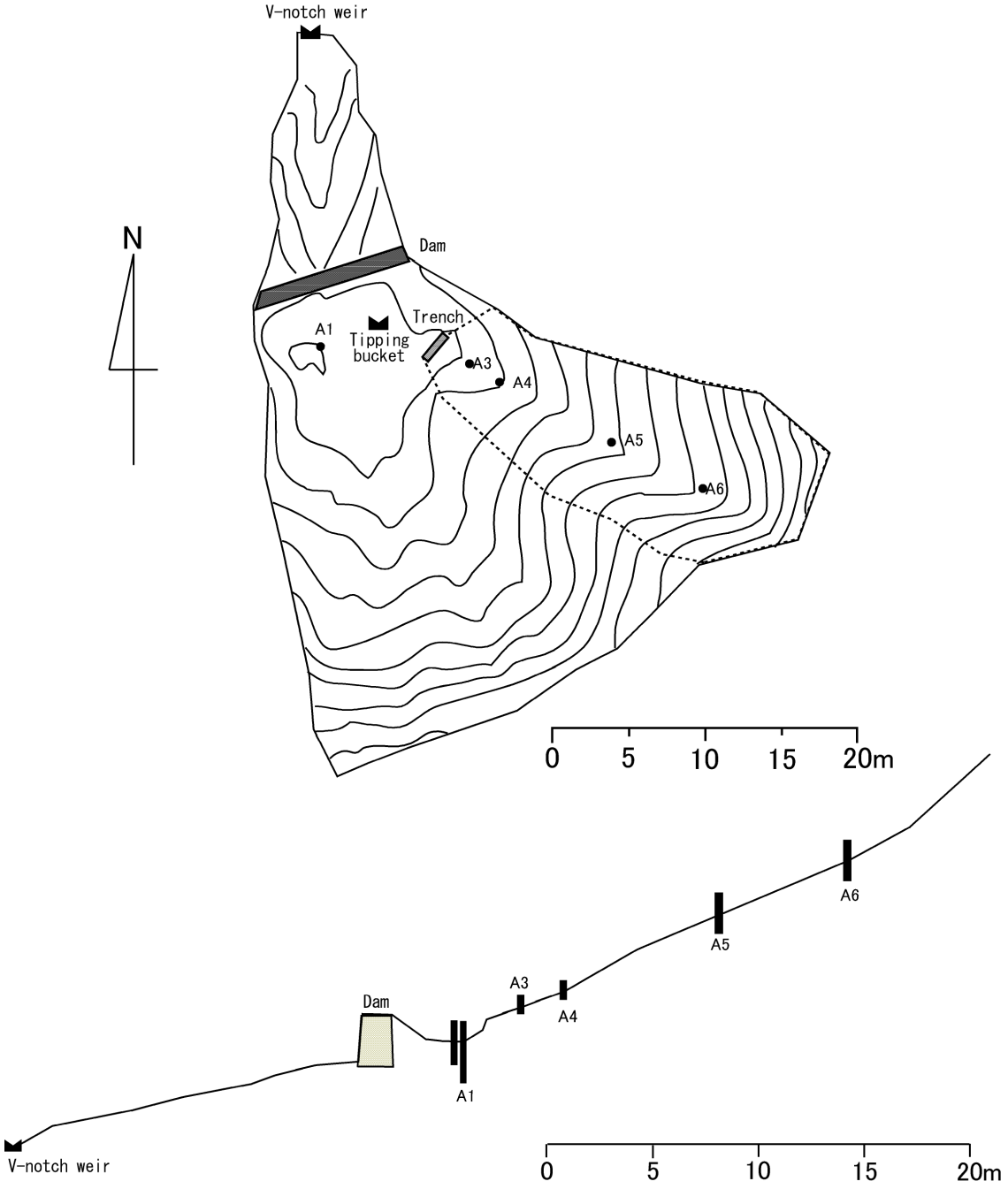

Figure 2.9 Ground surface topography and a longitudinal section of the Akakabe catchment

In order to study runoff generation and the hydrochemical processes of saturated throughflow during rainstorms within the hillslope area, a 0.02-ha hillslope plot was set up and a trench was installed. The longitudinal section and the soil depth distributions are shown in Figure 2.10. The soil depth, which was

measured using a boring stick at 48 points along the hollow of the plot, was distributed in the range of 20 cm to 126 cm. The mean soil depth of these 48 points was 0.7 m, with 31.2% having a soil depth less than 0.5 m and 18.8% having a depth greater than 1 m. The slope length is 49.8 m and the gradient is 23.4°.

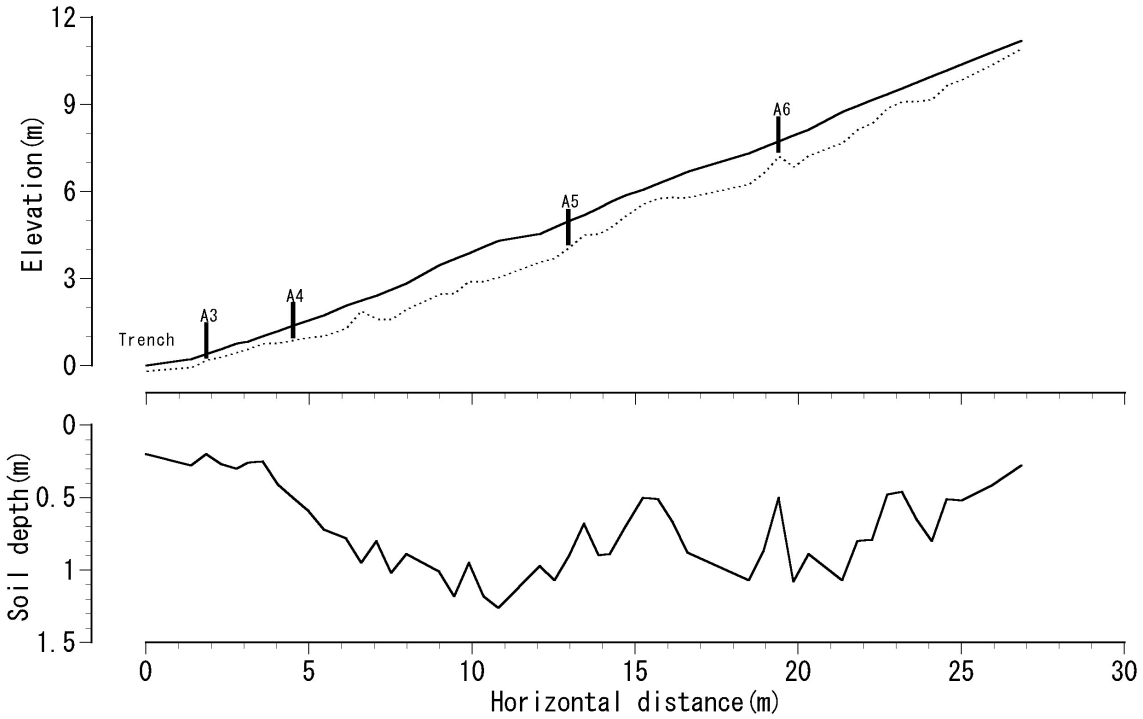

Figure 2.10 Longitudinal section of hillslope plot and soil depth distributions in the Akakabe catchment

2.1.3 Jakujo Rachidani Catchment

The Jakujo Rachidani catchment is within the Tanakami Mountains region, as is the Kiryu Experimental Watershed. In this area, hillside restoration works have been unsuccessful and the soils are predominantly eroded and bare. The topography and a longitudinal section of the lower part of the catchment are shown in Figure 2.11. The catchment area is 0.18 ha and the mean gradient in the valley is 34.1°. The mean annual rainfall and runoff from 1996 to 1999 were 1670.3 mm and 1093.5 mm, respectively. The Rachidani catchment is less than 5 km from the Kiryu Experimental Watershed (Figure 2.1), so the mean annual rainfall is similar. However, because the vegetation is immature and there is little evapotranspiration, the soil-water contents differ between the two catchments. The eroded Rachidani catchment has only a small area at the bottom part of the hollow (about 10% of the area) covered with *Pinus thunbergii* Parl. and *Chamaecyparis obtusa* Sieb. et Zucc. A 1-m high dam has been installed at the bottom of the

catchment, and upslope from the dam the soil formed from sediment is 70 m to 100 cm deep. Groundwater persists in the soil sediment zone year round; however, the scale of the saturated zone is small compared with that of the Matsuzawa catchment. The channel length from the spring (point SP in Figure 2.11) to the weir (point W) is about 3 m. More detailed descriptions of the topography and of the physical characteristics of the soil are given in Kimoto et al. (1999), and the chemical characteristics of the soil are detailed in Asano et al. (1998).

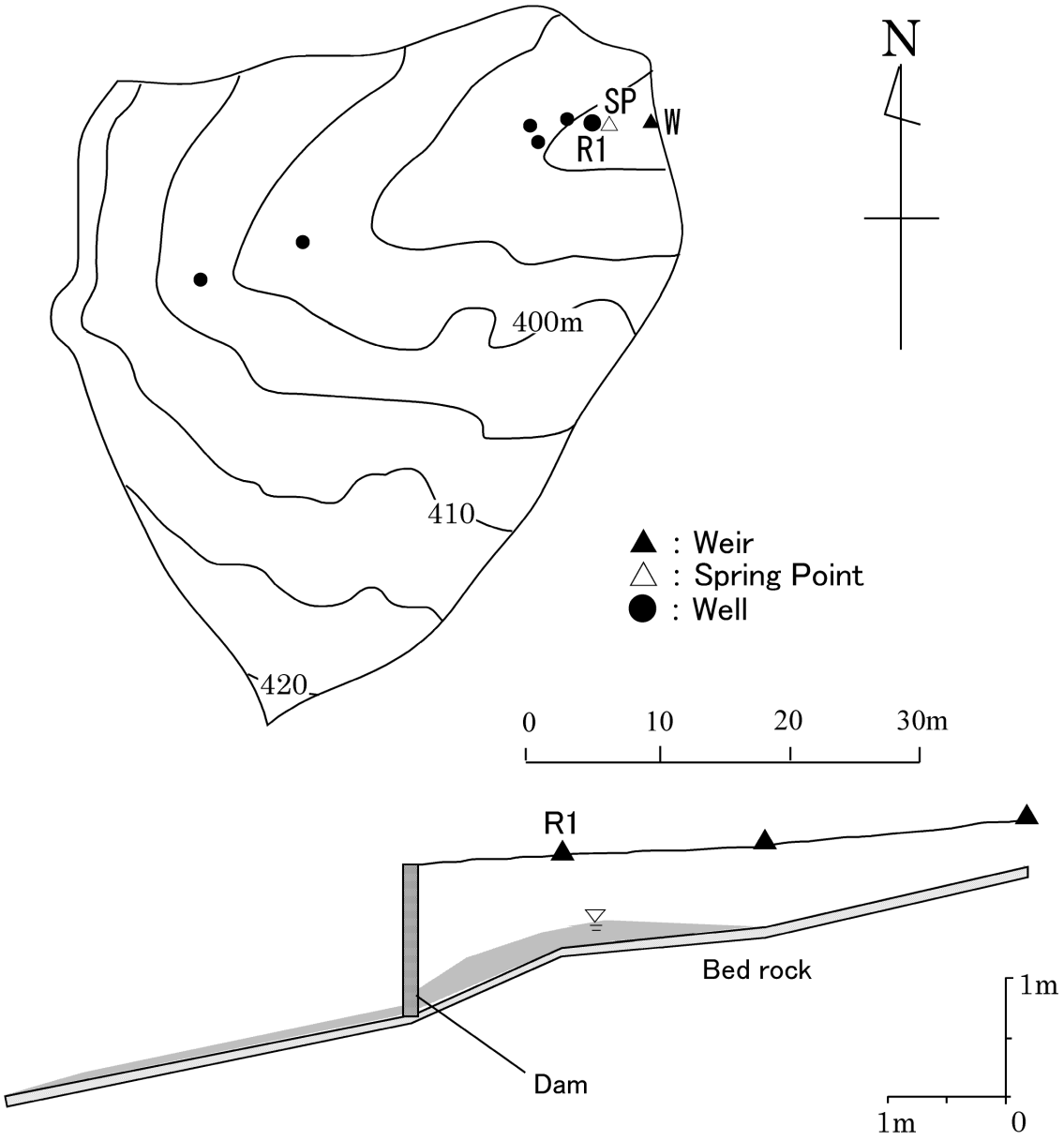

Figure 2.11 Ground surface topography and a longitudinal section of the Rachidani

2.1.4 Ashiu Toinotani Catchment

The Toinotani catchment is a headwater subcatchment of the Shimotani catchment (303 ha) in the Kyoto University Forest in Ashiu, located in the northern part of Kyoto Prefecture, Central Japan (see Figure 2.1). The topography and a longitudinal section of the lower part of the catchment are shown in Figure 2.12. The catchment area is 0.64 ha and the mean slope gradient is 35.9°. The altitude of the catchment ranges from 730 m to 830 m above sea level, with an average air temperature of 10.3°C. Mean annual rainfall and runoff from the Kamitani catchment (490 ha, adjacent to the Shimotani catchment) are 2885.3 mm (30% of which falls as snow) and 2448.1 mm, respectively (Nakashima and Fukushima, 1994). The catchment is covered by secondary forest growth of *Cryptomeria japonica* D. Don, with some broadleaf species (*e.g.*, *Betula grossa* Sieb. et Zucc.). The catchment is underlain by Paleozoic sedimentary rock. The outlets of some natural soil pipes were found about 10 m upstream from the weir along the longitudinal axis of the hollow, and the importance of pipe flow to storm runoff generation processes has been described (Uchida, 2000). Soil depth is about 10 cm around the spring outflow, and ranges from 20 cm to 80 cm around the pipe outlets. The channel length from the spring (point SP in Figure 2.12) to the weir (point W) is about 2 m. The outlet of one of the pipes is 6 m upstream from the spring outflow point (Pipe A), and six others occur 4 m upstream from Pipe A (Pipe group B) (Uchida, 2000).

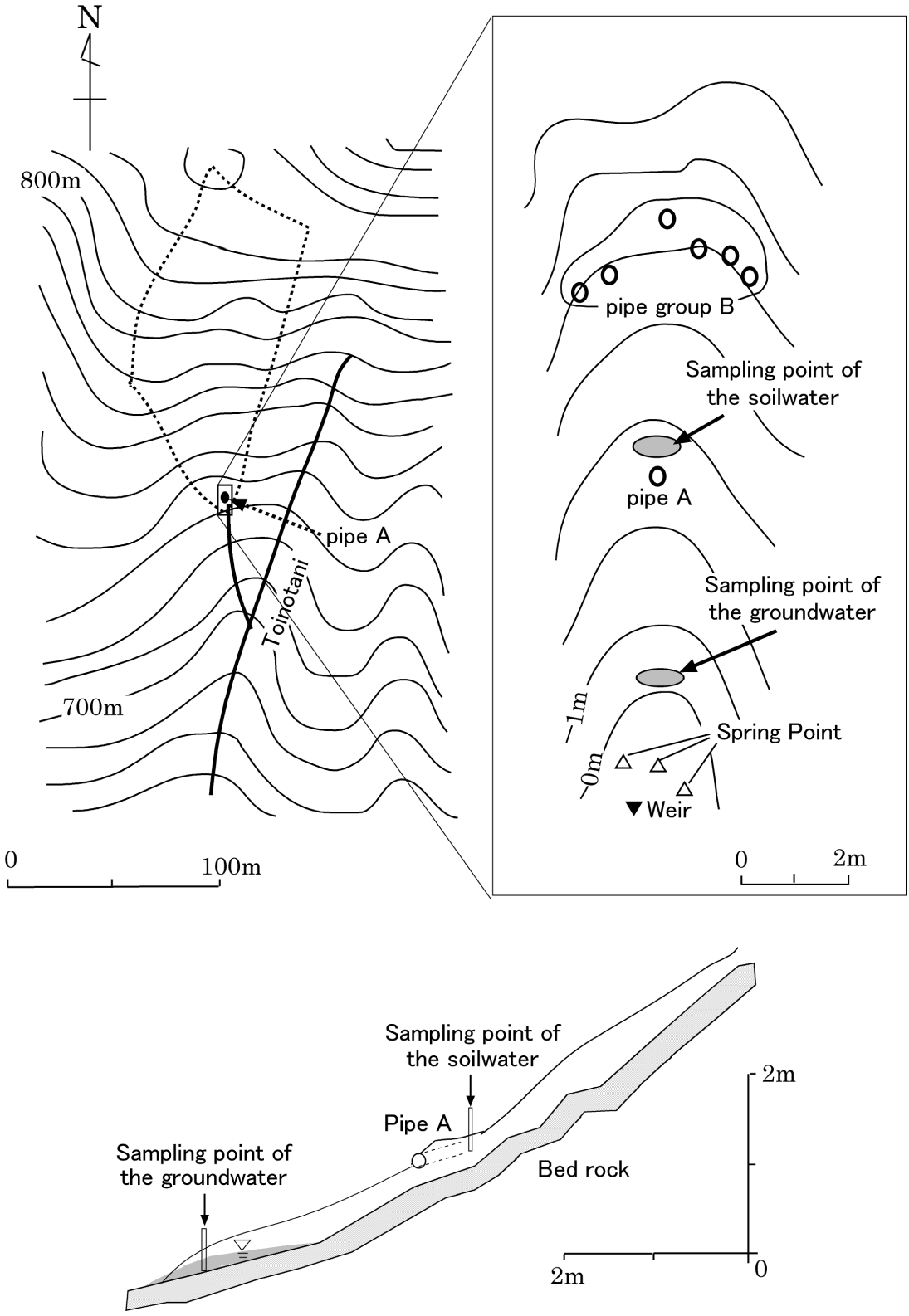

Figure 2.12 Ground surface topography and a longitudinal section of the Toinotani catchment

2.2 Hydrological and Hydrochemical Observations

2.2.1 Matsuzawa Catchment

The locations of the observation facilities are shown in Figure 2.4. Rainfall was measured using a tipping-bucket rain gauge at the meteorological station located at the center of the Kiryu Experimental Watershed (see Figure 2.2). Runoff from the Matsuzawa catchment was continuously measured at a 30° V-notch weir located downstream of the spring through which groundwater emerges to the surface. Groundwater levels were monitored manually using maximum groundwater level gauges at 39 observation wells throughout the catchment and using continuous automatic-recording tensiometers and a programmable data logger (Campbell, USA, CR-10X) in the lower part of the catchment at points G1, G2, G10, G11, G15, G34, GA, GB, GC, GD, GE, GF, and GH. The structure of the observation wells is shown in Figure 2.13. These wells were made of bore pipes 6 cm in diameter screened with small holes around their peripheries from top to bottom.

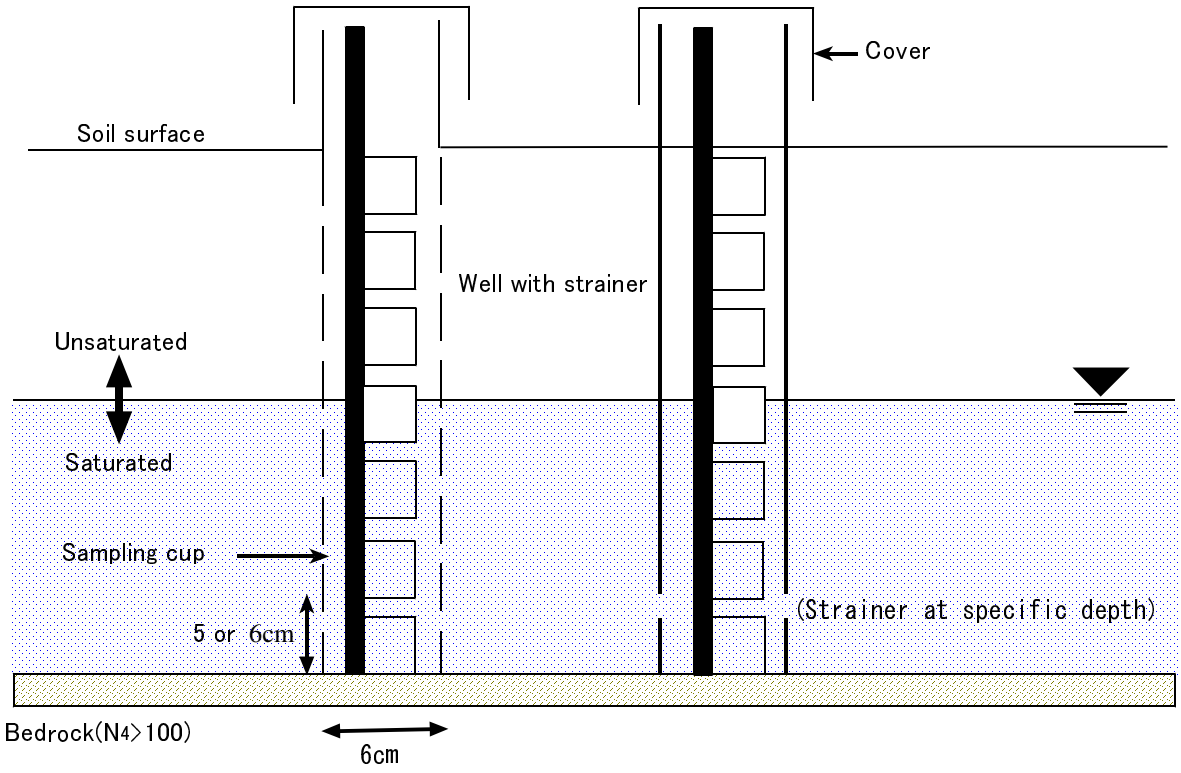

Figure 2.13 The structure of the observation wells (Maximum rise well)

The observation wells are of three types according to expected hydrological behavior; that is, the response of the groundwater level to rainstorms and the

general groundwater condition (Ohte et al., 1995). The three categories are as follows:

1) Saturated zone (SGW). This zone is saturated year-round and is adjacent to the stream. Points G1, G2, GE, GF, and G3 are located in this zone.

2) Transient saturated zone (TGW). This zone is situated at the edge of the saturated zone. During wet seasons, from spring to fall in this region, saturated conditions always occur. This zone is similar to the SGW zone at these times. The saturated condition disappears during the dry winter season. Points GA, GB, GC, GD, and GH are located in this zone.

3) Unsaturated hillslope zone (HGW). This zone has shallow soils and is located at the hillslope part of the catchment. It is not saturated continuously, but on occasion during rainstorms. Saturation disappears immediately after the rainstorms. Points G10, G11, and the other observation wells are located in this zone.

The depth of the representative observation wells for each zone, soil depth to bedrock, and the occasions when groundwater occurred at each point are shown in Table 2.2. In Figure 2.14, profiles of N_4 value at each point are shown. The observation wells in SGW are in very deep soil compared to those in zones TGW and HGW. The observation wells of GB, GC, and GD in TGW have been drilled down to bedrock.

Table 2.2 Hydrological classification and groundwater occurrence of observation wells

1996

Well	soil depth	well depth	Jun			Jul				Aug	Sep						Oct			Nov		Dec	
	(cm)	(cm)	12	20	26	3	10	19	20	10	3	12	14	20	25	27	9	15	30	5	19	3	19
Matsuzawa catchment																							
SGW																							
G1-75	470	75	◎	◎	◎	◎	◎	◎	◎	◎	◎	◎	◎	◎	◎	◎	◎	◎	◎	◎	◎	◎	◎
G2-177	446	177	◎	◎	◎	◎	◎	◎	◎	◎	◎	◎	◎	◎	◎	◎	◎	◎	◎	◎	◎	◎	◎
GE	350	185																			◎	○	◎
TGW																							
GC	82	217	◎	◎	◎	◎	◎	◎	◎	◎	◎	◎	◎	◎	◎	◎	◎	◎	◎	◎	◎	◎	◎
GD	30	179	×	◎	◎	◎	◎	◎	◎	◎	◎	◎	◎	◎	◎	◎	◎	◎	◎	◎	◎	○	◎
HGW																							
G10	26	25	○	○	○	×	○	×	×	○	○	○	○	×	×	×	×	○	×	○	×	×	○
G11	38	49	×	×	◎	○	○	×	×	×	○	○	○	×	×	×	×	○	×	×	×	○	×

1997

Well	soil depth	well depth	Jan		Feb	Mar			Apr		May	Jun			Jul				Aug		Sep	Oct			Nov		Dec	
	(cm)	(cm)	8	21	12	6	18	31	16	30	15	4	17	28	3	15	31	13	30	18	2	16	28	13	27	11	23
Matsuzawa catchment																											
SGW																											
G1-75	470	75	◎	◎	◎	◎	◎	◎	◎	◎	◎	◎	◎	◎	◎	◎	◎	◎	◎	◎	◎	◎	◎	◎	◎	◎	◎
G2-177	446	177	◎	◎	◎	◎	◎	◎	◎	◎	◎	◎	◎	◎	◎	◎	◎	◎	◎	◎	◎	◎	◎	◎	◎	◎	◎
GE	350	185	○	○	○	◎	◎	◎	◎	◎	◎	◎	◎	◎	◎	◎	◎	◎	◎	◎	◎	◎	◎	◎	◎	◎	◎
GF	356	200				○	×	◎	◎	◎	◎	◎	◎	◎	◎	◎	◎	◎	◎	◎	◎	◎	◎	◎	◎	◎	◎
TGW																											
GA	74	76												◎	◎	◎	◎	◎	◎	◎	◎	◎	◎	×	◎	◎	◎
GB	32	82												◎	◎	◎	◎	◎	◎	◎	◎	○	×	○	◎	◎	◎
GC	82	217	◎	◎	◎	◎	◎	◎	◎	◎	◎	◎	◎	◎	◎	◎	◎	◎	◎	◎	◎	◎	○	○	◎	◎	◎
GD	30	179	◎	◎	○	◎	◎	◎	◎	◎	◎	◎	◎	◎	◎	◎	◎	◎	◎	◎	◎	◎	○	○	◎	◎	◎
HGW																											
G10	26	25	×	×	×	×	×	○	○	×	○	×	×	○	○	○	○	○	×	○	○	×	×	×	○	○	×
G11	38	49	×	×	×	×	×	×	○	×	○	×	×	○	×	◎	○	○	×	○	○	×	×	×	○	○	×

◎ Continuous appearrance of groundwater
○ Groundwater remaining from last rain
× No groundwater

Table 2.2 (Continued)

1998

Well	soil depth (cm)	well depth (cm)	Jan 13	Feb 4	18	May 3	17	Apr 10	23	May 14	28	Jun 11	23	Jul 9	22	Aug 10	31	Sep 24	Oct 13	29	Nov 10	24	Dec 15	28
Matsuzawa catchment																								
SGW																								
G1-75	470	75	◎	◎	◎	◎	◎	◎	◎	◎	◎	◎	◎	◎	◎	◎	◎	◎	◎	◎	◎	◎	◎	◎
G2-177	446	177	◎	◎	◎	◎	◎	◎	◎	◎	◎	◎	◎	◎	◎	◎	◎	◎	◎	◎	◎	◎	◎	◎
GE	350	185	◎	◎	◎	◎	◎	◎	◎	◎	◎	◎	◎	◎	◎	◎	◎	◎	◎	◎	◎	◎	◎	◎
GF	356	200	◎	◎	◎	◎	◎	◎	◎	◎	◎	◎	◎	◎	◎	◎	◎	◎	◎	◎	◎	◎	◎	◎
TGW																								
GA	74	76	◎	◎	◎	◎	◎	◎	◎	◎	◎	◎	◎	◎	◎	◎	◎	◎	◎	◎	◎	◎	◎	○
GB	32	82	◎	◎	◎	◎	◎	◎	◎	◎	◎	◎	◎	◎	◎	◎	◎	◎	◎	◎	◎	○	○	×
GC	82	217	◎	◎	◎	◎	◎	◎	◎	◎	◎	◎	◎	◎	◎	◎	◎	◎	◎	◎	◎	◎	◎	○
GD	30	179	◎	◎	◎	◎	◎	◎	◎	◎	◎	◎	◎	◎	◎	◎	◎	◎	◎	◎	◎	◎	◎	○
HGW																								
G10	26	25	○	○	×	○	○	○	○	○	○	○	○	○	○	○	○	○	○	○	×	×	○	×
G11	38	49	×	○	×	×	×	◎	○	○	○	○	◎	○	○	×	×	○	○	○	×	×	×	×

1999

Well	soil depth (cm)	well depth (cm)	Jan 20	Feb 19	Mar 10	26	Apr 8	21	May 13	Jun 2	15	29	Jul 1	12	29	Aug 19	Sep 3	21	Oct 7	19	Nov 4	18	30	Dec 22
Matsuzawa catchment																								
SGW																								
G1-75	470	75	◎	◎	◎	◎	◎	◎	◎	◎	◎	◎	◎	◎	◎	◎	◎	◎	◎	◎	◎	◎	◎	◎
G2-177	446	177	◎	◎	◎	◎	◎	◎	◎	◎	◎	◎	◎	◎	◎	◎	◎	◎	◎	◎	◎	◎	◎	◎
GE	350	185	◎	◎	◎	◎	◎	◎	◎	◎	◎	◎	◎	◎	◎	◎	◎	◎	◎	◎	◎	◎	◎	◎
GF	356	200	◎	○	×	◎	◎	◎	◎	◎	◎	◎	◎	◎	◎	◎	◎	◎	◎	◎	◎	◎	◎	◎
TGW																								
GA	74	76	×	○	○	◎	◎	◎	◎	◎	◎	◎	◎	◎	◎	◎	◎	◎	◎	◎	◎	◎	◎	○
GB	32	82	○	○	○	◎	◎	◎	○	◎	◎	◎	◎	◎	◎	◎	○	○	◎	◎	◎	○	○	×
GC	82	217	×	○	○	◎	◎	◎	◎	◎	◎	◎	◎	◎	◎	◎	◎	◎	◎	◎	◎	◎	◎	○
GD	30	179	×	×	×	◎	◎	◎	◎	◎	◎	◎	◎	◎	◎	◎	◎	◎	◎	◎	◎	○	×	×
HGW																								
G10	26	25	×	○	×	○	×	○	○	○	○	○	○	×	×	○	×	○	○	×	○	○	×	×
G11	38	49	×	×	×	○	×	×	×	○	○	○	○	×	○	○	×	×	◎	○	×	×	×	×
Akakabe catchment																								
SGW																								
A1-175		175									◎	◎	◎	◎	◎	◎	◎	◎	◎	◎	◎	◎	◎	◎
A1-110		110					◎	◎	◎	◎	◎	◎	◎		◎	◎	◎	◎	◎	◎	◎	◎	◎	◎
HGW																								
A3		20									×	○	○	×	×	○	○	○	○	×	○	○	×	×
A4		30									×	○	○	×	×	○	○	○	○	×	×	×	×	×
A5		95									×	○	○	×	×	×	×	×	×	×	×	×	×	×
A6		94									×	○	○	×	×	○	×	○	○	×	×	×	×	×

2000

Well	soil depth (cm)	well depth (cm)	Jan 11	Feb 2	22	Mar 9	24	Apr 10	24	May 9	23	Jun 6	15	20	27	Jul 4	11	28	Aug 10	24	Sep 14	Oct 5	24	Nov 10	22	Dec 14	28
Matsuzawa catchment																											
SGW																											
G1-75	470	75	◎	◎	◎	◎	◎	◎	◎	◎	◎	◎	◎	◎	◎	◎	◎	◎	◎	◎	◎	◎	◎	◎	◎	◎	◎
G2-177	446	177	◎	◎	◎	◎	◎	◎	◎	◎	◎	◎	◎	◎	◎	◎	◎	◎	◎	◎	◎	◎	◎	◎	◎	◎	◎
GE	350	185	◎	◎	◎	◎	◎	◎	◎	◎	◎	◎	◎	◎	◎	◎	◎	◎	◎	◎	◎	◎	◎	◎	◎	◎	◎
GF	356	200	◎	◎	×	○	◎	◎	◎	◎	◎	◎	◎	◎	◎	◎	◎	◎	◎	◎	◎	◎	◎	◎	◎	◎	◎
TGW																											
GA	74	76	○	○	○	○	◎	◎	◎	○	◎	◎	◎	◎	◎	◎	◎	◎	○	○	◎	◎	◎	◎	◎	◎	◎
GB	32	82	×	○	○	○	◎	◎	◎	○	◎	◎	◎	◎	◎	◎	◎	◎	○	○	◎	◎	◎	◎	◎	○	○
GC	82	217	×	◎	○	◎	◎	◎	◎	◎	◎	◎	◎	◎	◎	◎	◎	◎	○	○	◎	◎	◎	◎	◎	◎	◎
GD	30	179	○	○	×	×	○	×	○	×	○	◎	◎	◎	◎	◎	◎	◎	○	○	◎	◎	◎	◎	◎	◎	○
HGW																											
G10	26	25	×	○	×	×	○	×	×	×	○	○	○	○	○	×	×	×	○	○	○	○	○	○	×	×
G11	38	49	×	×	×	×	×	×	×	×	×	×	×	○	×	×	×	×	×	○	○	×	○	○	○	×	×
Akakabe catchment																											
SGW																											
A1-175		175	◎	◎	◎	◎	◎	◎	◎	◎	◎	◎	◎	◎	◎	◎	◎	◎	◎	◎	◎	◎	◎	◎	◎	◎	◎
A1-110		110	◎	◎	◎	◎	◎	◎	◎	◎	◎	◎	◎	◎	◎	◎	◎	◎	◎	◎	◎	◎	◎	◎	◎	◎	◎
HGW																											
A3		20	○	○	○	○	○	×	○	×	○	○	○	○	○	○	×	○	○	○	○	○	○	○	○	×	×
A4		30	○	○	×	×	×	×	×	×	○	×	×	×	×	○	×	○	○	○	○	○	○	○	○	×	×
A5		95	×	×	×	×	×	×	×	×	×	×	×	×	×	×	×	×	×	×	×	×	×	×	×	×	×
A6		94	×	×	×	×	×	×	×	×	×	×	×	×	○	×	×	×	×	○	○	○	×	○	×	×	×

2001

Well	soil depth (cm)	well depth (cm)	Jan 11	31	Feb 14	Mar 8	27	Apr 18	May 9	24	Jun 12	26	Jul 18
Matsuzawa catchment													
SGW													
G1-75	470	75	◎	◎	◎	◎	◎	◎	◎	◎	◎	◎	◎
G2-177	446	177	◎	◎	◎	◎	◎	◎	◎	◎	◎	◎	◎
GE	350	185	◎	◎	◎	◎	◎	◎	◎	◎	◎	◎	◎
GF	356	200	◎	◎	◎	◎	◎	◎	◎	◎	◎	◎	◎
TGW													
GA	74	76	◎	◎	◎	◎	◎	◎	◎	◎	○	◎	◎
GB	32	82	◎	◎	◎	◎	◎	○	○	◎	○	◎	◎
GC	82	217	◎	◎	◎	◎	◎	◎	◎	◎	◎	◎	◎
GD	30	179	◎	◎	◎	◎	◎	◎	○	◎	○	◎	◎
HGW													
G10	26	25	○	○	○	○	×	×	×	○	○	○	○
G11	38	49	×	○	×	○	×	×	×	○	×	○	○
Akakabe catchment													
SGW													
A1-175		175	◎	◎	◎	◎	◎	◎	◎	◎	◎	◎	◎
A1-110		110	◎	◎	◎	◎	◎	◎	◎	◎	◎	◎	◎
HGW													
A3		20	○	○	○	○	×	×	○	○	○	○	○
A4		30	○	×	○	○	×	×	○	○	○	○	○
A5		95	×	×	×	×	×	×	×	×	×	×	×
A6		94	×	×	×	×	×	×	×	○	○	○	○

◎ Continuous appearrance of groundwater
○ Groundwater remaining from last rain
× No groundwater

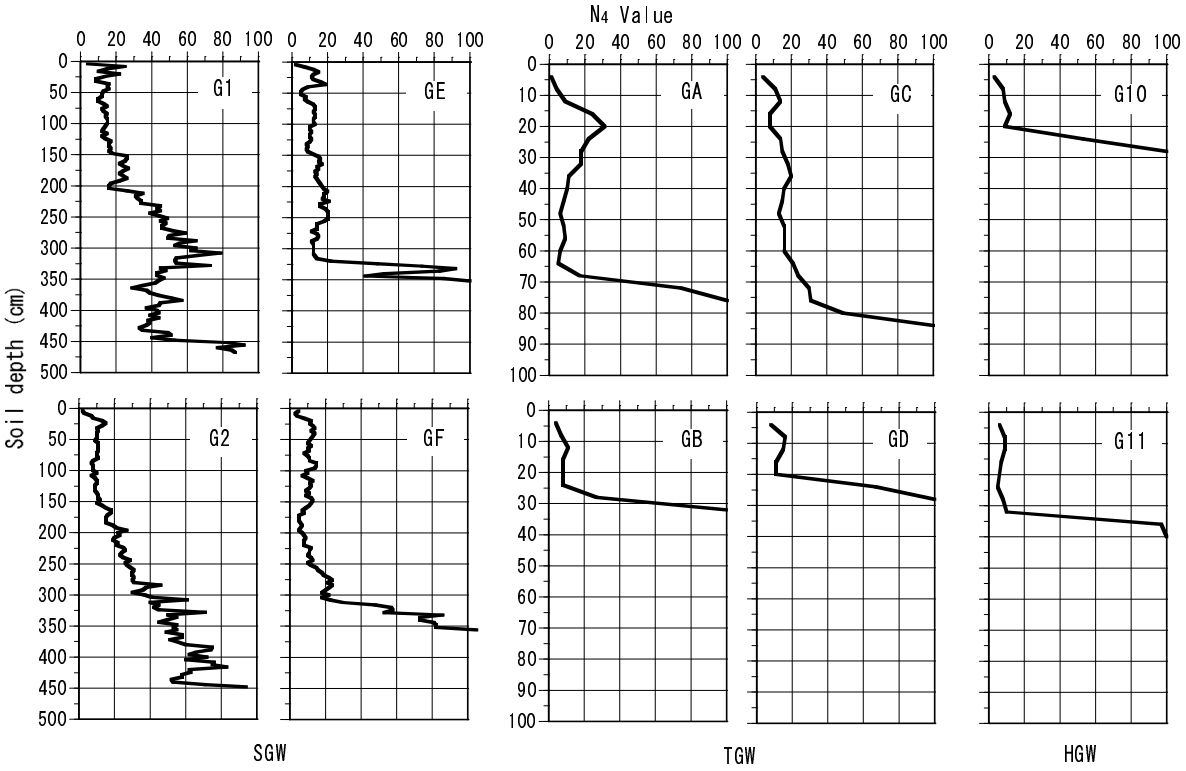

Figure 2.14 Vertical distribution of N_4 value

note: Pay attentions in the difference of Y axis in SGW and TGW, HGW

In the Matsuzawa catchment, areas downslope of the SGW and TGW zones correspond to the riparian zone, because these zones are adjacent to the stream channel and have a gentle slope. They are clearly distinguished from the upslope regions.

The groundwater volume existing on the bedrock was calculated based on the intensive observations of groundwater levels in the lower part of the catchment. A 2-m mesh grid was superimposed on maps of the soil surface (Figure 2.4) and the bedrock surface (Figure 2.5) and groundwater levels for each grid cell were calculated by interpolating the observed groundwater levels. These were then multiplied by the area of a grid cell (4 m^2) and summed. Saturated soilwater content was uniformly assumed to 0.5.

Observations began in June 1996. Samples were collected biweekly (regular sampling) and during rainstorms (event sampling). The groundwater samples were taken from the cups immersed in the maximum rise well (Figure 2.13). Streamwater samples were collected regularly by manual sampling at point ST, and using two automatic samplers (American Sigma, USA, Model 900&702).

Spring water samples were collected manually at point SP.

Rainfall and throughfall were sampled using bottles with funnels 21 cm in diameter. The rainfall was collected at the meteorological station at the center of the Kiryu Experimental Watershed (Figure 2.2) and throughfall was collected at four points within the catchment (Figure 2.4). The concentrations of throughfall were estimated from the weighted mean values obtained at four points.

2.2.2 Akakabe Catchment

The locations of the observation facilities are shown in Figure 2.9. The runoff from the Akakabe catchment was measured using a 30° V-notch weir. Saturated throughflow occurring within the hillslope plot was directed from the trench to 200-cc capacity tipping buckets and samples were taken (hereafter, these samples are referred to as "trench water"). Automatic recording tensiometers were installed at point A1 in the soil sediment zone at a depth of 137 cm and at four points (A3-A6) in the hillslope plot at the soil-bedrock interface depth to measure groundwater levels. Observation wells were installed next to each tensiometer and samples of the groundwater were taken for chemical analysis. At the point A1, two wells were installed at different depths (110 cm and 175 cm).

2.2.3 Rachidani Catchment

The runoff from the catchment was measured using a 90° V-notch weir. Samples were collected during rainstorms. The groundwater was sampled by the same method as that used in the Matsuzawa catchment. Streamwater samples were collected at point W (Figure 2.11) using an automatic sampler (American Sigma, USA, Model 702). Rainfall was bottle-sampled using funnels 21 cm in diameter.

2.2.4 Toinotani Catchment

The outflow of Pipe A was directed to 500-cc capacity tipping buckets. Runoff from the catchment was measured using a 45° V-notch weir. The groundwater and soilwater samples were collected by using a tension lysimeter during rainfall. A silicon rubber tube was connected to a porous cup and water was extracted by suction using a hand pump when it reached the volume required for chemical analysis. Streamwater samples were collected at the weir (see Figure 2.12) using an automatic sampler (American Sigma, USA, Model 900). The throughfall samples were collected after rainfall by the same method as that used

in the Matsuzawa catchment.

2.3 Chemical Analysis

In situ measurements for each sample included pH using a glass electrode (TOA, Japan, HM-12P), electrical conductivity (HORIBA, Japan, ES-12), temperature, and partial pressure of dissolved CO_2. Dissolved pCO_2 was directly measured with a sensor (TOA, Japan, CE-331) (Ohte et al., 1995).

Samples were sealed in 50-ml polyethylene bottles and refrigerated until analyzed for inorganic solutes. The analyses for solute concentrations were carried out in a laboratory at Kyoto University. The samples were filtered through a 0.45-μm-pore cellulose acetate filter, and concentrations of major ions (Na^+, NH_4^+, K^+, Ca^{2+}, Mg^{2+}, Cl^-, NO_3^-, and SO_4^{2-}) were measured by ion chromatography (SHIMADZU, Japan, HIC-6A). HCO_3^- concentrations were calculated from pH and pCO_2 values (details described by Ohte et al., 1995). SiO_2 concentrations were measured using an inductively coupled plasma (ICP) emission spectrometer (SEIKO, Japan, SPS1500 VR).

Samples for organic carbon analysis were filtered through precombusted filters (Whatman GF/F), sealed in precombusted 30-ml glass vials, and frozen until analyzed. Dissolved organic carbon (DOC) concentrations were measured using a total organic carbon analyzer (SHIMADZU, Japan, TOC-5000). The three-dimensional fluorescence excitation-emission spectra of DOC were measured using a fluorescence spectrophotometer (HITACHI, Japan, F-4500). Fluorescence occurs when electrons within molecules that have previously been excited by a high-energy light source emit energy in the form of light. In three-dimensional fluorescence spectrometry, emission and excitation wavelengths are each scanned sequentially and fluorescence intensity is expressed as a contour graph, the excitation-emission matrix (EEM). Each dissolved organic substance has a characteristic EEM depending on the composition or structure of component groups of humic substances present.

The excitation wavelength was scanned from 225 nm to 400 nm at 5-nm intervals and the emission wavelength from 225 nm to 500 nm at 1-nm intervals at scan speeds of 1200 or 2400 nm/min. For each measurement, fluorescence was calibrated against a quinine sulfate unit (QSU) (*e.g.*, Mopper and Schultz, 1993; Suzuki et al., 1997). One QSU is the fluorescence intensity at excitation wavelength 345 nm and emission wavelength 450 nm of a solution of 1 μg/l quinine sulfate in 0.01N H_2SO_4.

References

Asano, Y., Ohte, N., Katsuyama, M. and Kobashi, S. (1998) Impacts of forest succession on the hydrogeochemistry of headwaters, Japan, *In* Headwaters: water resources and soil conservation (proceedings of Headwater '98, the fourth international conference on headwater control, Merano, Italy, April 1998), Haigh, M. J., Krecek, J., Rajwar, G. S., Kilmartin, M. P. (Eds.), A. A. Balkema Rotterdam, pp. 85-95.

Beven, K. J. and Kirkby, M. J. (1979) A physically-based variable contributing area model of basin hydrology, Hydrol. Sci. Bull., 24, pp. 43-69.

Beven, K. (1997) TOPMODEL: A critique, Hydrol. Process., 11, pp. 1069-1085.

Hobara, S., Tokuchi, N., Ohte, N., Nakanishi, A. Katsuyama, M. and Koba, K. (2001) Mechanism of nitrate loss from a forested catchment following a small-scale, natural disturbance, Can. J. For. Res., 31, pp. 1326-1335.

Kim, J. S. (1990) Variations of soil moisture and groundwater table in a small catchment, Ph. D. thesis, Kyoto Univ. Kyoto, Japan, 87pp.

Kimoto, A., Uchida, T., Asano, Y., Mizuyama, T. and Li, C. (1999) Surface runoff generation of devastated weathered granite mountains -Comparison between Dahou experimental basin in the southern part of China and Jakujo Rachidani experimental basin in Tanakami mountains-, J. Jpn. Soc. Erosion. Control. Engng., 51, pp. 13-19 (in Japanese with English summary).

Mopper, K. and Schultz, C. A. (1993) Fluorescence as a possible tool for studying the nature and water column distribution of DOC components, Mar. Chem., 41, pp. 229-238.

Nakashima, T. and Fukushima, Y. (1994) Characteristics of streamflow at two source watersheds of the Yura River in highland area of Kyoto University Forest in Ashiu, Bull. Kyoto Univ. For., 66, pp. 61-75 (in Japanese with English summary).

Ohte, N., Tokuchi, N. and Suzuki, M. (1995) Biogeochemical influences on the determination of water chemistry in a temperate forest basin: Factors determining the pH value, Water Resour. Res., 31, pp. 2823-2834.

Ohte, N., Tokuchi, N. and Suzuki, M. (1997) An in situ lysimeter experiment on soil moisture influence on inorganic nitrogen discharge from forest soil, J. Hydrol., 195, pp. 78-98.

Quinn, P. F., Beven, K. J. and Lamb, R. (1995) The $\ln(\alpha/\tan\beta)$ index: How to calculate it and how to use it within the TOPMODEL framework, Hydrol. Process., 9, pp. 161-182.

Suzuki, Y., Nagao, S., Nakaguchi, Y., Matsunaga, T., Muraoka, S. and Hiraki, K. (1997) Spectroscopic properties of fluorescent substances in natural waters (1), Geochemistry, 31, pp. 171-180 (in Japanese with English summary).

Uchida, T. (2000) Effects of pipeflow on storm runoff generation processes at forested headwater catchments, Ph. D. thesis, Kyoto Univ. Kyoto, Japan, 119pp.

Chapter 3
Groundwater Dynamics and Hydrological Pathways

3.1 Introduction

This chapter discusses the hydrological pathways within the catchments, as determined by the results of intensive hydrometric observations. Based on the groundwater dynamics observed in the Matsuzawa and Akakabe catchments, the hydrological processes from the rainfall to the stream have been deduced. The differences between the hydrological processes occurring in the two catchments, and the reasons for these differences, are also discussed.

3.2 Groundwater Dynamics in Akakabe Catchment

Figure 3.1 shows the direct runoff ratios in the Akakabe catchment and in the hillslope plot. In this study, the total runoff from the hillslope plot is regarded as direct runoff, because it is generated only during rain. The direct runoff rates were calculated following the method of Hewllet and Hibbert (1967); this method has also been used in other studies (*e.g.*, Harr,1977; Tsujimura et al., 2001). A line is projected from the beginning of any stream rise at a slope of 0.55 l/s/km^2/hr (0.0019 mm/hr/hr) to its intersection with the falling limb of the hydrograph. This line was determined after examining many hydrographs from about 200 water-years of collected records for fifteen small forested catchments.

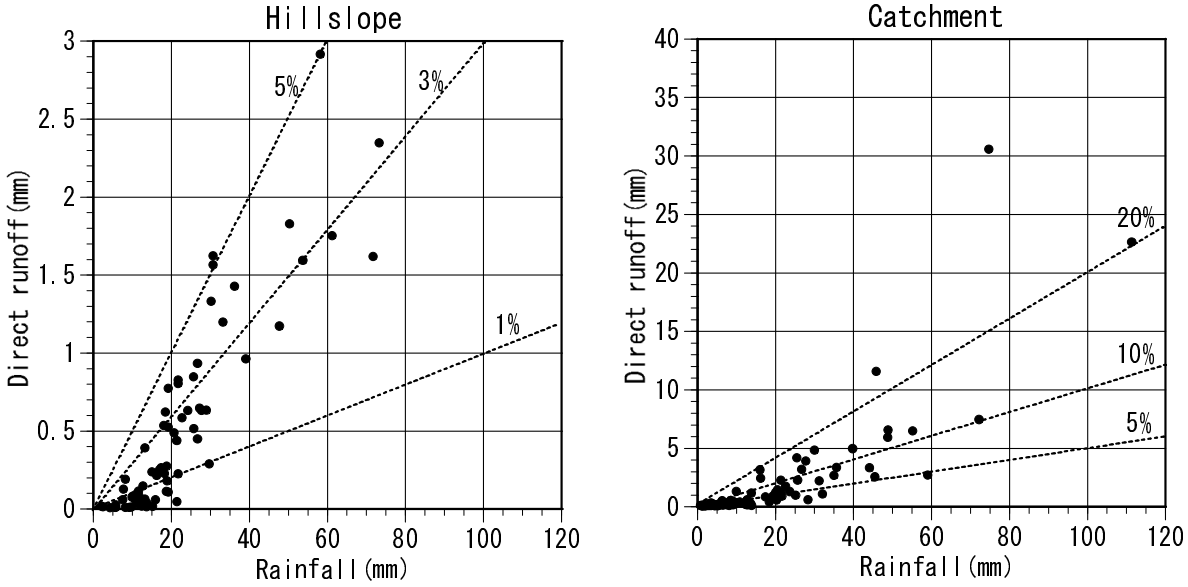

Figure 3.1 Direct runoff ratios in the Akakabe catchment and in the hillslope plot

Runoff was generated from the hillslope plot even when the total rainfall was less than 10 mm. However, the direct runoff ratio was low, at less than 1%, when the total rainfall was less than 20 mm, about 3% when the total rainfall was more than 20 mm, and only rarely exceeded 5%. The direct-runoff ratio of the whole catchment was about 5% when total rainfall was less than 20 mm and increased with increasing total rainfall to a maximum of about 20%.

Histograms of the frequency of occurrence of saturated throughflow to the rainfall at each point within the hillslope plot are presented in Figure 3.2. Saturated throughflow was more frequent from small rainstorms at the lower slope points. The occurrence frequency of the trench water was similar to that at A3, located at the foot of the hillslope. In Figure 3.3, the relationship between the maximum groundwater levels at each point and the total discharge rate from the hillslope are shown. A clear correlation appears for site A3, and discharge from the hillslope was not observed when saturated throughflow did not occur at A3. On the other hand, no clear correlation is apparent at A4 and A6, so it can be deduced that the discharge from the hillslope was mainly composed of saturated throughflow occurring at A3.

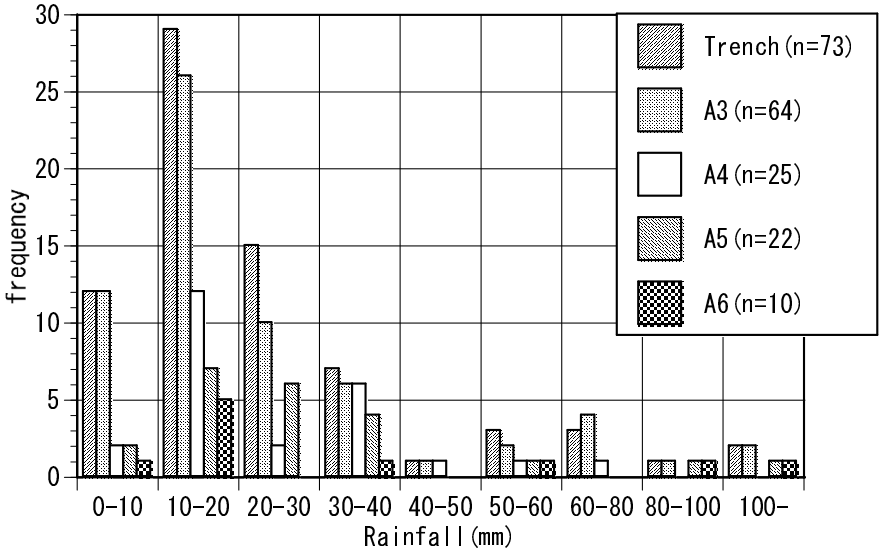

Figure 3.2 Histograms of the frequency of the saturated throughflow occurrence to the rainfall in each point within the hillslope plot

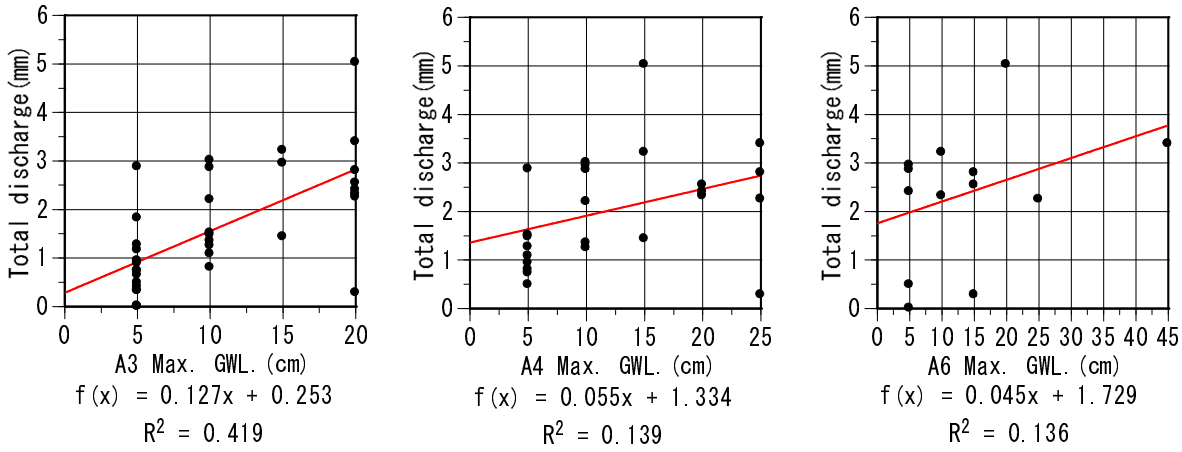

Figure 3.3 Relationship between the maximum groundwater levels of each point and the total discharge rate from the hillslope

As shown in Figure 3.1, the direct-runoff ratio in the hillslope plot was less than 5% of the total rainfall. Thus, 95% of the total rainfall was distributed between evapotranspiration and deep seepage, based on the water budget within the hillslope. Akakabe (1999) estimated evapotranspiration from the assumed soil column within the hillslope plot based on the water budget, and found a good fit to the estimated evapotranspiration in the Kiryu Experimental Watershed derived by Suzuki et al. (1980) by the method of short-term water budget estimation. Akakabe et al. (1999) also reported a strong positive correlation between the mean soil-water content and deep seepage within the hillslope. Terajima et al. (1993) estimated the deep-seepage water from the water budget in granitic catchments, and the deep-seepage water ratio to rainfall was higher in smaller headwater catchments. More than 30% of the rainfall was deep seepage in a 0.87-ha catchment. These facts imply that deep seepage is an important component of the water budget within a hillslope, especially in the middle or upper hillslope regions where water made little contribution to discharge through the trench. The annual mean evapotranspiration (the difference of the total rainfall and the total discharge rate) in the Kiryu Experimental Watershed averaged about 46% of the annual rainfall from 1972 to 2001. Thus, deep seepage in the hillslope is estimated as about 50% of the total rainfall.

The rainfall, discharge rates from the catchment and the hillslope plot, and the groundwater level at A1 during two rainstorms are presented in Figure 3.4. The total rainfalls in (a) and (b) were 75.67 mm and 55.47 mm, respectively. Runoff from the hillslope was maintained during each rainstorm but ceased soon after the

rainfall stopped. The peak of the A1 groundwater level in the soil sedimentation area was delayed by a few hours from the peak discharge from the hillslope. This means that the groundwater in the soil sedimentation area was recharged not only by the saturated throughflow occurring on the soil-bedrock interface but also by another component with lower velocity. Bedrock flow, derived from deep seepage flowing down through the bedrock, can be identified as this lower velocity component. The peak discharge rate in the catchment preceded the groundwater peak, so some component of runoff that did not pass through the soil sedimentation area, such as channel precipitation, may have contributed to the peak discharge. In addition, the annual discharge rate from the Akakabe catchment was similar to that of the Kiryu Experimental Watershed, where deep seepage must be relatively small because of the large watershed area (Table 2.1). Therefore, baseflow from the Akakabe catchment may be sustained by bedrock groundwater in addition to groundwater in the soil sedimentation area.

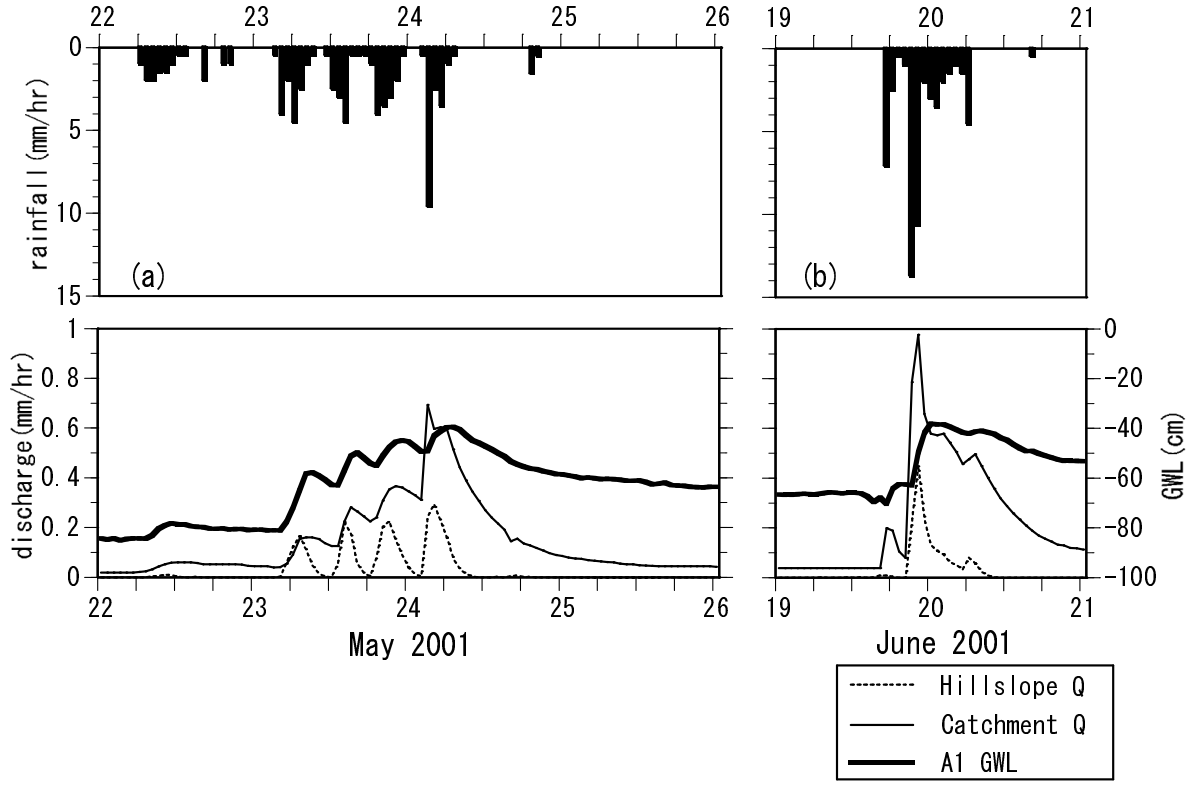

Figure 3.4 Rainfall, discharge rates from the catchment and the hillslope plot, and the groundwater level at A1 during two rainstorms in the Akakabe catchment

3.3 Groundwater Dynamics in the Matsuzawa Catchment

The direct runoff ratio in the Matsuzawa catchment is shown in Figure 3.5. The ratios were calculated following the method of Hewllet and Hibbert (1967), as in the Akakabe catchment. The overall direct-runoff ratio is about 5% to the total rainfall, and smaller than that in the Akakabe catchment.

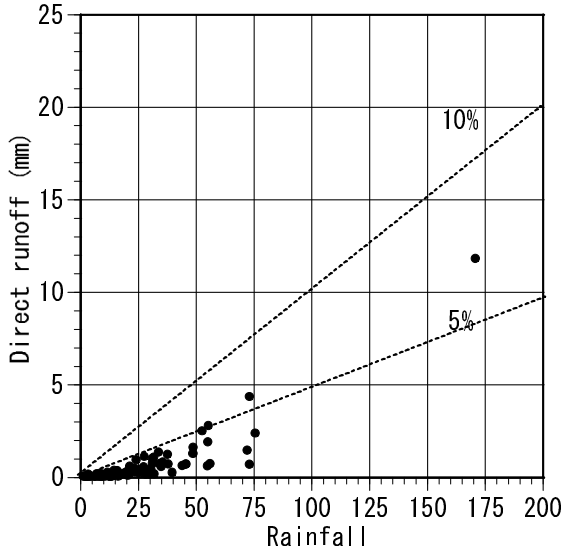

Figure 3.5 Direct runoff ratio in the Matsuzawa catchment

The variations of the groundwater levels (or hydraulic potentials) along the cross and longitudinal sections and the hydraulic gradient during rainstorms are shown in Figure 3.6 (a-h) and Figure 3.7, respectively. The total rainfall was 165.58 mm and the total discharge was 27.40 mm during the period of observation. The four observed sections are the two longitudinal sections, line SP-G1-GE-GF in SGW and line SP-GA-GB-GC-GD in TGW; and the cross sections, lines G10-GB-GH-GE and G11-GC-GF across the HGW-TGW-SGW regions. The hydraulic gradient in the downward direction is defined as positive in this study. No antecedent rainfall was recorded during the ten days prior to each event. The peak discharge rate occurred at the same time as the peak rainfall was recorded, but the peak groundwater volume was delayed by a few hours.

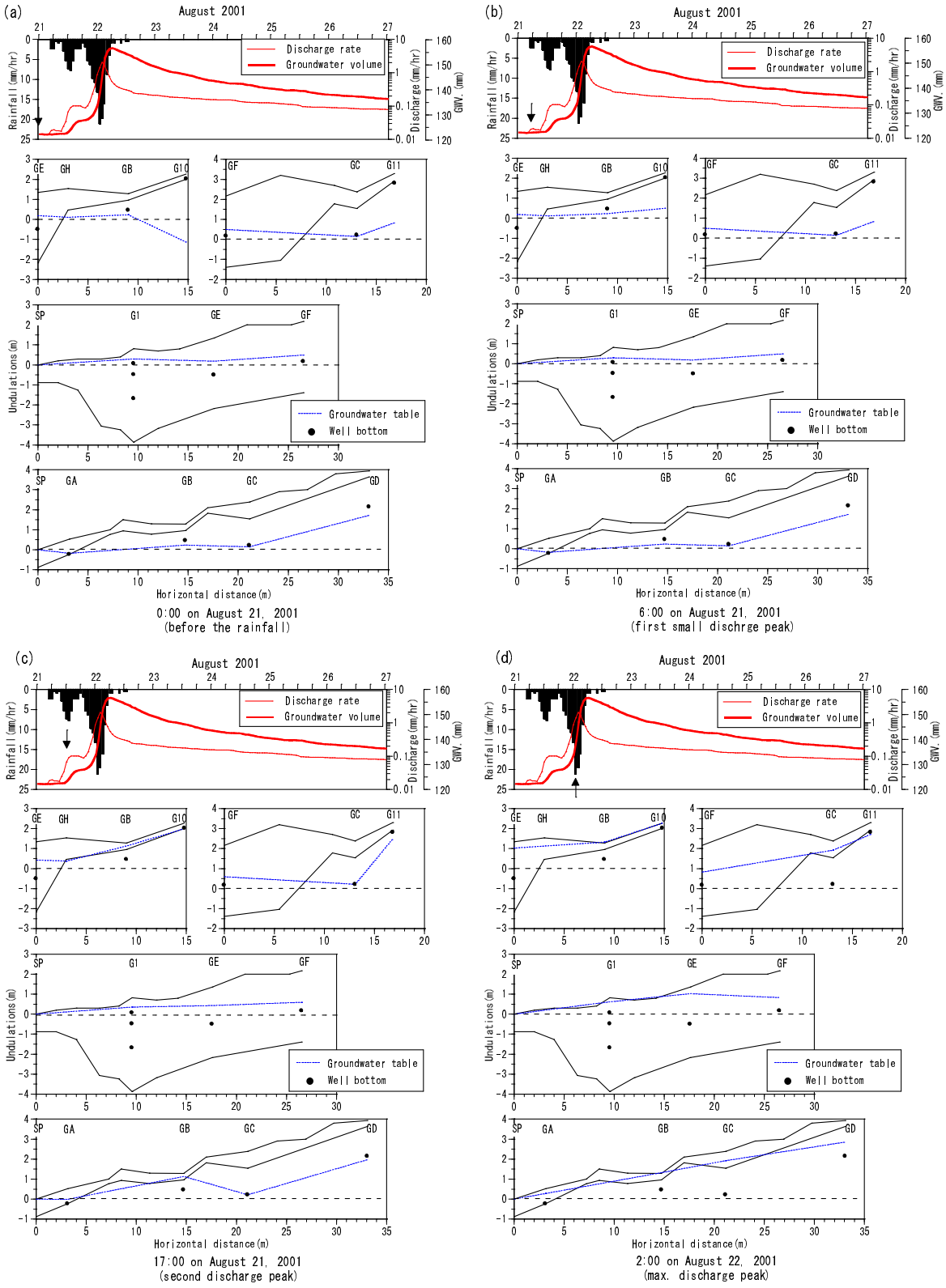

Figure 3.6 Temporal variations of the groundwater levels along the cross and longitudinal sections during the rainstorms

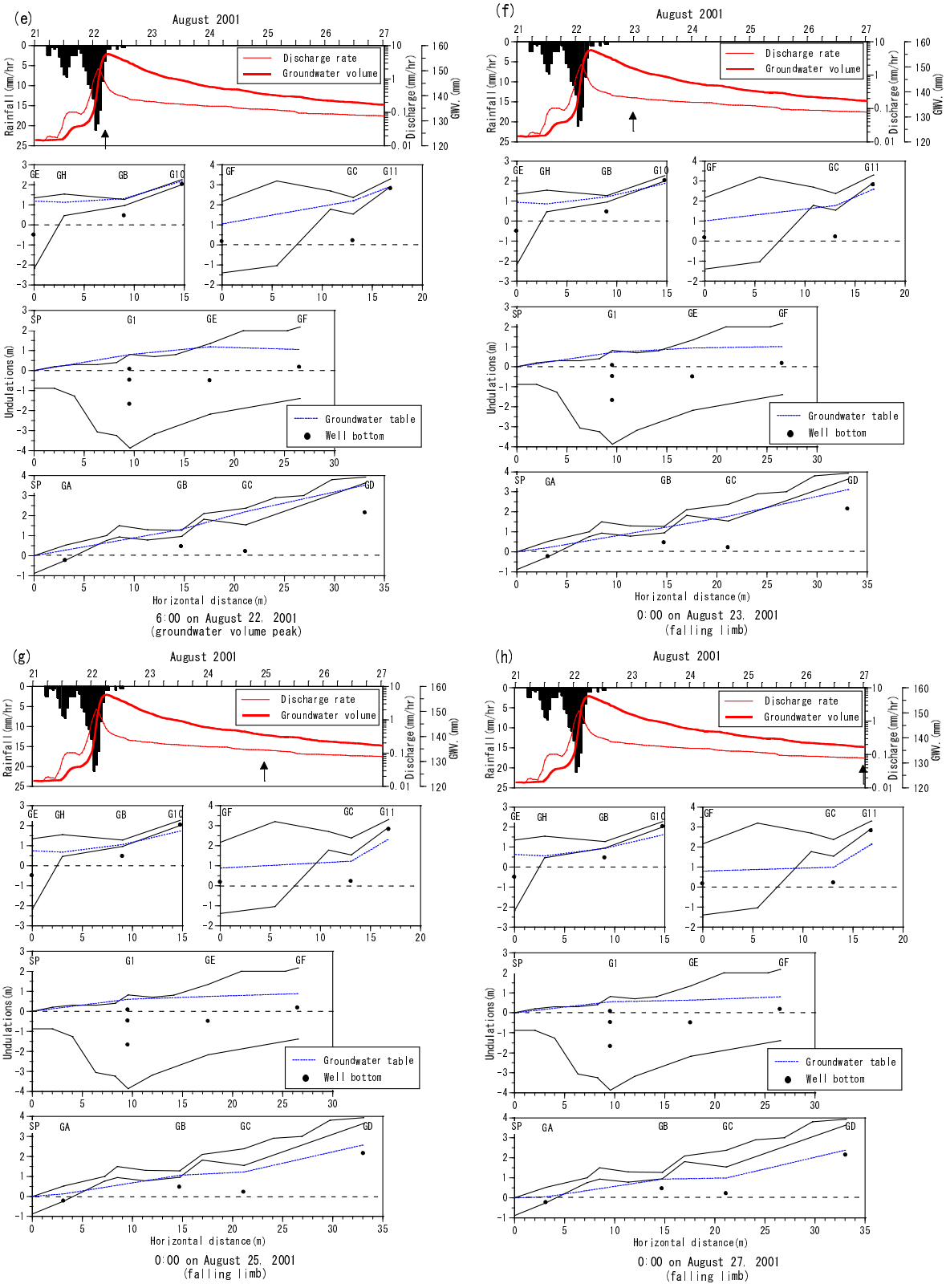

Figure 3.6 (Continued)

Comparing the soil-surface and bedrock topography in each section, the soil is shallow and the bedrock surface is parallel to the soil surface in HGW and TGW. In SGW the soil is deep, and a large depression of the bedrock exists around the spring outflow point (SP). Before rainfall (a), a positive hydraulic gradient was observed only from G1 to SP within SGW. The hydraulic gradient was negative from GA, at the nearest observed point to SP. Therefore, the discharge rate during the dryer conditions was maintained by groundwater flow from SGW around SP. When rainfall started (b), the hydraulic potential in HGW responded in a short time only at G10. Saturated throughflow occurred from G10 in HGW toward GB in TGW, and the groundwater level at GB rose sharply as the rainfall continued (c). Comparing the hydraulic responses to the rainfall between G10 and G11 in HGW, or GB and GC in TGW, the groundwater level rose faster at G10 and GB, the nearer points to SP.

When the discharge rate was maximum (d), the groundwater levels around GB in TGW or GE in SGW rose, and the hydraulic gradient from GH in TGW to GE in SGW reached its maximum; SGW had been recharged near the soil surface. In addition, the groundwater level at GC was raised by the occurrence of saturated throughflow from G11 in HGW to GC in TGW, and the water moved toward GF in SGW. The groundwater level at GE in SGW approached the soil surface and a positive hydraulic gradient from GE toward SP was observed. However, the hydraulic gradient from GF to GE was negative at this time. This phenomenon is called "groundwater ridging" (Novakowski and Gillham, 1988; Sklash, 1990) and, according to Kim (1990), is important to the runoff generation processes in this catchment. Furthermore, the hydraulic gradient from GA to SP changed to positive at this time, meaning that the area contributing to the discharge broadened out.

When the groundwater volume reached its maximum (e), the groundwater levels in upslope SGW and TGW rose, and during the falling limbs (f, g, h), the groundwater levels in SGW, particularly in the upslope SGW, continued at a high level, though the groundwater levels in TGW had declined earlier. This implies that groundwater in the soil above the bedrock in TGW flowed down to SGW through the surface soil with high transmissivity. The discharge rate at the falling limb was maintained by groundwater flow from the upslope SGW region.

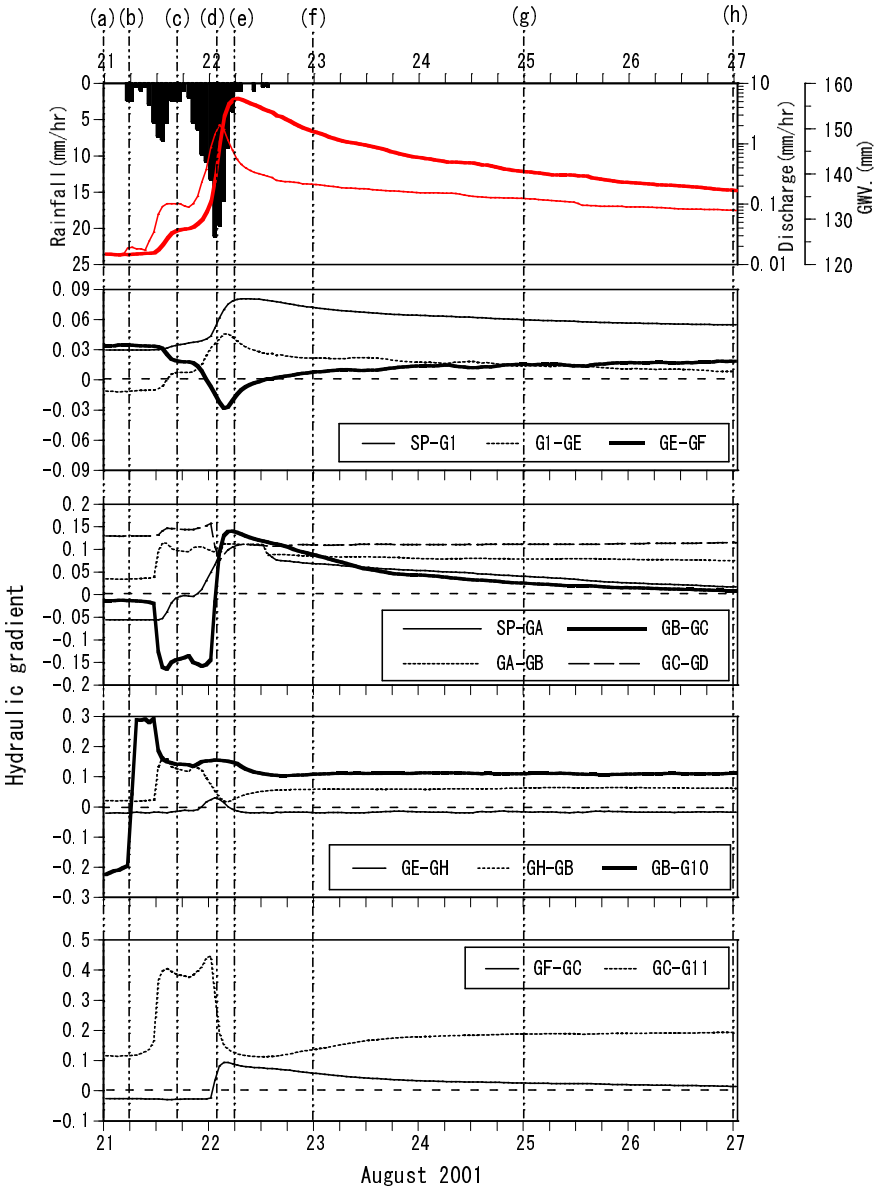

Figure 3.7 Temporal variations of the hydraulic gradient during the rainstorms

3.4 Groundwater Dynamics within the Bedrock

The relationship between the N_4 value and the saturated hydraulic conductivity is shown in Figure 3.8. The soil samples were taken within the Matsuzawa catchment with 100-cc core samplers. Samples were divided into five classes by their N_4 values, 0–20, 20–40, 40–60, 60–80, and over 80; four soil cores were sampled in each class. As the N_4 value increased (that is, as the soil became harder), the saturated hydraulic conductivity decreased. Even in the highest class, with N_4 over 80, (which can be considered as nearly corresponding to bedrock), the

hydraulic conductivity was of the order of 10^{-3} or 10^{-4}; thus, the bedrock is not impermeable. The observation wells in TGW were drilled into the bedrock, and groundwater was sampled even during the dry season (mainly winter in this region) (Table 2.2). As shown in Figure 2.7, the Matsuzawa catchment is covered by shallow soil, except in the central part, and 62.4% of the catchment area has a soil depth of less than 1 m. As the Matsuzawa and Akakabe catchments adjoin each other and have the same bedrock material, deep seepage must contribute significantly to the water budget within the hillslope of the Matsuzawa catchment, as in the Akakabe catchment (Paragraph 3.1). Therefore, groundwater present within the bedrock of TGW must be derived mainly from deep seepage water from HGW in the Matsuzawa catchment. The bedrock water in TGW must move within the bedrock and recharge the deep layer of SGW.

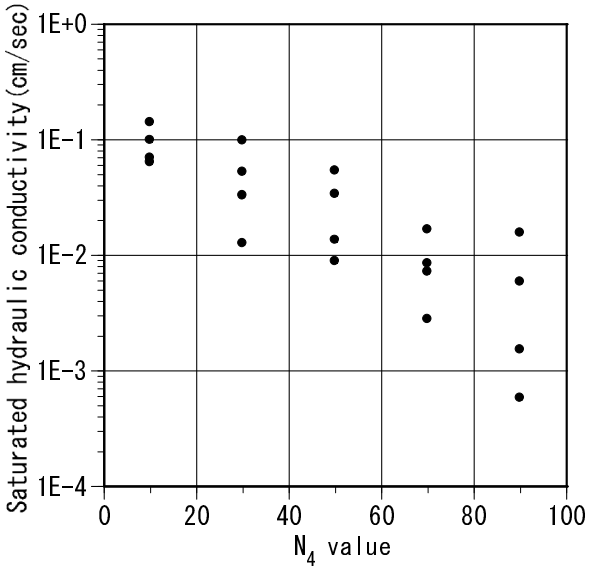

Figure 3.8 Relationship of the N_4 value and saturated hydraulic conductivity

As shown in Table 2.1, the annual discharge from the Matsuzawa catchment was small compared to those of the Kiryu and Akakabe catchments. The hydrographs in Kiryu, Matsuzawa, and Akakabe catchments in the year 2000 are presented in Figure 3.9. The baseflow in the Matsuzawa catchment was smaller than that in the Kiryu Experimental Watershed. The groundwater volume in the Matsuzawa catchment varied little during the year (for example, it was 118.5 mm at January 1 2000 and 121.7 mm at December 31 2000); thus, the variations of groundwater storage were probably small. These facts mean that significant amounts of deep-seepage water, or groundwater present in the deeper layers of soil in SGW, may bypass the gauging weir in the Matsuzawa catchment.

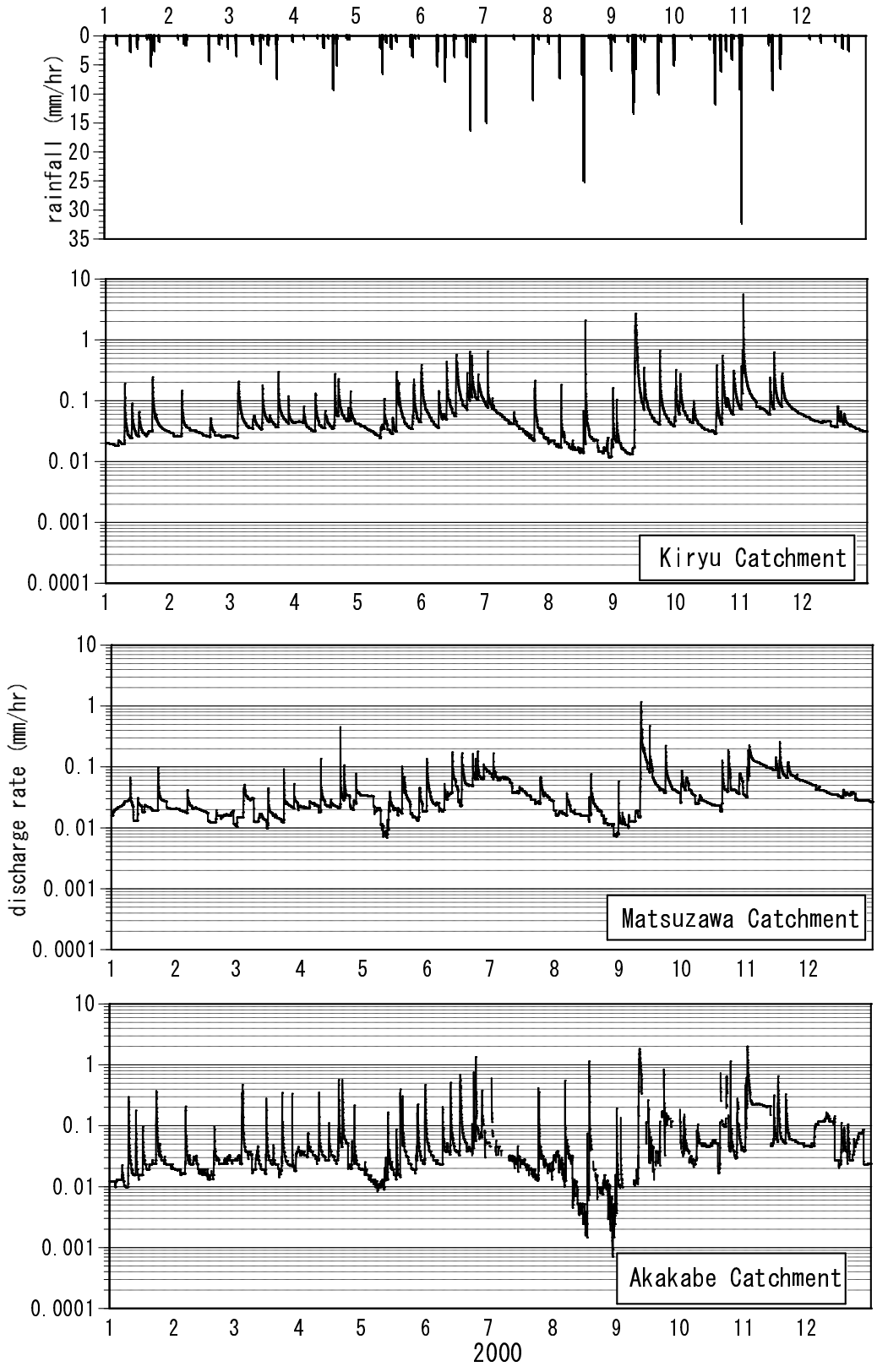

Figure 3.9 Hydrographs in the Kiryu, Matsuzawa, and Akakabe catchments in the year 2000

3.5 Differences in the Hydrological Pathways in the Matsuzawa and Akakabe Catchments

Comparing the annual hydrographs of the Akakabe and Matsuzawa catchments (Figure 3.9) shows that variations in the discharge rate were smaller in the Matsuzawa catchment. In the Akakabe catchment, the discharge rate varied considerably, particularly the noticeable decrease in Aug 2000. These differences must be caused by differences in groundwater storage or the volume of groundwater present. In the Matsuzawa catchment, deep soils are present in the depression of the bedrock, and a large volume of groundwater accumulates there. In contrast, in the Akakabe catchment the area of the soil sedimentation zone is small; thus, the groundwater storage is small. The large volume of groundwater in the Matsuzawa catchment acts as a buffer and maintains a stable discharge rate during the dry season or rainstorms. The differences in the direct-runoff ratio in the two catchments (Figures 3.1, 3.5) are caused by the differences in groundwater storage.

The schematic diagrams of the hydrologic pathways in the Matsuzawa and Akakabe catchments are presented in Figure 3.10. In the Matsuzawa catchment, TGW is formed at the interface of HGW with shallow soil and a high gradient, and SGW with deep soil and a low gradient. The water is divided into two components at the hillslope (HGW), the largest part of the catchment: saturated throughflow generated on the soil-bedrock interface, and bedrock flow derived from deep seepage. These components flow down on the soil-bedrock interface and within the bedrock of TGW, and recharge the shallow layer and deep layer of SGW, respectively. In SGW, little of the groundwater in the deep layer can discharge from the spring outflow because of the depression of the bedrock. The discharge from TGW contributes to the stormflow. In the Akakabe catchment, part of the bedrock flow recharges SGW and the other part contributes directly to the streamwater. These differences result from variations in the bedrock topography of the catchments.

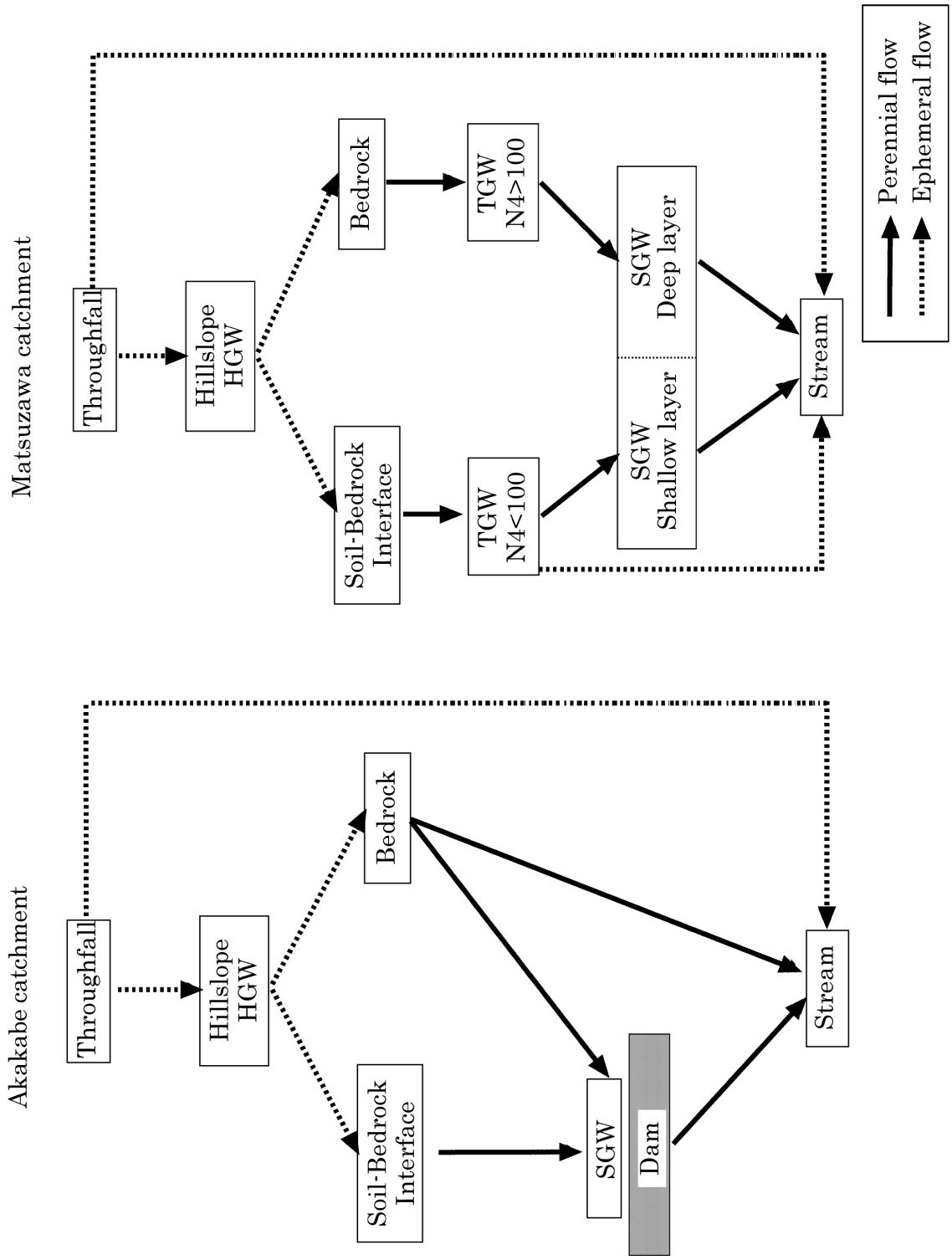

Figure 3.10 Schematic Diagram of Hydrological Pathways in the Matsuzawa and Akakabe catchment

3.6 Conclusions

The importance of bedrock flow to runoff generation processes in mountainous catchments has been pointed out in recent reports (*e.g.*, Montgomery et al., 1997; Onda et al., 2001). The existence of hydrological pathways through the bedrock in was also shown in the two catchments studied. However, the roles of these pathways in the hydrological processes in these two catchments differ, because the bedrock topography and the configurations of groundwater storage are different. These differences in the hydrological processes impact on hydrochemical processes in the groundwater and streamwater, as is discussed in the following chapters.

References

Akakabe, T. (1999) Estimation of Evaporation from forest catchment based on the measured soil water content, the Master's thesis, Kyoto Univ. Kyoto, Japan, 26pp. (in Japanese)

Harr, R. D. (1977) Water flux in soil and subsoil on a steep forested slope, J. Hydrol., 33, pp. 37-58.

Hewlett, J. D. and Hibbert, A. R. (1967) Factors affecting the response of small watersheds to precipitation in humid areas, Sopper, W. E. and Lull, H. W. (eds.), International Symposium on Forest Hydrology, Pergamon Press, Oxford, pp. 275-290.

Kim, J. S. (1990) Variations of soil moisture and groundwater table in a small catchment, Ph. D. thesis, Kyoto Univ. Kyoto, Japan, 87pp.

Montgomery, D. R., Dietrich, W. E., Torres, R., Anderson, S. P., Heffner, J. T. and Loague, K. (1997) Hydrologic response of a steep, unchanneled valley to natural and applied rainfall, Water Resour. Res., 33, pp. 91-109.

Novakouski, K. S. and Gillham, R. W. (1988) Field investigations of the nature of water-table response to precipitation in shallow water-table environments, J. Hydrol., 97, pp. 23-32.

Onda, Y., Komatsu, Y., Tsujimura, M. and Fujihara, J. (2001) The role of subsurface runoff through bedrock on storm flow generation, Hydrol. Process., 15, pp. 1693-1706.

Sklash, M. G. (1990) Environmental isotope studies of storm and snowmelt runoff generation, Anderson, M. G. and Burt, T. P. (eds.), Process studies in hillslope hydrology, John Wiley and Sons, Chichester, pp. 401-436.

Suzuki, M. (1980) Evapotranspiration from a small catchment in hilly mountains (I) Seasonal variations in evapotranspiration, rainfall interception and transpiration, J. Jap. For. Soc., 62, pp. 46-53.

Terajima, T., Mori, A. and Ishii, H. (1993) Comparative study of deep percolation amount in two small catchments in granitic mountain, J. Jpn. Assoc. Hydrol. Sci., 23, pp. 105-118. (in Japanese with English summary)

Tsujimura, M., Onda, Y., Komatsu, Y., Shimizu, T., Matsumura, K., Nakagawa, Y. and Matsui, T. (2001) Runoff and chemical characteristics in stream water of hilly headwater basins underlain by gravel and weathered granite, J. Japan Soc. Hydrol & Water Resour., 14, pp. 229-238. (in Japanese with English summary)

Chapter 4
Geographic Sources of Streamwater and Their Hydrochemistry

4.1 Introduction

Several studies have employed three-component mixing models to describe catchment runoff (DeWalle et al., 1988; Bazemore et al., 1994; Rice and Hornberger, 1998), emphasizing the importance of geographic source distributions (Christophersen et al., 1990; Hooper et al., 1990; Ogunkoya and Jenkins, 1993). However, the geographic extent of each contributing end-member; that is, the linkage between the hillslope and riparian zones, is not well understood (Hooper et al., 1998).

In this chapter, the spatial distributions of the chemistries of the rainfall, throughfall, groundwater, spring water, and streamwater are presented, and their determining factors are discussed. Using the spatial distributions of solutes and the hydrological pathways described in **Chapter 3**, the geographic source chemistry of the streamwater is also discussed.

4.2 Spatial Variability of Groundwater Chemistry

The solute concentrations (SiO_2, Na^+, NH_4^+, K^+, Ca^{2+}, Mg^{2+}, Cl^-, NO_3^-, SO_4^{2-}, HCO_3^- and DOC) in the rainfall, throughfall, groundwater, spring water, and streamwater in the Matsuzawa and Akakabe catchments and in the streamwater sampled at the gauging weir in the Kiryu Experimental Watershed (Figure 2.2) are shown in Figure 4.1. Throughfall was not sampled in the Akakabe catchment, but the throughfall concentrations in the Matsuzawa catchment, sampled at the same time as the other parameters, are shown in Figure 4.1.

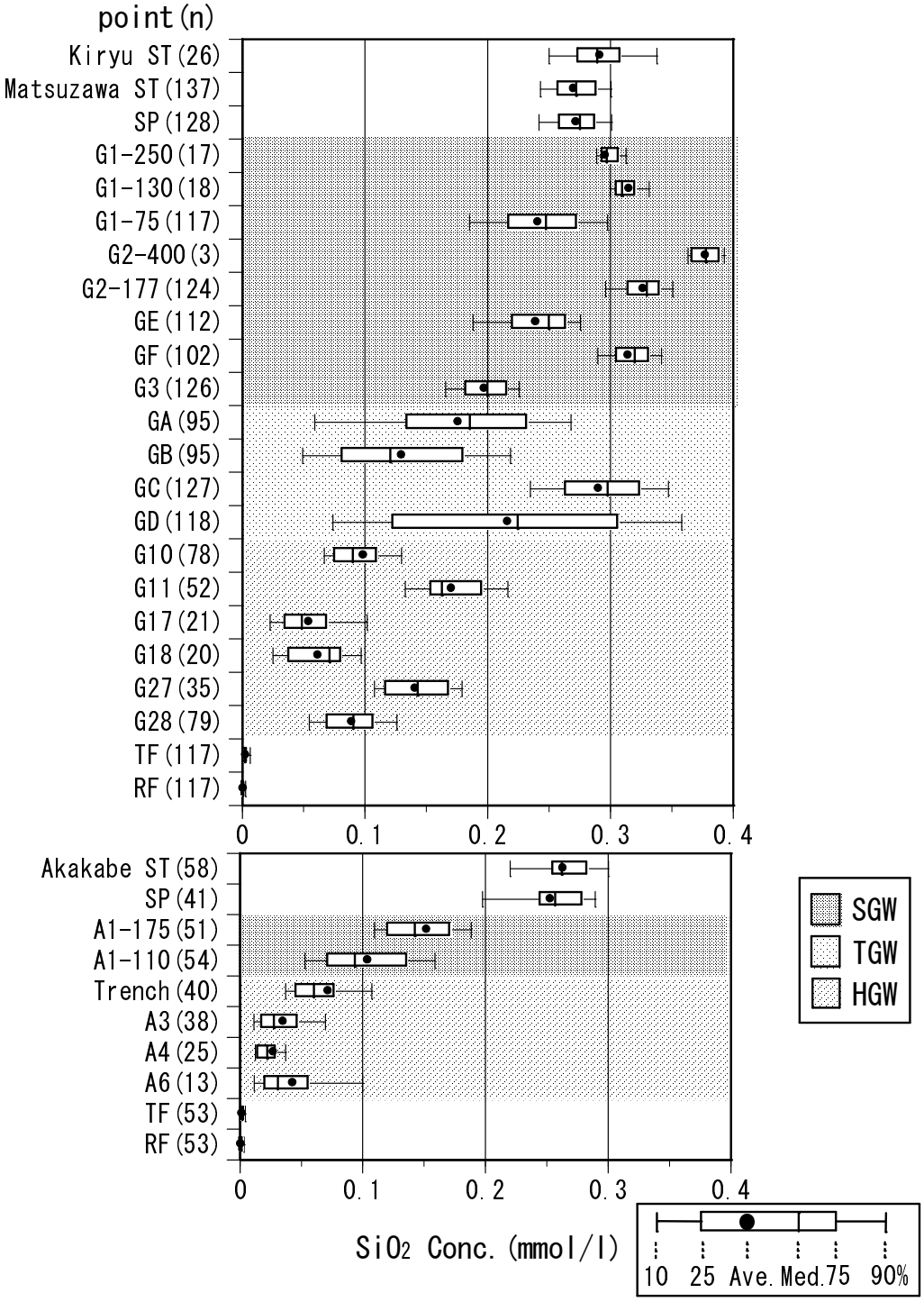

Figure 4.1 Solute concentrations of Rainfall, Throughfall, Groundwater, Spring water and Streamwater

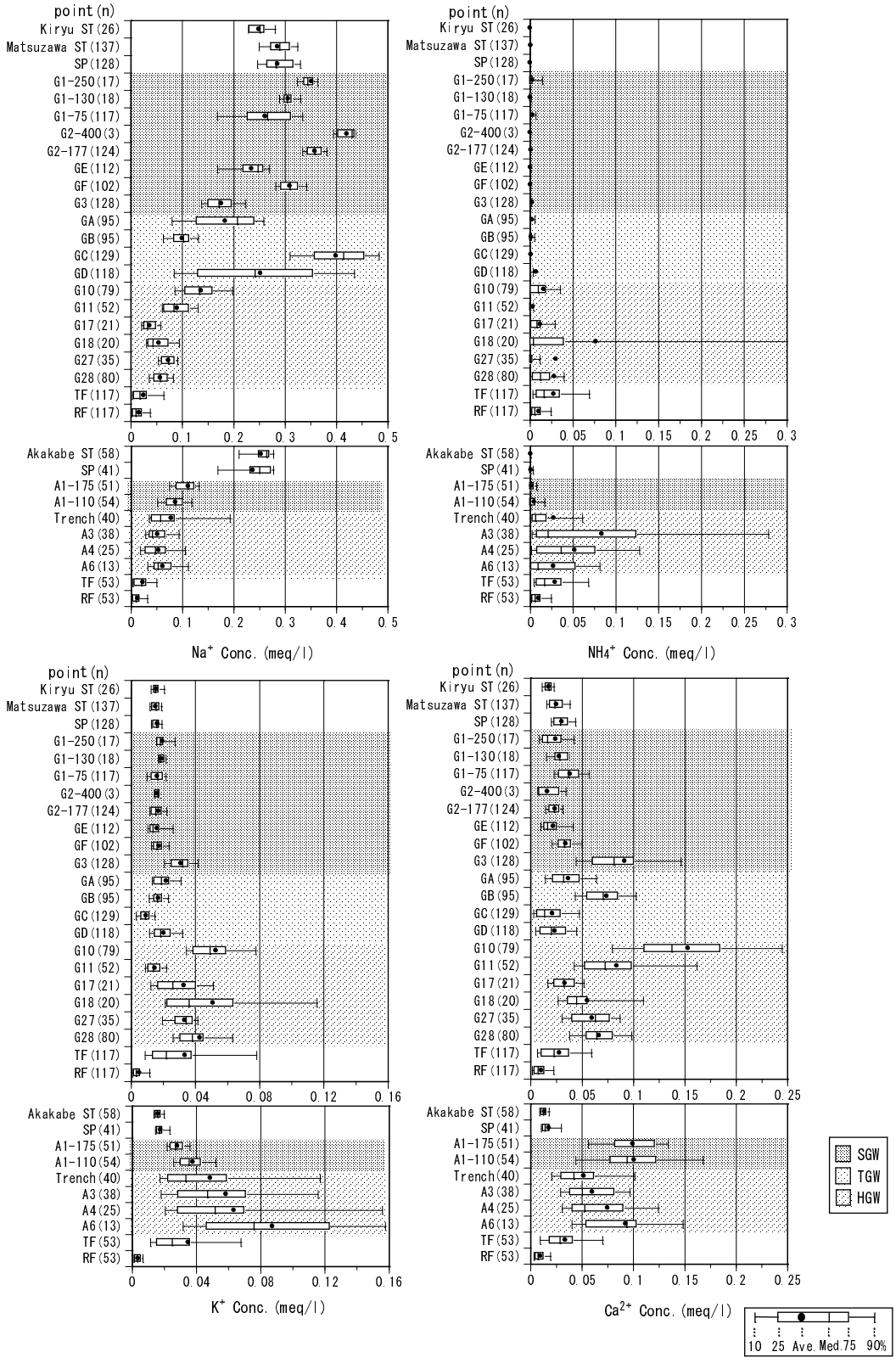

Figure 4.1 (Continued)

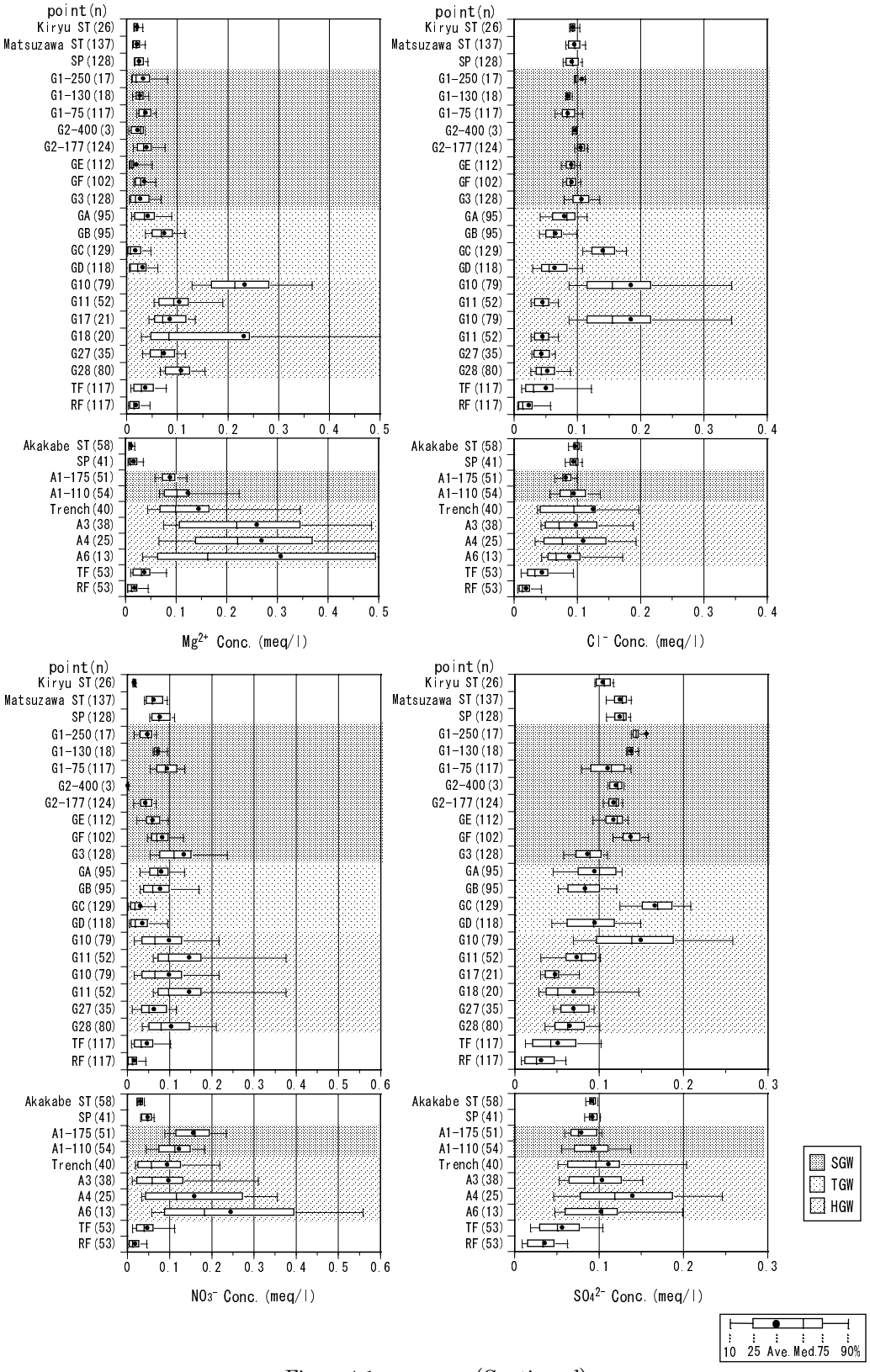

Figure4.1 (Continued)

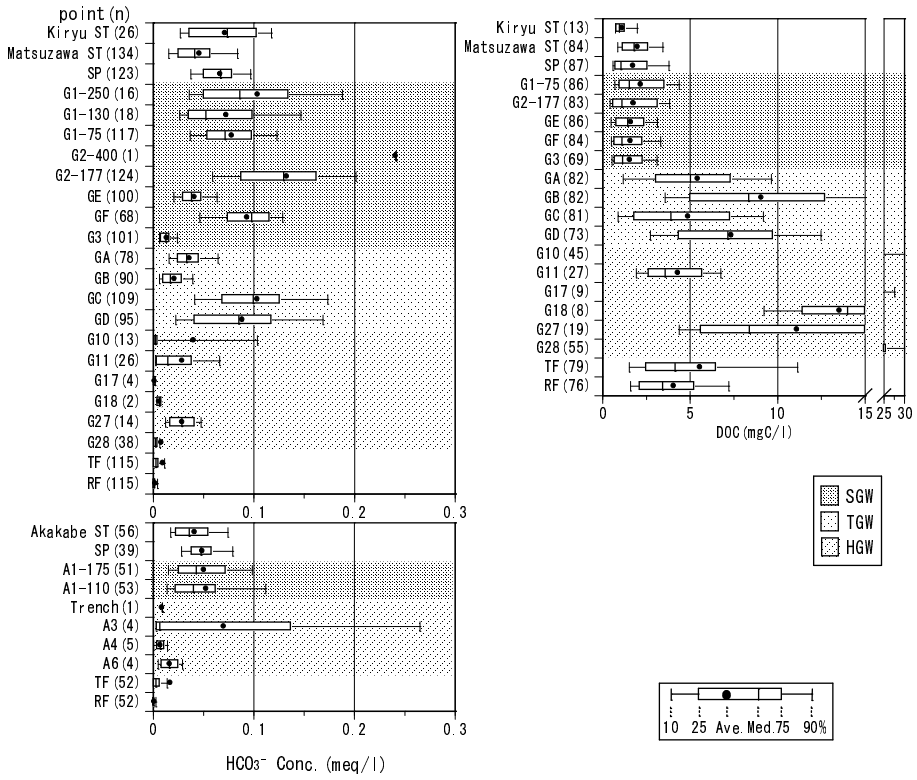

Figure4.1 (Continued)

Two patterns of concentration variations were recognized in the Akakabe catchment, depending on the group of chemical species involved. Both groups exhibited low concentrations in rainfall and throughfall, but the first group (SiO_2, Na^+, Cl^-, SO_4^{2-}, and HCO_3^-) showed higher concentrations in the processes involving lateral water flow, throughflow and streamflow, while the highest concentrations of the second group (NH_4^+, K^+, Ca^{2+}, Mg^{2+}, and NO_3^-) were in the hillslope zone, with lower levels in the flowing-water processes. These patterns were similar to those in the Matsuzawa catchment (Ohte et al., 1991; Shimada et al., 1993); however, the variations within and between sampling points were smaller in the Akakabe catchment. This chapter focuses on identifying the potential contributing sources (end-members) and their chemistry, and the spatial distributions of concentrations of SiO_2, which is commonly used as a tracer to separate runoff components. SiO_2 is the chemical species most directly related to weathering reactions. It is not a significant component of precipitation, is not significantly affected by nutrient cycling in vegetation, and is only weakly affected by ion-exchange processes (White, 1995). Concentrations of SiO_2 generally increase with depth (*e.g.*, Rice and Hornberger, 1998; Stonestrom et al., 1998), and are generally higher in bedrock

flow than in saturated throughflow at the soil-bedrock interface (Peters et al., 1998; McGlynn et al., 1999; Uchida et al., 2001).

As discussed in **Chapter 3**, throughfall was divided into two components within the hillslope: saturated throughflow generated at the soil-bedrock interface and bedrock flow derived from deep seepage. Lower SiO_2 concentrations were observed at the HGW zone (A6, A4, A3, and trench water in the Akakabe catchment and G28, G27, G18, G17, G11, and G10 in the Matsuzawa catchment), where the saturated throughflow was sampled during rainstorms, although there was considerable variability among hillslopes in the Matsuzawa catchment. In the TGW zone of the Matsuzawa catchment, the SiO_2 concentrations varied greatly between and within the sampling points, and lower concentrations were observed in GA and GB, located at the downslope. Lower concentrations were observed at G1-75 and GE in SGW, relative to the other points in SGW of the Matsuzawa catchment. Vertical distributions in concentrations at the same point were observed in the riparian zone; G1-75 (75 cm in depth) had lower concentrations than G1-130 (130 cm), G1-250 (250 cm), and G2-177 (177 cm, nearby G1). Additionally, the highest concentrations were observed at G2-400, which is the deepest point around the spring, although the number of samples was small because of the short observation period. Thus, there were vertical distributions in SiO_2 concentrations and some concentration layers had formed within the riparian SGW. Concentrations in the spring water and the streamwater were similar, and within the range of variation in SGW, intermediate between the SGW shallow layer (G1-75) and SGW deep layer (G2-177). The streamwater concentrations were similar in the Matsuzawa and the Akakabe catchments and slightly higher at the outlet of the Kiryu Experimental Watershed.

4.3 Hydrochemical Processes of Groundwater

In Figure 4.2 (a) and (b), the relationship of the maximum groundwater levels and the SiO_2 concentrations in the regular sampling program at GA and GC in TGW are shown, with the depth to bedrock ($N_4 = 100$). Results were classified depending on whether saturated throughflow occurred at G11 in HGW, where it flows into GC in Figure 4.2 (b). The observation well at GA was installed to a depth of 76 cm, close to the bedrock depth (74 cm). The SiO_2 concentrations decreased with rising groundwater levels at this point. On the other hand, the observation well at GC was installed to a depth of 217 cm, much deeper than the bedrock (82 cm). Thus, as discussed in **Chapter 3**, it can be considered that bedrock

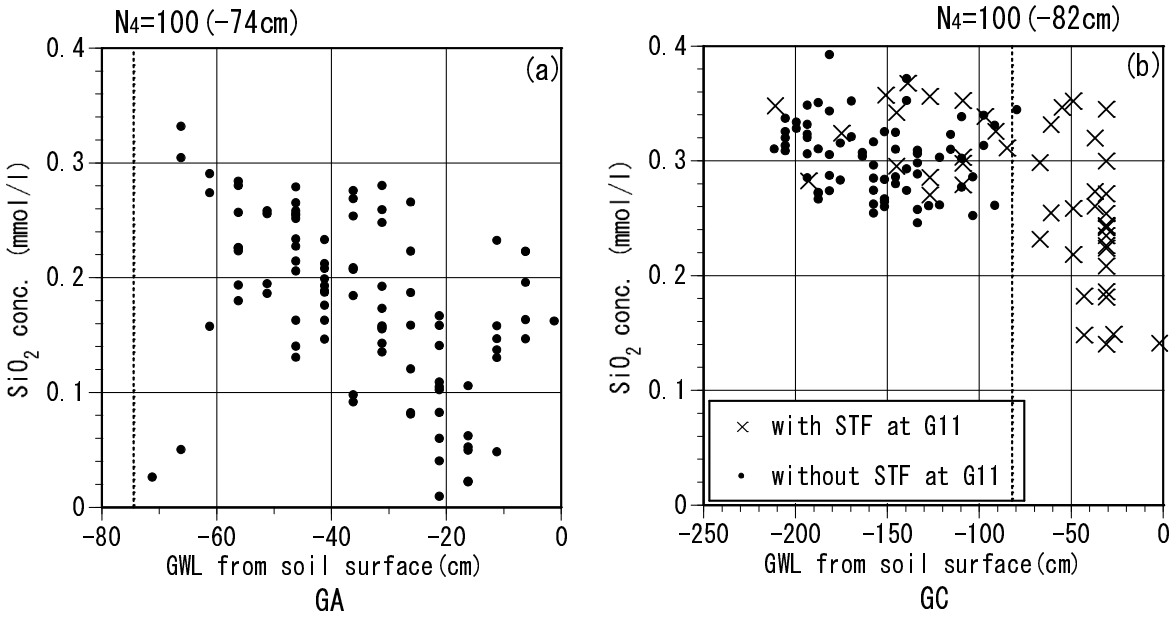

Figure 4.2 Relationship of groundwater levels and SiO_2 concentrations at GA and GC

note: "STF" denotes the subsurface storm flow.

groundwater derived from deep seepage at HGW was sampled here when the groundwater levels existed below the bedrock. Groundwater sampled below the bedrock had high SiO_2 concentrations, 0.31 mmol/l on average. This concentration was similar to those in SGW, such as GF, G1-130, or G2-177 (see Figure 4.1). When the groundwater level rose above the bedrock depth, lower concentrations were observed, as at GA. Also, when the groundwater levels at GC rose above the bedrock depth, saturated throughflow always occurred at G11. The vertical distribution of SiO_2 concentrations at GC when groundwater levels were high is summarized in Table 4.1. Vertical variability of SiO_2 concentration occurred when saturated throughflow occurred at G11; lower concentrations were detected in the shallow layers and higher concentrations in the deep layers; vertical variability was not observed in the absence of saturated throughflow at G11. The short-term variations in SiO_2 concentrations and groundwater levels and the groundwater temperature at GC during a rainstorm are presented in Figure 4.3. The total

Table 4.1 Vertical distributions of SiO_2 concentrations at GC

Date	Throughflow occurrence at G11	Max. GWL (cm)	Shallow layer sampling depth (cm)	Shallow layer concentration (mmol/l)	Deep layer sampling depth (cm)	Deep layer concentration (mmol/l)
Sep 14, 2000	○	-31	-73～-31	0.14	-217～-181	0.28
Nov 10, 2000	○	-31	-73～-31	0.22	-217～-181	0.29
Jan 31, 2001	×	-115	-145～-115	0.27	-217～-187	0.27
Mar 8, 2001	×	-97	-127～-97	0.24	-217～-181	0.24

rainfall was 56.5 mm during this period. The SiO_2 concentrations decreased with rising groundwater levels. However, the concentrations declined when they approached the bedrock depth, not when the groundwater levels started rising. The groundwater temperature rose suddenly at the same time. The temperatures of source waters are relatively constant at the time scale in which streamflow is generated during storms in small watersheds (Shanley and Peters, 1988); thus, if the temperatures among the source waters differ significantly, the changes in water temperature imply the arrival of contributions from other sources. Therefore, variation in the groundwater temperature at GC indicates that another runoff component with a higher water temperature from a different source had mixed with the groundwater already present. The soil temperature is higher near the surface in summer; for example, the air temperature at 10:00 on June 19 2001, when the observations in Figure 4.3 were conducted, was 24.6℃, and the temperatures of the unsaturated soil at 10 cm, 30 cm, 60 cm, 100 cm, and 200 cm in depth were 20.7℃, 18.6℃, 16.0℃, and 13.6℃, respectively. Thus, the water component that mixed with the groundwater at GC had a lower SiO_2 concentration and higher water temperature, and had passed near the soil surface.

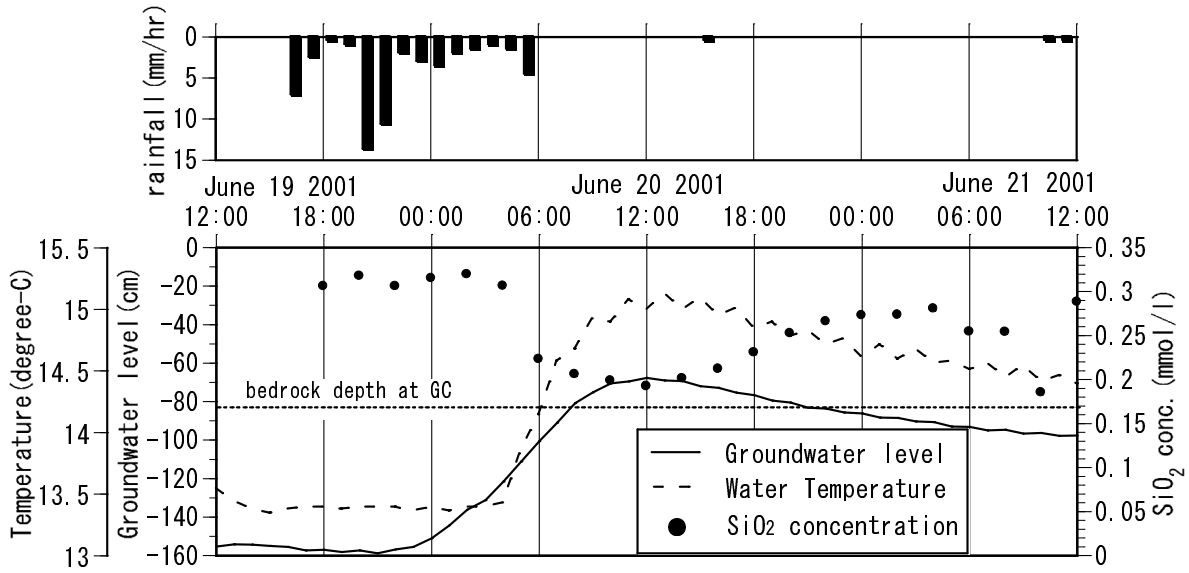

Figure 4.3 Short-term variations of SiO_2 concentrations and groundwater levels and groundwater temperature at GC

The long-term variations in SiO_2 concentrations at G11 in HGW, GC in TGW, and GF in SGW are shown in Figure 4.4. The seasonal variations in SiO_2 concentration at G11, which reached a maximum in September (the wet season) and a minimum in March (the dry season), are evident. Insufficient samples were

obtained during the dry winter season. The seasonal variations at GC had similar timing and higher concentrations. These results imply that the groundwater below the bedrock was recharged by deep-seepage water and had high SiO_2 concentrations in TGW. During rainstorms, the groundwater levels at TGW rose above the bedrock depth, and the SiO_2 concentrations decreased because of the recharge by saturated throughflow generated at the soil-bedrock interface in HGW.

The seasonal variability at GF, shown in Figure 4.4, was similar to that at GC, though the amplitude was smaller. The fact that groundwater at GC continued to be present during the dry winter (Table 2.2) indicates that bedrock flow recharged SGW with high SiO_2 concentration water throughout the year. During rainstorms, saturated throughflow occurred at HGW flowing down on the soil-bedrock interface in TGW and recharging SGW (see **Chapter 3**). This component may recharge the shallow layer of SGW because of the bedrock topography of the catchment. The SiO_2 concentrations in the saturated throughflow were lower; therefore, the concentrations in SGW were temporarily diluted, particularly during the rainy season.

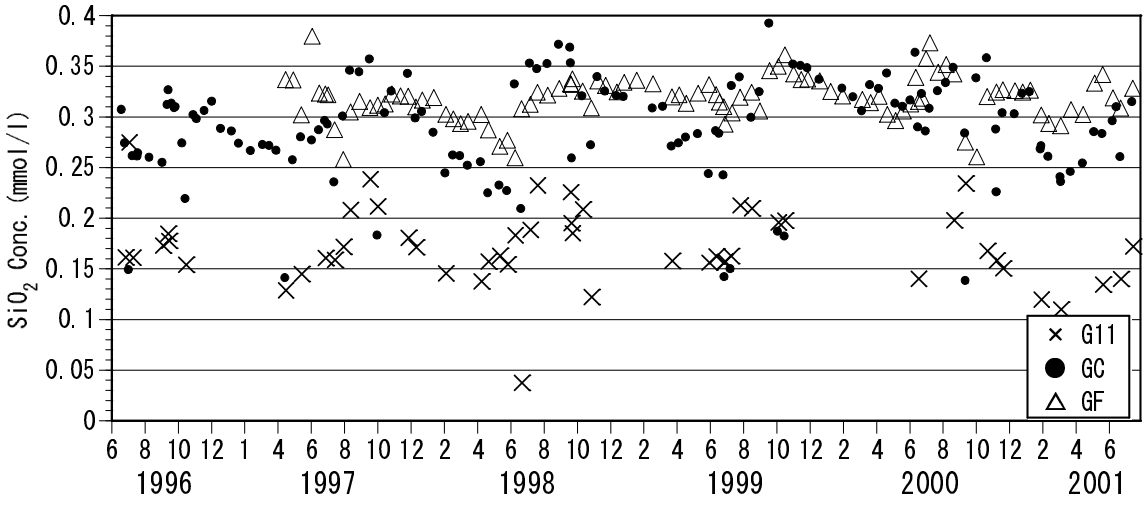

Figure 4.4 Long-term variations of SiO_2 concentrations at G11, GC, and GF

As mentioned above, the vertical distributions of SiO_2 concentrations in SGW were generated by the differences in permeability of the soil and the bedrock, the differences of SiO_2 concentrations in the saturated throughflow and the bedrock flow, and the bedrock topography of the catchment. As the SiO_2 concentration in G2-400, the deepest zone within SGW around the spring, was much higher, bedrock groundwater with high SiO_2 concentrations contributed more to the deeper groundwater. Additionally, G1-75 and GE, located near the spring, had lower SiO_2

concentrations than those observed in the other SGW wells (Figure 4.1). This must have arisen from the responses of the groundwater levels to rainstorms, as discussed in **Chapter 3**; the groundwater levels responded to rainfall earlier at the points nearer to the spring in all zones. In other words, at points close to the spring, the soil became saturated and groundwater was generated even by small rainstorms. The SGW wells, located near the spring, were frequently affected by the presence of groundwater in TGW with low SiO_2 concentrations, and consequently maintained lower concentrations.

A vertical distribution of SiO_2 concentration was present at A1 in SGW in the Akakabe catchment, similar to that observed in the Matsuzawa catchment. This may be due to the contribution of bedrock groundwater to the deeper groundwater in SGW, in addition to vertical infiltration processes (Shimada et al., 1993). However, the SiO_2 concentrations in SGW in the Akakabe catchment were much lower than those in the Matsuzawa catchment, and similar to the concentrations at GA or GB, so the contribution of the bedrock water may be relatively small. These differences may depend on the presence or absence of a TGW zone and, ultimately, on the catchment area or the bedrock topography. In the Akakabe catchment, saturated throughflow with low SiO_2 contributed directly to SGW. The highest concentrations were observed in the spring water and the streamwater. Therefore, bedrock groundwater with high SiO_2 must contribute more to these waters. The streamwater concentrations at the outlet of the Kiryu Experimental Watershed were slightly higher than those in the Matsuzawa and the Akakabe catchments, perhaps because the fraction of deep seepage water that bypassed the gauging weir was smaller in the Kiryu Experimental Watershed than in the two subcatchments.

4.4 Mean Residence Time of Groundwaters in the Matsuzawa Catchment

The mean residence times (MRTs) of the groundwaters and the streamwater (Kabeya, personal communication, 2001), which were estimated by using regular sampling of stable isotopes in the waters, and the estimates of turnover time, calculated from the discharge rate and the groundwater volume of the Matsuzawa catchment, are shown in Table 4.2. In the estimations of MRT from the $d^{18}O$ and/or dD, the input value (throughfall) is transformed to the output (groundwater or streamwater) by means of the convolution integral (Stewart and McDonnell, 1991; Rodhe et al., 1996; Vitvar and Balderer, 1997). In this study, the d-excess was used for the estimations.

$$d = \delta D - 8\delta^{18}O$$

$$C_{out}(t) = \int_0^{\infty} g(t')C_{in}(t-t')dt'$$

$$g(t) = \frac{1}{\tau}\exp(-\frac{t}{\tau})$$

where C_{in} is the d-excess of the throughfall and C_{out} is that of the groundwater, the spring water, or the streamwater, as appropriate. The $g(t')$ is the system-response function, which specifies the distribution of the transit times of water within the system (*e.g.*, Zuber, 1986), and the well-mixed exponential model is assumed in this study. Here t represents calendar time and the integration is carried out over the transit times (t'). The mathematical development of the formulas that express the mean residence time is detailed in Kubota (2000).

The turnover time is defined by the following equation (Zuber, 1986):

$$T = V_m / Q$$

where Q is the discharge rate of the catchment and V_m is the volume of the mobile water in the catchment. In this study, the annual mean daily discharge rate and the annual mean daily groundwater volume were designated Q and V_m, respectively.

Table 4.2 Mean residence times of the groundwaters in the Matsuzawa catchment (Kabeya, personal communication, 2001)

	point	days
MRT	G10※	0.0
	GA※	383.0
	GB	16.3
	GC	380.2
	GD※	470.9
	GF	221.7
	G1-75	167.1
	Spring	206.4
	Stream	222.7
T.T		137.9

※Not with complete accuracy of the estimations by the limited sampling numbers.

Groundwaters in GA, GB, GC, GD, G10 were sampled from Apr. 1999 to Dec. 2000.

Spring, stream and the other groundwaters were sampled from May 1998 to Dec. 2000.

MRT: Mean residence time, T.T: Turnover time of the groundwater in 2000

Variations in MRT between sample points were particularly large within TGW. The MRT at GC, where the well was drilled into the bedrock and the contribution of the bedrock water was relatively large, was greater than at GB, where the sampling depth of the groundwater was shallow and the contribution of the saturated throughflow was relatively large. The MRT in SGW, recharged by both the saturated throughflow and the bedrock flow, was intermediate between the MRT at GB and that at GC. In addition, the MRT at G1-75, located in the riparian zone, was smaller than at GF, located upslope in SGW. Thus, the riparian groundwater in SGW was more affected by the groundwater with a shorter MRT. The fact that the MRT of the streamwater was larger than that at G1-75 indicates that some other component with longer MRT, that is, water derived from the bedrock water, contributed to the streamwater. The turnover time of the groundwater was shorter than the MRT of the streamwater because the calculation of the turnover time considered both baseflow and stormflow conditions, but only baseflow conditions were considered in the estimations of MRT based on the results of regular sampling. This implies that during stormflow conditions, the runoff components, which have smaller MRT, (*i.e.*, the 'new' water), must contribute to the stormflow. Kabeya (personal communication, 2001) found a positive correlation between the mean residence time and SiO_2 concentration of the groundwater. These facts indicate the importance of the mean residence time in determining the details of the hydrochemical processes.

4.5 Chemistry of Potential Geographic Sources of Streamwater

The SiO_2 concentrations in the streamwater and in the potential geographic sources in the Matsuzawa catchment are compared herein. The SiO_2 concentrations in the streamwater were intermediate between those in the SGW shallow layer and the SGW deep layer, and higher than those in throughfall and groundwater present at the soil-bedrock interface in TGW ($N_4 < 100$). Considering the other solute concentrations in the potential geographic sources and the streamwater (see Figure 4.1), the concentrations of Na^+, Cl^-, and SO_4^{2-} were similar to the pattern exhibited by SiO_2. The concentrations of Ca^{2+}, NO_3^-, and DOC were higher in the SGW shallow layer and lower in the SGW deep layer than in the streamwater; however, the vertical variations of Cl^- and DOC in SGW were small. There were no clear variation patterns in the concentrations of NH_4^+, K^+, and Mg^{2+} between the potential geographic sources. The HCO_3^- concentrations were high within SGW, and higher than in the streamwater. The decrease of HCO_3^-

concentrations in the streamwater accompanied a rise in pH value, which was caused by the degassing of CO_2 due to turbulence in the groundwater flow from the spring (Ohte et al., 1995).

Although the bedrock groundwater, which may affect the streamwater chemistry, was not sampled in the Akakabe catchment, it must have higher concentrations of SiO_2, Na^+, Cl^-, and SO_4^{2-} and lower concentrations of Ca^{2+}, Mg^{2+}, and NO_3^- than those in the SGW groundwater or streamwater, if it is assumed that the streamwater is formed by mixing of SGW groundwater and bedrock groundwater, as the SGW deep-layer groundwater in the Matsuzawa catchment would indicate. As mentioned above, the SGW deep-layer groundwater is recharged mainly by bedrock groundwater. The bedrock material is the same in the Matsuzawa and the Akakabe catchments, so the bedrock groundwater is likely to have a similar chemical composition.

4.6 Conclusions

Spatial variability in groundwater chemistry has been demonstrated, especially in the vertical distribution in the riparian groundwater of headwater catchments. This variability is produced by differences of chemistry in the saturated throughflow generated at the soil-bedrock interface and the bedrock flow originating in deep seepage at the hillslope. The former component recharges the shallow layer of the groundwater volume and the latter component recharges the deep layer of the groundwater. The chemical signature of each flow is conserved, with little mixing within the body of the groundwater. The mean residence time of groundwater composed mainly of saturated throughflow is shorter than that of groundwater composed mainly of bedrock flow. Since many of the reactions are related to the biogeochemical environment, for example, interactions between the water and the surrounding soil material, and since the reactions are time dependent, the distributions of the mean residence times of groundwaters are related to the distributions of the groundwater and streamwater chemistry.

In recent studies, the importance of the contribution of bedrock groundwater to streamwater from small mountainous catchments has been demonstrated (Mulholland, 1993; Anderson et al., 1997). Hill (1990) showed that the groundwater in the riparian zone, which controls the runoff generation processes (Kendall et al., 1999; McGlynn et al., 1999) and the hydrochemical processes (Cirmo and McDonnell, 1997) of the streamwater, is composed of shallow and deep groundwater with distinguishable chemical regimes. It was determined

from this study that the vertical distribution of groundwater chemistry in the riparian zone is generated by the vertical distribution of the bedrock groundwater contribution to the groundwater within the catchment, depending on the catchment scale and the bedrock topography.

Reference

Anderson, S. P., Dietrich, W. E., Torres, R., Montgomery, D. R. and Loague, K. (1997) Concentration-discharge relationships in runoff from a steep, unchanneled catchment, Water Resour. Res., 33, pp. 211-225.

Bazemore, D. E., Eshleman, K. N. and Hollenbeck, K. J. (1994) The role of soil water in stormflow generation in a forested headwatar catchment: synthesis of natural tracer and hydrometric evidence, J. Hydrol., 162, pp. 47-75.

Christophersen, N., Neal, C., Hooper, R. P., Vogt, R. D. and Anderson, S. (1990) Modelling streamwater chemistry as a mixture of soilwater end-members - a step towards second-generation acidification models, J. Hydrol., 116, pp. 307-320.

Cirmo, C. P. and McDonnell, J. J. (1997) Linking the hydrologic and biogeochemical controls of nitrogen transport in near-stream zones of temperate-forested catchments: a review, J. Hydrol., 199, pp. 88-120.

DeWalle, D. R., Swistock, B. R. and Sharpe, W. E. (1988) Three-component tracer model for streamflow on a small Appalachian forested catchment, J. Hydrol., 104, pp. 301-310.

Hill, A. R. (1990) Groundwater cation concentrations in the riparian zone of a forested headwater stream, Hydrol. Process., 4, pp. 121-130.

Hooper, R. P., Christophersen, N. and Peters, N. E. (1990) Modelling streamwater chemistry as a mixture of soilwater end-members - an application to the Panola Mountain catchment, Georgia, U.S.A, J. Hydrol., 116, pp. 321-343.

Hooper, R. P., Aulenbach, B. T., Burns, D. A., McDonnell, J., Freer, J., Kendall, C. and Beven, K. (1998) Riparian control of stream-water chemistry: implications for hydrochemical basin models, Hydrology, Water Resources and Ecology in Headwaters (Proceedings of Headwater '98, the fourth international conference on headwater control, Merano, Italy, April 1998), pp. 451-458.

Kendall, K. A., Shanley, J. B. and McDonnell, J. J. (1999) A hydrometric and geochemical approach to test the transmissivity feedback hypothesis during snowmelt, J. Hydrol., 219, pp. 188-205.

Kubota, T. (2000) On the formulas expressing mean residence time of subsurface water, I. Japan Soc. Hydrol. & Water Resour., 13, pp. 472-475(in Japanese with English summary).

McGlynn, B. L., McDonnell, J. J., Shanley, J. B. and Kendall, C. (1999) Riparian zone flowpath dynamics during snowmelt in a small headwater catchment, J. Hydrol., 222, pp. 75-92.

Mulholland, P. J. (1993) Hydrometric and stream chemistry evidence of three storm flowpaths in Walker Branch Watershed, J. Hydrol., 151, pp. 291-316.

Ogunkoya, O. O. and Jenkins, A. (1993) Analysis of storm hydrograph and flow pathways using a three-component hydrograph separation model, J. Hydrol., 142, pp. 71-88.

Ohte, N., Tokuchi, N. and Suzuki, M. (1991) Variations in qualities of groundwater and stream water correspond to hydrological cycling in forested watershed, Bull. Kyoto Univ. For., 63, pp. 69-81. (in Japanese with English summary)

Ohte, N., Tokuchi, N. and Suzuki, M. (1995) Biogeochemical influences on the determination of water chemistry in a temperate forest basin: Factors determining the pH value, Water Resour.Res., 31, pp. 2823-2834.

Peters, N. E., Ratcliffe, E. B. and Tranter, M. (1998) Tracing solute mobility at the Panola Mountain Research Watershed, Georgia, USA: variations in Na^+, Cl^-, and H_4SiO_4 concentrations, Hydrology, Water Resources and Ecology in Headwaters (Proceedings of Headwater '98, the fourth international conference on headwater control, Merano, Italy, April 1998), pp. 483-490.

Rice, K. C. and Hornberger, G. M. (1998) Comparison of hydrochemical tracers to estimate source contributions to peak flow in a small, forested, headwater catchment, Water Resour. Res., 34, pp. 1755-1766.

Rodhe, A., Nyberg, L. and Bishop, K. (1996) Transit times for water in a small till catchment from a step shift in the oxygen 18 content of the water input, Water Resour. Res., 32, pp. 3497-3511

Shanley, J. B. and Peters, N. E. (1988) Preliminary observations of streamflow generation during storms in a forested Piedmont watershed using temperature as a tracer, J. Contam. Hydrol., 3, pp. 349-365.

Shimada, Y., Ohte, N., Tokuchi, N. and Suzuki, M. (1993) A dissolved silica budget for a temperate forested basin, Tracers in Hydrology (Proceeding of Yokohama Symposium), IHAS publ., No. 215, pp. 79-88.

Stewart, M. K. and McDonnell, J. J. (1991) Modeling base flow soil water residence times from deuterium concentrations, Water Resour. Res., 27, pp. 2681-2693.

Stonestrom, D. A., White, A. F. and Akstin, K. C. (1998) Determining rates of chemical weathering in soils - solute transport versus profile evolution, J. Hydrol., 209, pp. 331-345.

Uchida, T., Asano, Y., Ohte, N. and Mizuyama, T. (2001) Contribution of bedrock groundwater on perennial spring at a forested headwater catchment, J. Japan Soc. Hydrol & Water Resour., 31, pp. 59-72. (in Japanese with English summary)

Vitvar, T. and Balderer, W. (1997) Estimation of mean water residence times and runoff generation by ^{18}O measurements in a Pre-Alpine catchment (Rietholzbach, Eastern Switzerland), Appl. Geochem., 12, pp. 787-796.

White, A. F. (1995) Chemical weathering rate in soils, White, A. F., Brantley, S. L. (Eds.), Chemical weathering rates of silicate minerals. Mineralogical Soc. Amer., Washington, DC, Reviews in Mineralogy, 31, pp. 407-458.

Zuber, A. (1986) Mathematical models for the interpretation of environmental radioisotopes in groundwater systems, *In* Handbook of Environmental Isotope Geochemistry, vol 2, part B, Fritz, P. and Fontes, J. C. (Eds.), Elsevier, Amsterdam, pp. 1-59.

Chapter 5
Hydrochemical Processes of Baseflow

5.1 Introduction

As mentioned in the **Chapter 4**, the riparian groundwater, the potential geographic source of the streamwater, shows vertical distributions in solute concentrations in the Matsuzawa catchment, and the baseflow SiO_2 concentration is intermediate between the concentrations in the shallow and deep layers of the SGW (Figure 4.1). In this chapter, the effects of this spatial variability of groundwater chemistry on the seasonality of the streamwater chemistry baseflow conditions are discussed, using a two-component mixing model with a SiO_2 tracer.

5.2 Temporal Variations of Streamwater Chemistry

The long-term variations of SiO_2 concentration in the streamwater in the Matsuzawa catchment, at sites G1-75 (representative of the SGW shallow layer)

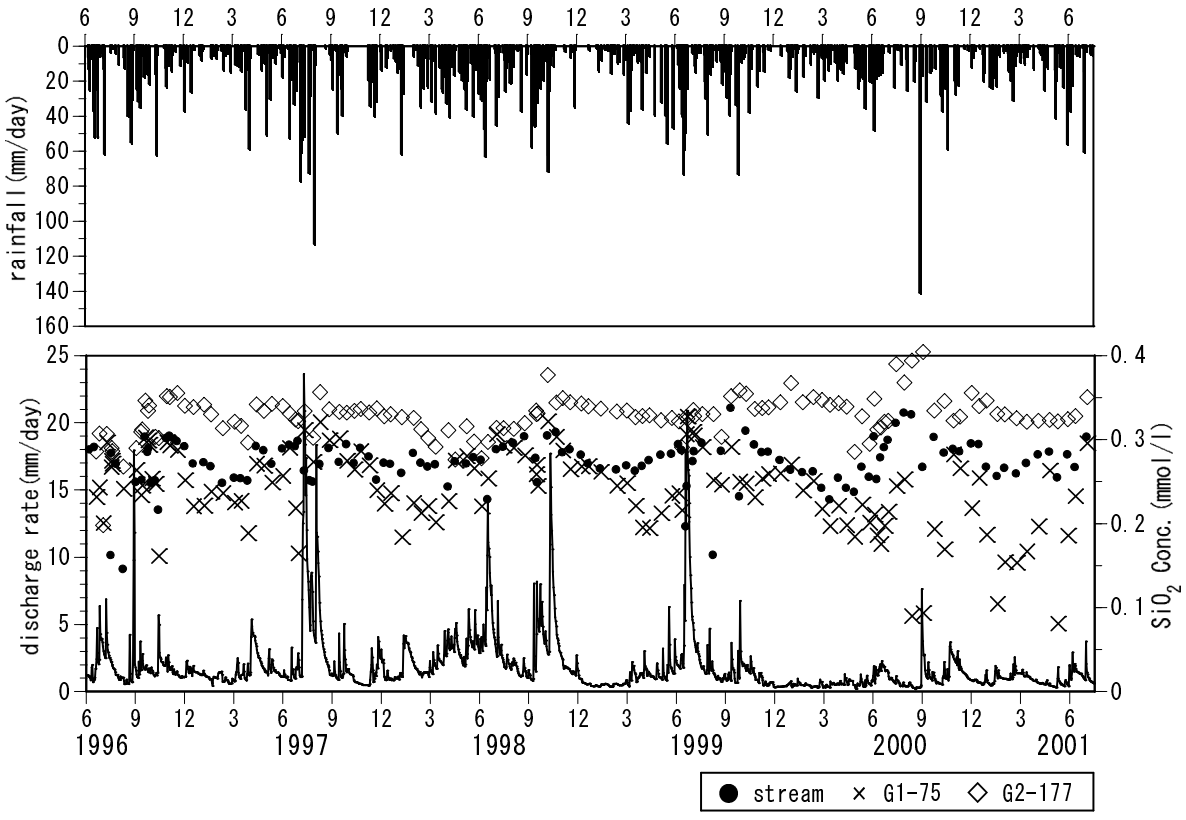

Figure 5.1 Long-term variations of SiO_2 concentration of streamwater, SGW shallow and deep layer in the Matsuzawa catchment

and G2-177 (representative of the SGW deep layer), are shown in Figure 5.1. The streamwater SiO_2 concentrations were intermediate between these groundwater concentrations. The coefficients of variation of concentrations at each of the observation points during the period of observation were 10.5% in the streamwater, 19.8% at G1-75, and 7.7% at G2-177. The concentrations at G1-75 had large seasonal variability, with lower concentrations in the dry season and higher concentrations in the rainy season. These variations are similar to the seasonality exhibited at G11, GC, and GF (see Figure 4.4). On the other hand, the seasonal variability was small at G2-177. The seasonality of streamwater SiO_2 concentrations was similar in phase, but with a smaller range. Comparing the concentrations of the streamwater, G1-75, and G2-177 at each sampled observation, the SiO_2 concentration was highest at G2-177 and lowest at G1-75 in 79.5% of cases, and highest at G2-177 and lowest in the streamwater in 19.7% of cases. Therefore, it may be considered that the streamwater during baseflow conditions was composed substantially of a mixture of the groundwaters in the shallow and deep layers of the SGW in the Matsuzawa catchment. When the concentrations at G1-75 were higher than in the streamwater, a runoff component other than that from the SGW, with lower SiO_2 concentration, may have contributed to the streamwater.

The long-term variations of SiO_2 concentrations in the streamwater in the Akakabe catchment, the groundwater at A1-175, and trench water are shown in Figure 5.2. The streamwater SiO_2 concentrations had little seasonality, with a minimum in March or April and a maximum in September or October, except for the extremely dry summer of August, 2000, when the highest concentrations were observed. The seasonality in A1-175 was similar to that of the streamwater, though the concentrations were lower. In August 2000, especially high concentrations were detected at each observation point. In Figure 5.3, the variations of the groundwater level at A1 and the pressure heads upslope (near A6) and downslope (A4) from March 2000 to November 2000 at a depth of 30 cm are shown. The dry conditions began abruptly in early July and continued until September. Higher concentrations were observed at each point during this period, and it is clear that the concentrations in the streamwater increased with the progress of the dry conditions. In the trench water a "flushing effect" (the phenomenon where the concentrated solutes within the soil are flushed out after a dry period; Walling and Foster, 1975) might have occurred during this period. The concentrations at A1-175 were raised by the admixing of trench water, which had high concentration. In

addition, the contribution of bedrock flow with high concentration might have increased proportionately when the saturated throughflow decreased. Similarly, it seems likely that the relative contribution of bedrock flow might have increased in the streamwater with the continuation of dry conditions and as higher SiO_2 concentrations were measured.

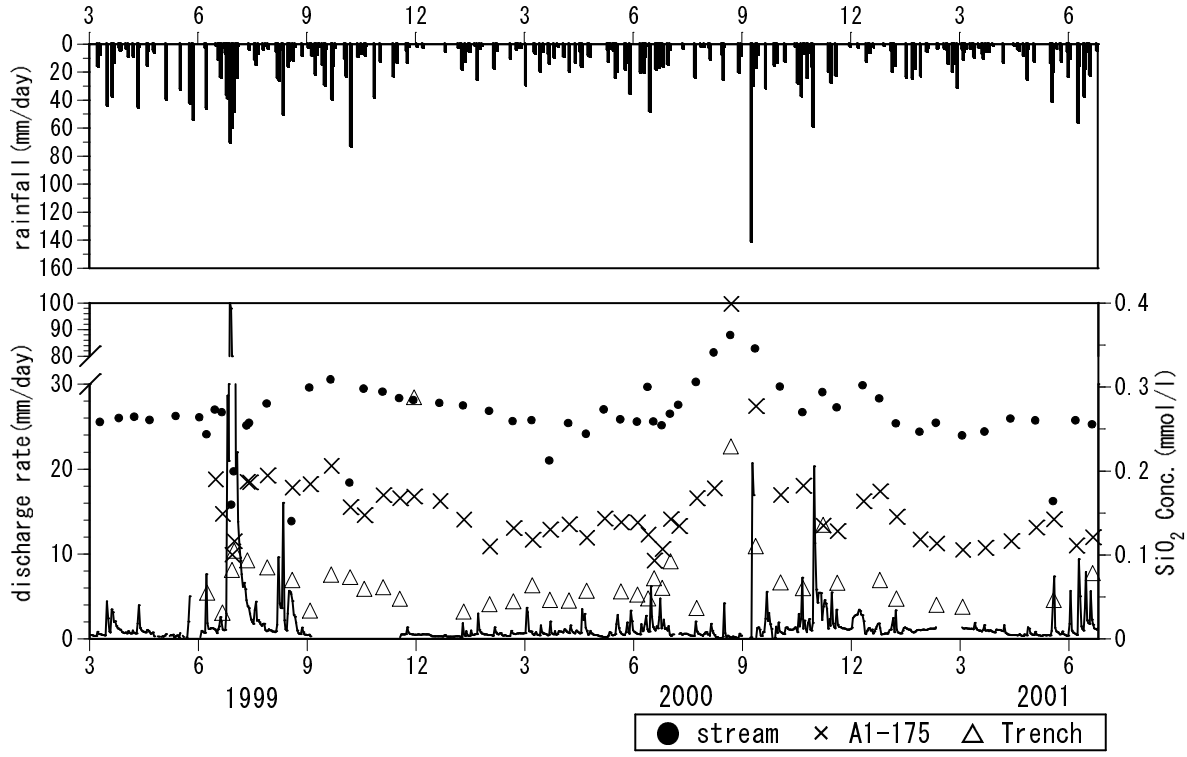

Figure 5.2 Long-term variations of SiO_2 concentration of streamwater, SGW and Trench water in the Akakabe catchment

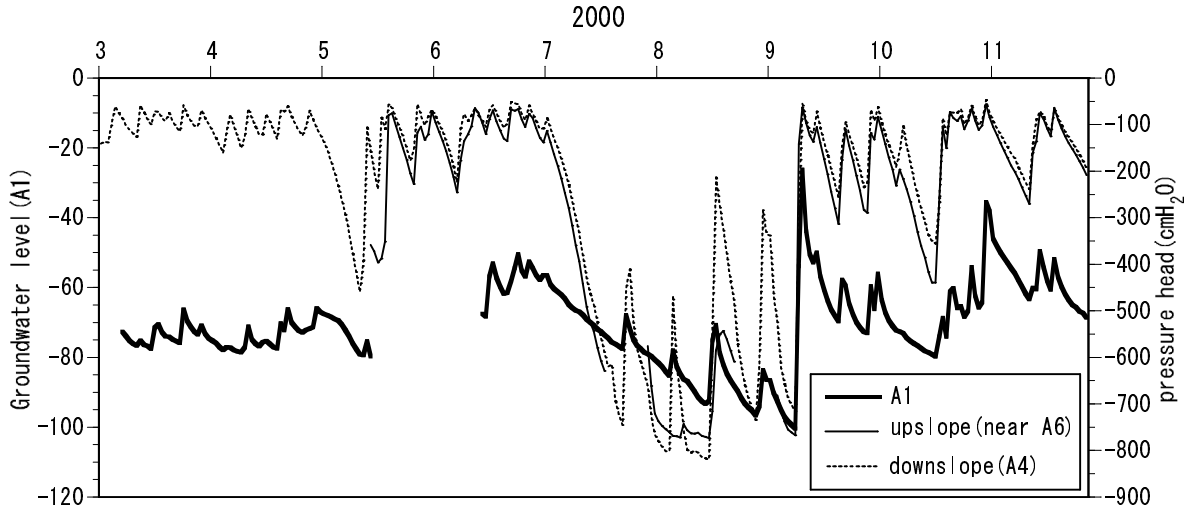

Figure 5.3 SGW groundwater level and 30-cm depth pressure head at hillslope in the Akakabe catchment

5.3 Two-component Mixing Model of Baseflow for the Matsuzawa Catchment

Assuming that the baseflow consisted of a mixture of waters from the shallow and deep levels of the SGW, the contribution of each component was calculated by using SiO_2 concentrations at G1-75 and G2-177 as a tracer. These contributions were calculated by solving the following simultaneous mass balance equations:

$$f_s + f_d = 1$$
$$C_s f_s + C_d f_d = C_{st}$$

where C is the concentration of the tracer and the subscripts s, d, and st refer to the SGW shallow-layer component, the SGW deep-layer component, and the streamwater, respectively. The f refers to the fraction of each component contributing to the streamwater. These equations were solved for each available set of streamwater chemistry data.

The temporal variations of the proportion from G1-75 are shown in Figure 5.4. The G1-75 proportion was higher after the large discharge peaks and during the dry season. These higher contributions after large discharge peaks must have been caused by the fact that the discharge rate from the SGW shallow layer increased with rising groundwater levels. As discussed in **Chapter 3**, the groundwater volume rose to a maximum later than the discharge peak; higher groundwater levels continued in the upslope SGW zone, and the source area spread upslope. The SiO_2 concentrations in G1-75 groundwater and in the streamwater

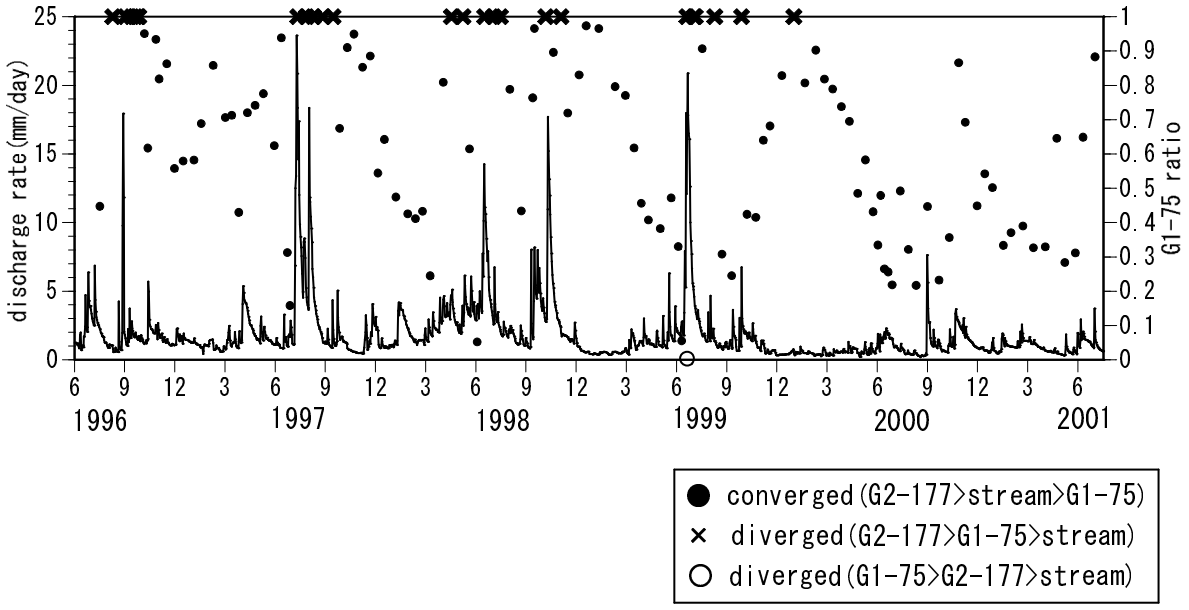

Figure 5.4 Temporal variations of SGW shallow layer contributions

note: the diverged values are plotted as "1" or "0".

were higher in the rainy season (Figure 5.1). This seasonality was caused by the contribution from the upslope SGW, with high SiO_2 concentrations, through the SGW shallow layer. At the peak discharge rate, higher SiO_2 levels were sometimes measured in G1-75 groundwater than in the streamwater. At these times, runoff components with low SiO_2 levels, other than groundwater from the shallow and deep layers in SGW, must have contributed to the streamwater (see **Chapter 6**).

Schematic diagrams of the hydrochemical processes of the baseflow in the Matsuzawa catchment using the two-component mixing model are presented in Figure 5.5. The contribution from the SGW shallow layer was higher during the dry period, as was seen in the winter season of 1999–2000, when the discharge rate was especially small. These phenomena seem to relate closely to the bedrock topography of the Matsuzawa catchment, where there is a large depression in the bedrock upslope of the spring outflow (see Figure 2.7 and 2.8). Groundwater has been present at G1-75 since 1996, and discharge from the SGW shallow layer has not ceased, even in the driest season. On the other hand, the groundwater of the SGW deep layer, pooled in the depression of the bedrock, may have been unavailable for discharge when the groundwater level decreased. Thus, only the groundwater of the shallow layer around the spring contributed to the stream during the dry season. The SiO_2 concentrations in G1-75 were lower in the dry seasons, so the streamwater SiO_2 concentrations were lower at these times.

During the wetting period, the contribution from the SGW shallow layer decreased. As discussed in **Chapters 3** and **4**, saturated throughflow did not occur in HGW and, therefore, the groundwater levels in TGW did not rise to the surface during relatively small rainfalls. On the other hand, groundwater existed below the soil-bedrock interface in TGW even in the dry season (see Table 2.2), indicating that the SGW deep layer was recharged by bedrock flow from TGW during wetting periods. This means the bedrock flow responses relatively fast to rainfall. As the discharge rate from the SGW deep layer increased with the increasing volume of groundwater in this layer, the contribution from the SGW shallow layer became proportionately lower. SiO_2 concentrations increased with contribution from the SGW deep layer, which had high SiO_2 concentrations during this period.

The contribution from the SGW shallow layer decreased during the drying period, because the discharge rate from the SGW shallow layer decreased as the groundwater level was depressed. With reduction in the fluxes from the upslope SGW toward the spring outflow, the supply of groundwater with high SiO_2 concentrations to the SGW shallow layer became exhausted, and even during this

period the riparian SGW shallow layer was diluted by rainwater or saturated throughflow from the downslope TGW. Thus, the groundwater SiO_2 concentrations declined in the SGW shallow layer around the spring, and consequently the SiO_2 concentrations in the streamwater also declined.

The hydrochemical processes of the baseflow in the Matsuzawa catchment have been explained on the basis of the two-component mixing model of the shallow and deep layers of the SGW, and the seasonality of the streamwater chemistry has been shown to result from variations in the mixing-ratio, particularly from changes in the contribution from the SGW shallow layer. In the Akakabe catchment, bedrock groundwater, which is one of the main components contributing to the streamwater, was not sampled, and the chemistry or discharge rate of that component is unknown, so the contribution of each runoff component could not be determined. However, since the bedrock groundwater chemistry observed in a small headwater granitic catchment close to the Kiryu Experimental Watershed was constant (Uchida et al., 2001), the bedrock groundwater in the Akakabe catchment probably corresponds to the groundwater in the SGW deep layer in the Matsuzawa catchment. The seasonality of the streamwater SiO_2 concentrations in the Akakabe catchment is caused by the changing contribution of the groundwater in the soil sedimentation zone, A1, which could be considered equivalent to the groundwater from the SGW shallow layer in the Matsuzawa catchment. The most important difference in the baseflow hydrochemistry of the two catchments is that the bedrock groundwater passes through the riparian groundwater in one, and not in the other. Soil has accumulated in a large depression on the bedrock of the Matsuzawa catchment, forming a riparian zone with abundant groundwater. The bedrock groundwater is pooled in this zone. In the Akakabe catchment, in contrast, the soil-sedimentation area is relatively small, with thin soil. As mentioned in **Chapter 4**, the groundwater in the riparian zone (soil-sedimentation zone) is strongly affected by saturated throughflow occurring at the soil-bedrock interface; however, the bedrock groundwater contributes little. There is a sizeable difference between the solute concentrations of the streamwater and the groundwater in SGW in the Akakabe catchment, resulting in the contribution of the groundwater in SGW being relatively small during the baseflow condition, and the riparian zone control of baseflow hydrochemistry is relatively weaker in this catchment than in the Matsuzawa catchment.

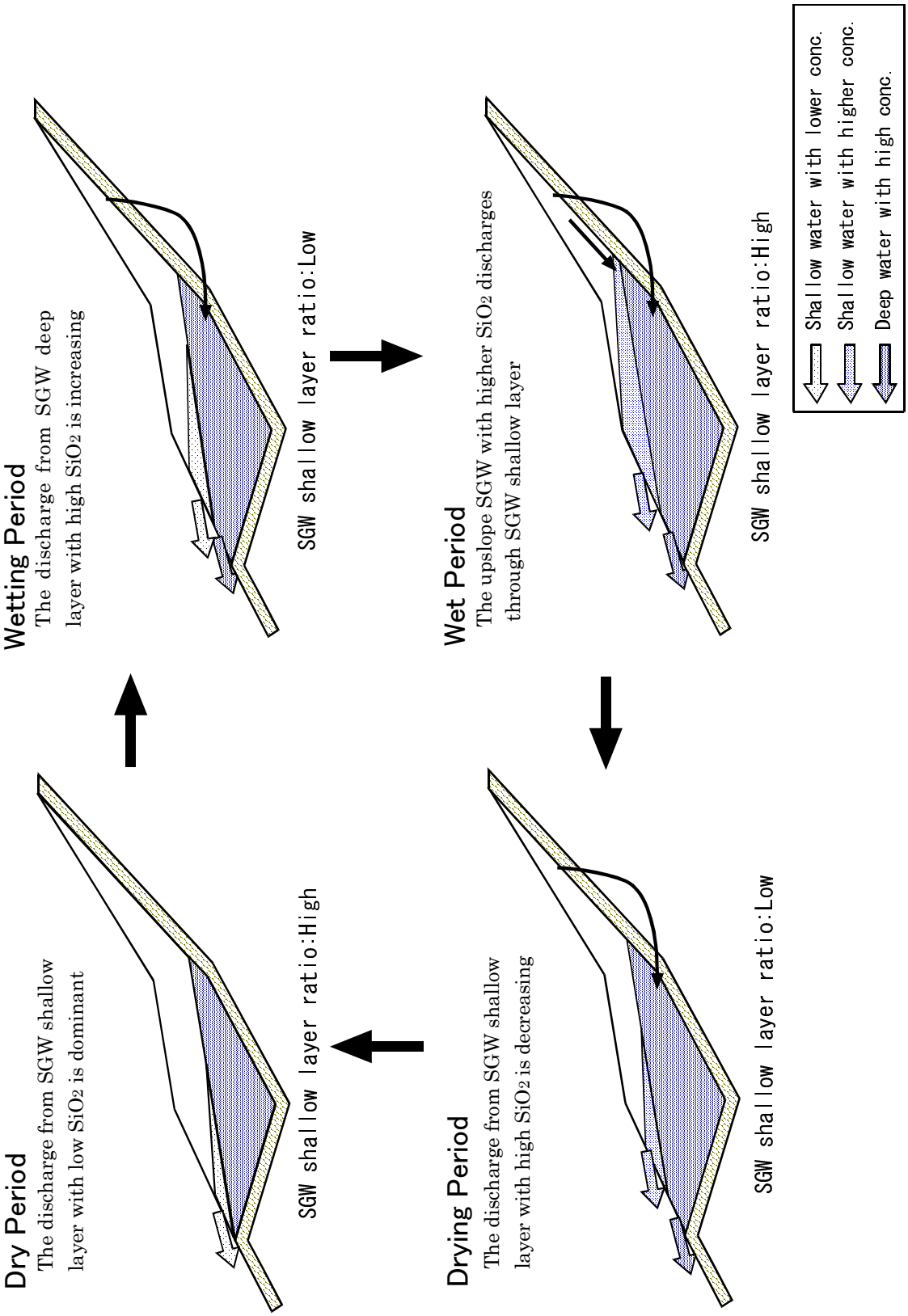

Figure 5.5 Schematic diagrams of baseflow generations and hydrochemical processes of the Matsuzawa catchment

5.4 Conclusions

In some previous studies (Sklash, 1990; Burns et al., 2001), riparian groundwater has been considered to be one of the sources of streamwater and to have a homogeneous chemistry similar to that of streamwater. Others have pointed out that groundwater dynamics within the riparian zone affect tracer concentrations (Hill, 1993; Tanaka and Ono, 1998) or biogeochemical processes (Mulholland, 1992; Lischeid, 2001). Thus, it is necessary to reevaluate the heterogeneities of groundwater chemistry when applying the mixing-model approach to the study of runoff generation and hydrochemical processes within the riparian zone. Following Hill (1990), this study shows that medium- or long-term phenomena, such as the seasonality of baseflow chemistry, are largely affected by the spatial variability of the groundwater chemistry within the riparian zone.

References

Burns, D. A., McDonnell, J. J., Hopper, R. P., Peters, N. E., Freer, J. E., Kendall, C. and Beven, K. (2001) Quantifying contributions to storm runoff through end-member mixing analysis and hydrologic measurements at the Panola Mountain Research Watershed (Georgia, USA), Hydrol. Process., 15, pp. 1903-1924.

Hill, A. R. (1990) Groundwater cation concentrations in the riparian zone of a forested headwater stream, Hydrol. Process., 4, pp. 121-130.

Hill, A. R. (1993) Base cation chemistry of storm runoff in a forested headwater wetland, Water Resour Res., 29, pp. 2663-2673.

Lischeid, G. (2001) Conservative mixing or chemically reacting: scale-dependency of processes at the stream water-groundwater interface, Impact of Human Activity on Groundwater Dynamics (Proceedings of a symposium held during the Sixth IAHS Scientific Assembly at Maastricht, The Netherlands, July 2001) IAHS Publ. 269, pp. 199-204.

Mulholland, P. J. (1992) Regulation of nutrient concentrations in a temperate forest stream: Roles of upland, riparian, and instream processes, Limnol. and Oceanogr., 37, pp. 1512-1526.

Sklash, M. G. (1990) Environmental isotope studies of storm and snowmelt runoff generation, Process studies in hillslope hydrology. edited by Anderson, M. G. and Burt, T. P., John Wiley and Sons, Chichester, pp. 401-436.

Tanaka, T. and Ono, T. (1998) Contribution of soil water and its flow path to

stormflow generation in a forested headwater catchment in central Japan, Hydrology, Water resources and Ecology in Headwaters (Proceeding of the HeadWater '98 Conference held at Merano, Italy, April 1998), pp. 181-188.

Uchida, T., Asano, Y., Ohte, N. and Mizuyama, T. (2001) Contribution of bedrock groundwater on perennial spring at a forested headwater catchment, J. Japan Soc. Hydrol & Water Resour., 31, pp. 59-72. (in Japanese with English summary)

Walling, D. E. and Foster, I. D. L. (1975) Variations in the natural chemical concentration of river water during flood flows, and the lag effect: some further comments, J. Hydrol., 26, pp. 237-244.

Chapter 6
Hydrochemical Processes of Stormflow

6.1 Introduction

How runoff is generated in a watershed governs, to a large extent, the temporal changes in streamwater chemistry during storm runoff events (Sklash, 1990). Many studies of small catchments have used hydrograph separation techniques to identify the principal source components of Stormflow, or to clarify how the mechanisms controlling streamwater chemistry behave and how they may change during stormflow (see reviews in Buttle, 1994; and Genereux and Hooper, 1998). The tracer-based hydrograph separation technique involves the use of a mixing model for the stream. Christophersen et al. (1990) and Hooper et al. (1990) considered that streamwater chemistry is determined by the mixing of spatially different soilwater components, and called this technique "End-members mixing analysis" (EMMA).

In this chapter, the hydrochemical processes that occur during rainstorms are considered from three aspects: 1) the scale of the rainfall, 2) the differences between the hydrological processes in different catchments, and 3) the source area of the stormflow. Hydrograph separations using EMMA were undertaken with certain tracers, including a new tracer—the fluorescence of dissolved organic carbon.

6.2 Hydrochemical Processes of Stormflow in the Matsuzawa Catchment: A Three-component End-member Analysis

6.2.1 Introduction

Herein, the results of intensive hydrometric and hydrochemical observations at the Matsuzawa catchment for three consecutive rainstorms are presented, and EMMA is used to quantitatively estimate the processes controlling streamwater chemistry during rainstorms.

6.2.2 Rainstorm Characteristics

The rainstorm characteristics are summarized in Table 6.1. Event M97-1 was caused by Typhoon No. 9708, and Event M97-3 was caused by Typhoon No. 9709. The rainfall of Event M97-2 was caused by a seasonal rain front.

Table 6.1 Rainstorm characteristics of the Matsuzawa catchment

		Event M97-1	Event M97-2		Event M97-3
			(first half)	(second half)	
Observed period	(from)	Jun 28, 1997	Jul 9, 1997	Jul 12, 1997	Jul 25, 1997
	(to)	Jun 29, 1997	Jul 11, 1997	Jul 16, 1997	Jul 27, 1997
Total rainfall	(mm)	37.4	136.5	114.5	80.5
Max. rainfall intensity	(mm/10min)	4.5	14	13.5	3
Total discharge	(mm)	3.6	20.0	91.0	22.2
Max. discharge intensity	(mm/10min)	0.1	0.4	0.3	0.1
Antecedent precipitation (5 days)	(mm)	19.2	1.9	138.4	0
Antecedent precipitation (10 days)	(mm)	76.5	31.3	164.3	52.3

6.2.3 Hydrologic Responses of Groundwater Levels

The contour maps of groundwater levels at the peak discharge rate of each rainstorm and temporal variations of groundwater levels at points G1, GC, and G10 are shown in Figure 6.1. Points G1, GC, and G10 represent SGW, TGW, and HGW, respectively. The starting point of groundwater levels is the spring outflow (SP). In Event M97-1, the duration of the saturated condition was short at point G10, and the variations of groundwater levels at points G1 and GC were small relative to the other rainstorms. The contour map showed that only the groundwater in SGW around the spring (SP) discharged to the stream, and the groundwater in TGW flowed into SGW. In Event M97-2, saturation overland flow started at around 11:00 on July 12 and continued even after the rainfall ceased; therefore, Event M97-2 was divided into two halves, with July 12 as the boundary date. In the first half of Event M97-2, the saturated condition continued at point G10 and the groundwater level at point GC rose sharply. These facts imply that HGW was saturated and the saturated throughflow at the soil-bedrock interface discharged down into TGW, causing the groundwater levels to rise sharply in TGW (as seen in **Chapter 3**). The contour map further showed that the groundwater levels of TGW rose and the fluxes toward SGW increased. In the second half of Event M97-2, the groundwater levels of TGW rose even more, and fluxes directly toward SP also occurred as the fluxes toward SGW increased. Saturation overland flow occurred at the peak of the discharge rate and continued contributing to the streamflow. In Event M97-3, the range of the variations in groundwater level is the same as for those noted in Event M97-1, but the duration of the saturated condition at point G10 was longer and the groundwater levels were higher, especially at point GC. The contour map showed that the fluxes from TGW toward SP continued.

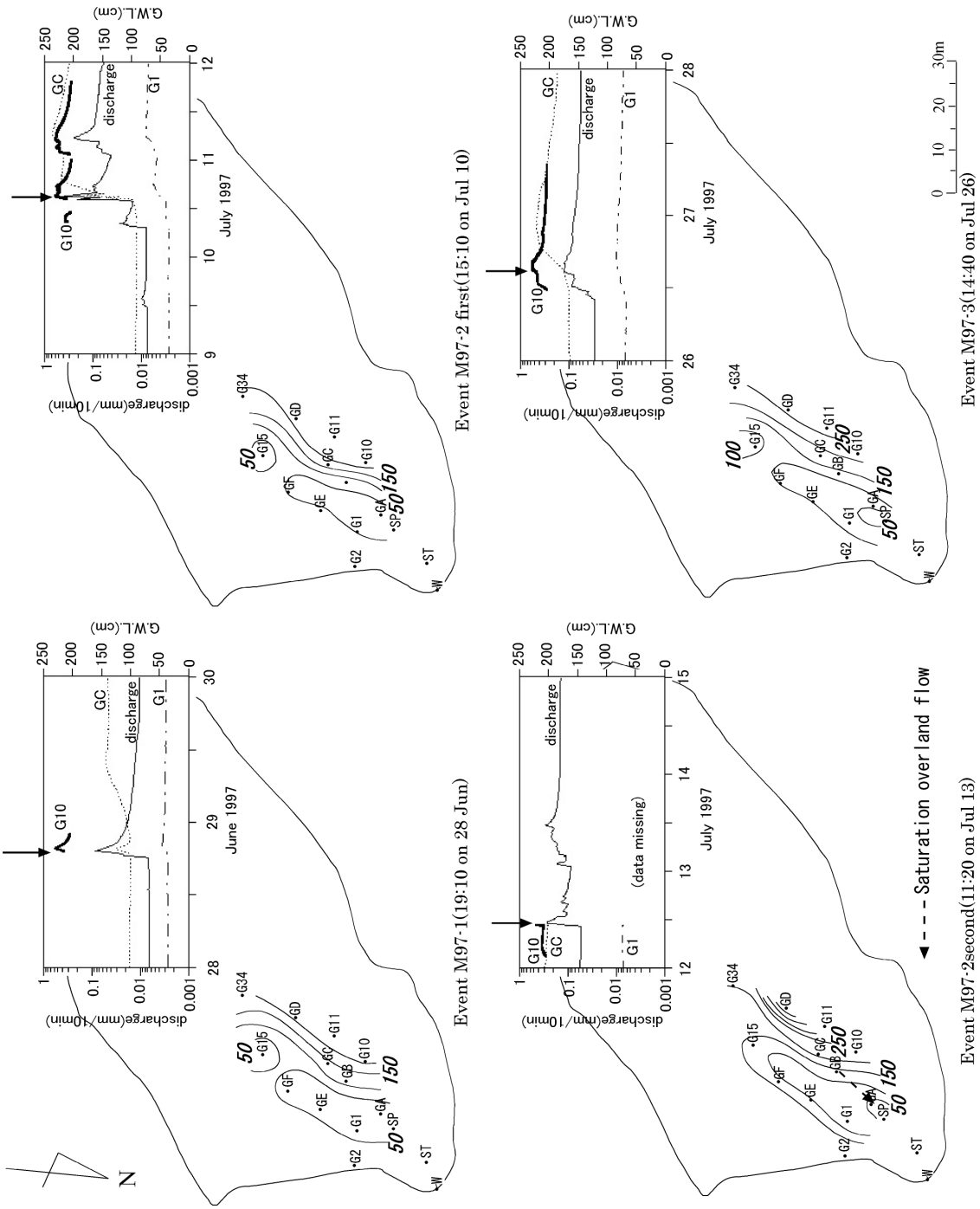

Figure 6.1 Contour maps of groundwater levels at the peak of discharge rate of each rainstorm

6.2.4 Spatial Distribution of Tracer Concentrations

Na^+ and SO_4^{2-} were selected as tracers, because this combination provides the best separation of sources. Large spatial variations in the concentrations of these solutes were seen between the groundwater zones, similar to those observed for SiO_2 concentration, as noted in **Chapter 4** (see Figure 4.1). There were also large spatial and temporal variations in the concentrations within TGW. The ion compositions from the long-term regular sampling of groundwater and streamwater in the Matsuzawa catchment are shown in Figure 6.2. The concentration of Na^+ in rainfall and throughfall is very low, and increases in the soil profile due to chemical weathering. Na^+ is the most dominant cation in the streamwater of this catchment. SO_4^{2-} exists in the throughfall to a certain extent from acid deposition over this catchment, and is concentrated in the soil. SO_4^{2-} is the most dominant anion in the streamwater.

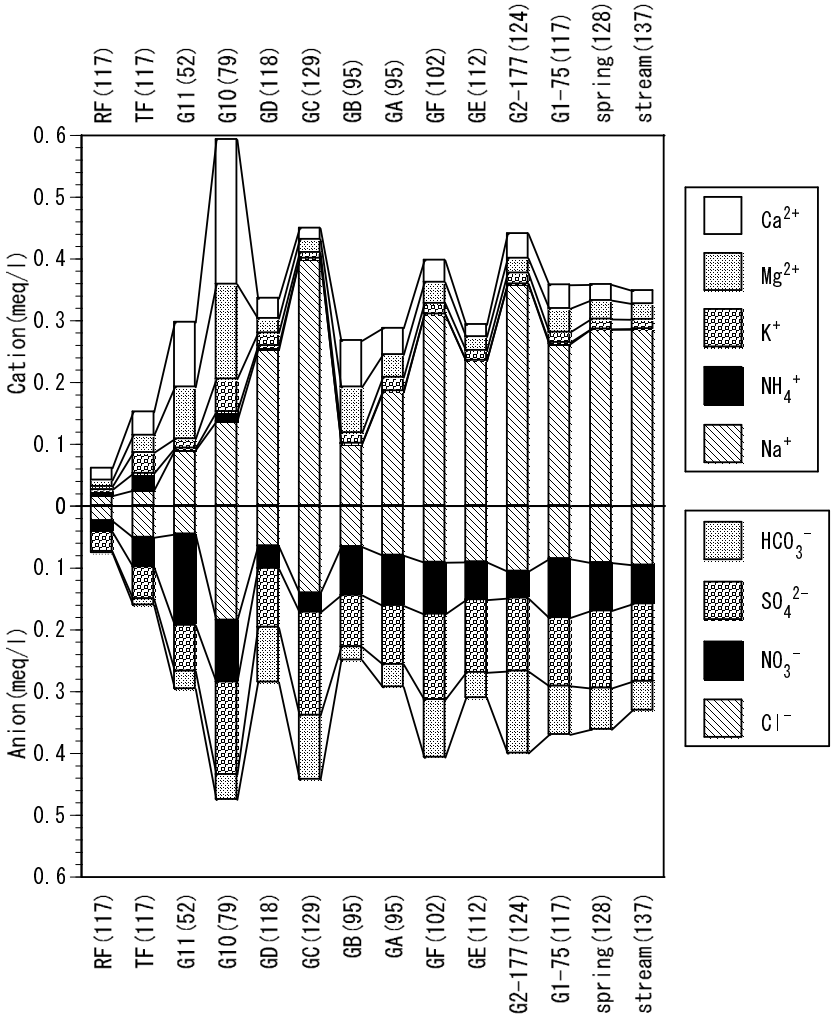

Figure 6.2 Ion compositions of the Matsuzawa catchment

note: Each value was averaged data of regular sampling.

6.2.5 Temporal Variations in Streamwater Chemistry

Temporal variations in rainfall, discharge rate, and Na^+ and SO_4^{2-} concentrations for each rainstorm are shown in Figure 6.3. Na^+ and SO_4^{2-} concentrations were inversely related to the discharge rate. Shanley and Peters (1993) found that streamwater sulfate concentration increased as flow increased at their Panola Mountain, Georgia site, because an increasing proportion of shallow, high-sulfate groundwater and soilwater contributed to the streamflow. In the Matsuzawa catchment, however, SGW groundwater SO_4^{2-} concentrations were similar to those in the streamwater (and lower in the others), so the streamwater must have been diluted. After the rainfall ceased, these concentrations returned to prestorm levels in Event M97-1 and Event M97-3. However in the second half of Event M97-2, Na^+ concentration remained below prestorm levels even after the rainfall ceased.

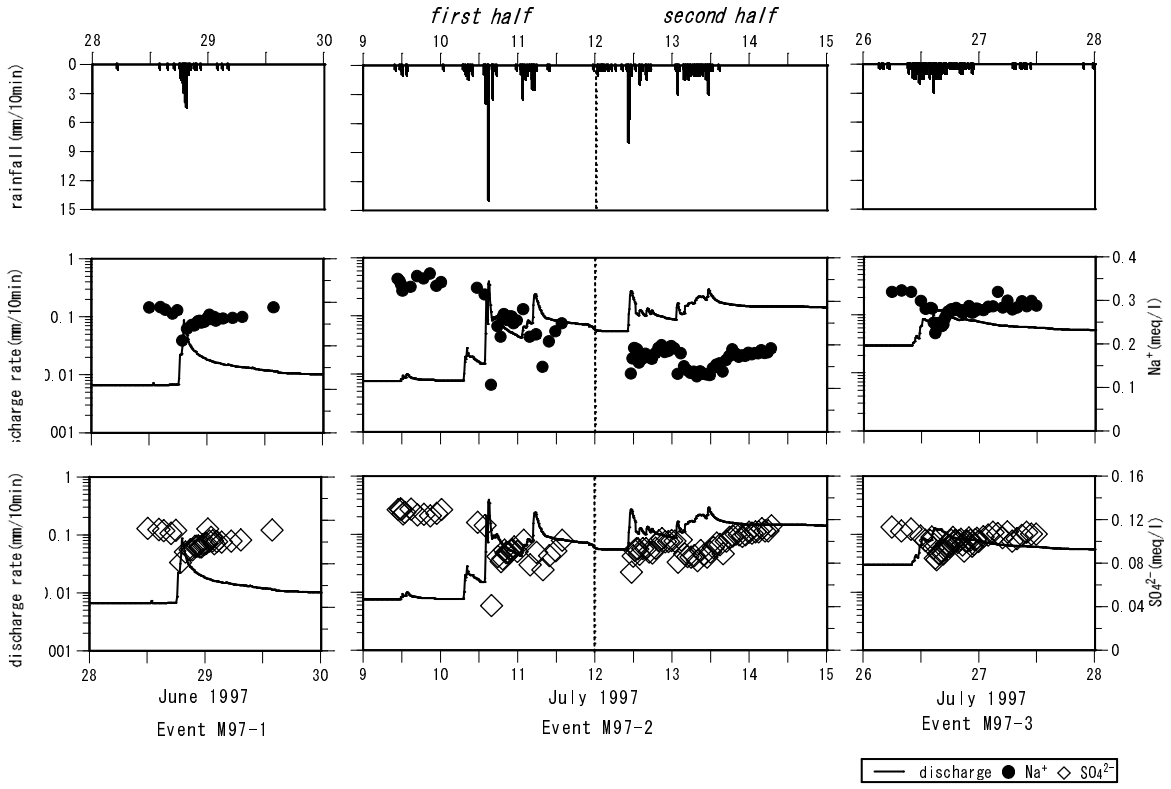

Figure 6.3 Temporal variations in rainfall, discharge rate and Na^+ and SO_4^{2-} concentrations of the Matsuzawa catchment

6.2.6 Analysis of the End-members

The changes in the streamwater chemistry during and after rainstorms were caused by changes in the mixing ratio of the water components that contribute to the streamwater runoff. EMMA was applied to each event to quantitatively evaluate the contribution of each component.

The results of hydrometric observations (see **Chapter 3** and Figure 6.1) indicate that SGW shallow layer, SGW deep layer, TGW, and throughfall can all contribute to stormflow. As noted in **Chapter 5**, baseflow chemistry was controlled by the mixing of SGW shallow-layer and SGW deep-layer waters. During rainstorms, however, the SGW shallow layer is strongly affected by the saturated throughflow generated at the soil-bedrock interface; that is, HGW or TGW, as noted in **Chapter 4**. Therefore, in the study of rainstorms (short-term phenomena), the SGW shallow layer should not be treated as an end-member, because this would be contrary to the assumption of independence of the end-members, which must be significantly different from each other (Christophersen et al., 1990). Therefore, the SGW deep layer can be treated as the first end-member of streamwater. The groundwater sampled from the G2-177 well before each rainstorm was used in the analysis.

Throughfall can be treated as the second end-member, because it is mixed directly into the streamwater as channel precipitation. According to Kim (1990), the spatial extent of the saturated zone and the variation of groundwater levels are mainly caused by the subsurface stormflow and are the main factors regulating the discharge rate during and after the rainfall. In addition, it is also clear that the groundwater level presents two different responses to rainfall: 1) when the rainfall is low and the soil is dry, only the saturated zone near the stream channel contributes to the discharge rate of the catchment; and 2) as the rainfall increases, the contribution of subsurface stormflow to the discharge rate increases. Thus, subsurface stormflow plays the role of the third end-member. As noted in **Chapter 3**, as the rainfall increases, saturated throughflow occurs on the soil-bedrock interface in HGW, flows down, and accumulates in TGW. The groundwater levels rise more rapidly in TGW than in SGW, and as a consequence, the hydraulic gradient becomes larger, with fluxes from the TGW zone to SGW to the stream discharge occurring, as seen in Figure 6.1. Hence, the groundwater in TGW can be treated as subsurface stormflow. The soilwater component is selected as one of the end-members in many studies (*e.g.*, Mulholland, 1993; Ohrui and Mitchell, 1999). The TGW groundwater plays the same role as soilwater because it develops in

response to rainstorms, and contributes to the discharge. The concentrations at the GC well sampled before each rainstorm were used in the analysis.

Three-component mixing diagrams are shown in Figure 6.4. The end-member of each event is as follows:

Event M97-1: SGW deep layer and throughfall (TF) (two components)

Event M97-2, 3: SGW deep layer, TGW, and TF (three components).

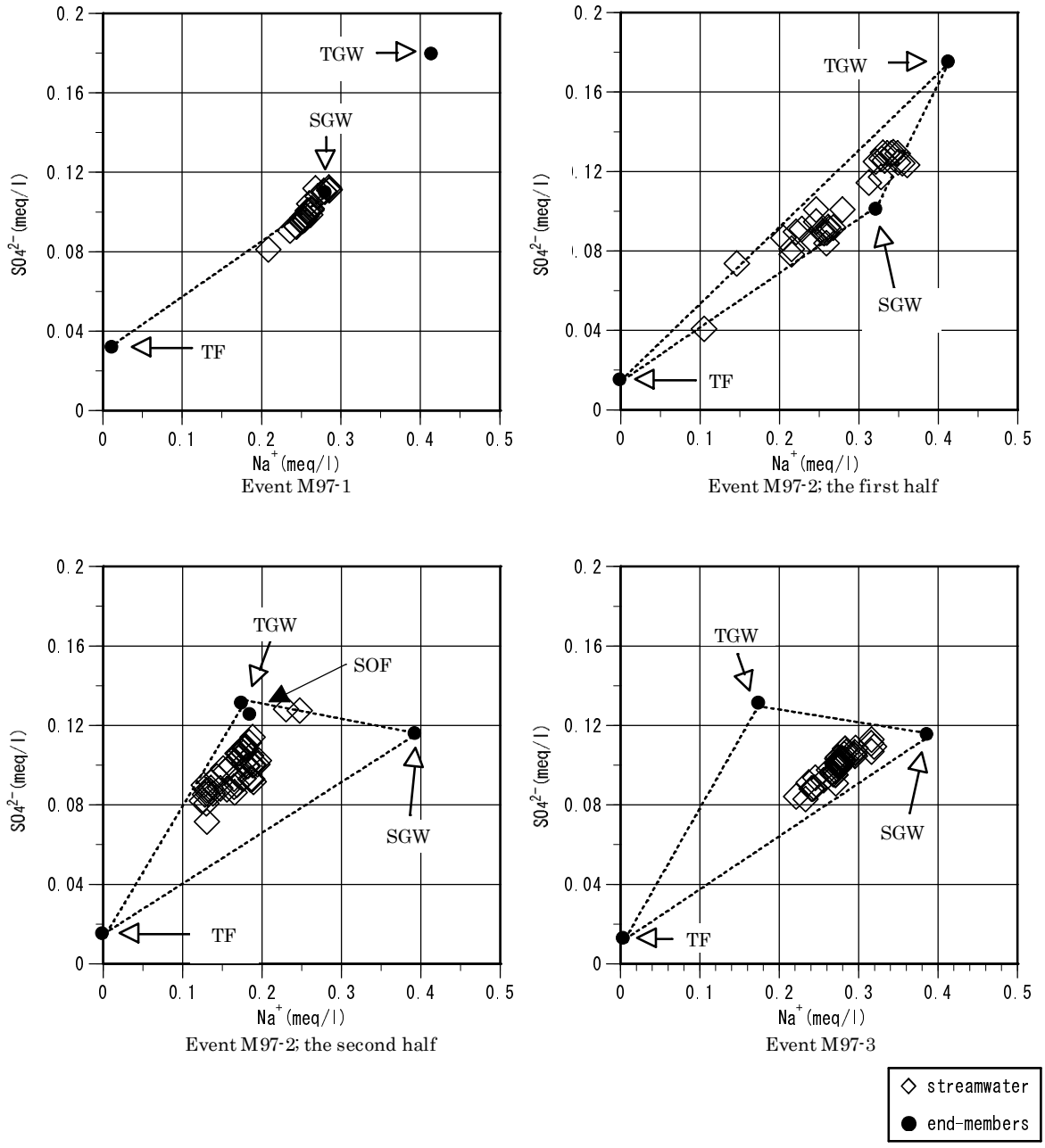

Figure 6.4 Three-component mixing diagram

note: "SOF" denotes saturation overland flow.

In Event M97-1, since the rainfall was light and short in duration compared to the other two events, the subsurface stormflow would have contributed little to the streamwater. In Event M97-2 and 3, the TGW component corresponding to subsurface stormflow contributed to the streamwater (see Figure 6.1). In both the first and second halves of Event M97-2 (comparing the right top panel and left bottom panel in Figure 6.4), the end-members were the same, but the shapes of the corresponding diagrams are considerably different. The concentration of the TGW component fluctuated greatly. The mechanism of this fluctuation is as follows (see **Chapter 3** and **Chapter 4**): the groundwater level at GC before Event M97-2 was below the bedrock depth and the groundwater chemistry was affected by groundwater flow through the bedrock, seeped at HGW. Saturated throughflow was generated at the soil-bedrock interface of HGW, the groundwater level of GC increased considerably, and the tracer concentrations changed. As noted in **Chapter 4**, the groundwater chemistry of GC is affected by the chemistry of the saturated throughflow generated at G11. Na^+ and SO_4^{2-} concentrations of G11 groundwater are lower than those at GC (see Figure 4.1); these tracer concentrations at GC are therefore diluted and this is reflected in the stormflow chemistry. Hooper et al. (1998) showed that the choice of one end-member ("A-horizon") (Hooper et al., 1990) was justified by the fact that a large change in the chemistry of this end-member was reflected in the streamwater chemistry throughout the long-term period of observation. The same effects occurred in this study, despite the short period of the phenomena. The chemistry of the saturation overland flow that occurred in the second half of Event M97-2 ("SOF" in Figure 6.4) is similar to that of the TGW component, because saturation overland flow was produced when the groundwater level of TGW reached the ground surface.

6.2.7 Contributions of Each Runoff Component

The runoff was separated into two components (as for Event M97-1) or three components (as for Event M97-2 and 3) using Na^+ and SO_4^{2-} concentrations. In Event M97-1, the hydrograph was separated into two components using Na^+ and SO_4^{2-}, respectively, and the results were then averaged.

The contributions of each end-member were calculated by solving the following simultaneous mass balance equations:

$$f_a + f_b + f_c = 1$$
$$C1_a f_a + C1_b f_b + C1_c f_c = C1_{st}$$
$$C2_a f_a + C2_b f_b + C2_c f_c = C2_{st}$$

where *C1* and *C2* are the concentrations of the tracers and the subscripts *a*, *b*, and *c* refer to each component of the three end-members. The subscript *st* refers to streamwater, and *f* refers to the fraction of each component that contributes to the streamwater. These equations were solved for each set of available streamwater chemistry data.

The results of hydrograph separations are shown in Figure 6.5. In Event M97-1, when the groundwater level was low, the SGW deep-layer component accounted for more than 90% of the throughout for most of the period, except at the peak of rainfall, when the throughfall component accounted for about 35%. In Event M97-2, the proportion of the TGW component increased as the saturated zone spread during the first half of the event, and after the occurrence of saturation overland flow (the second half), this component became dominant, accounting for about 80% after rainfall ceased. In Event M97-3, when groundwater levels were high, the SGW deep-layer component was dominant, while the TGW component accounted for about 20% throughout the observation period.

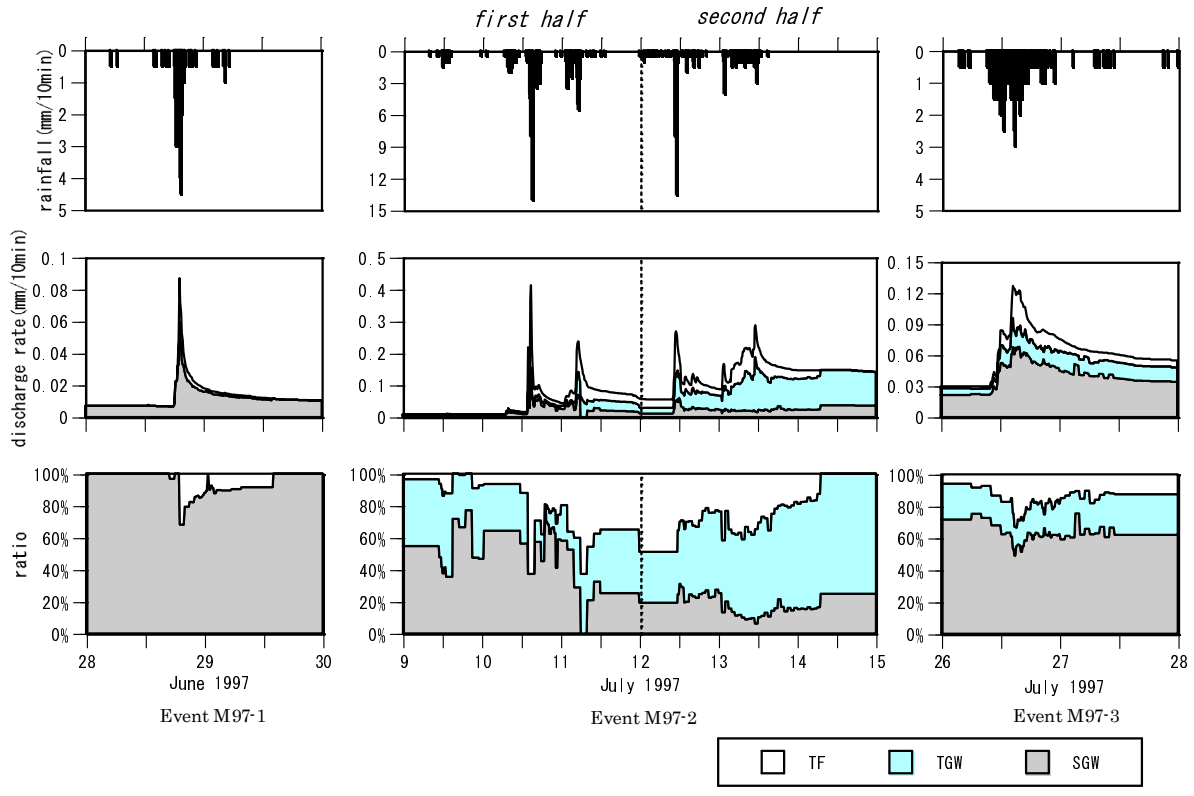

Figure 6.5 Hydrograph separations

6.2.8 Hydrochemical Processes of Stormflow

The results of analysis by the EMMA method, using Na^+ and SO_4^{2-} concentrations, indicate the importance of the contribution of the TGW component to the discharge rate and to streamwater chemistry in this catchment. The chemistry of the TGW component varies widely and is clearly different from the chemistry of the other components. The rise of groundwater levels and the spread of the saturated zone determine whether the TGW component contributes to the discharge rate, and whether this component discharges as subsurface flow or as overland flow. It was observed that when consecutive rainstorms occurred, the saturated zone enlarged with the continuation of rainfall. The hydrochemical processes of the streamwater are regulated by the source of solutes, hydrological pathways, and the contribution of each flow component. The spread of the saturated zone, which is decided by antecedent rainfall and by the total rainfall of each storm, impacts on these three factors, and on the streamwater chemistry.

6.3 Effects of Pathways and the Scale of the Riparian Zone on Stormflow Chemistry: Comparative Study in Four Catchments

6.3.1 Introduction

Herein, the results of comparative observations of the differences in the hydrological processes and in the vegetation of the catchments are discussed. In addition to the results from the Matsuzawa and the Akakabe catchments, the results from the Rachidani catchment, which has a small groundwater body and is unvegetated, and the Toinotani catchment, where pipe flow plays an important role in the hydrological processes, are included.

6.3.2 Hydrochemical Processes of Stormflow in the Akakabe Catchment

Event-based observations were conducted in the Akakabe catchment during two consecutive rainstorms. The rainstorm characteristics and the temporal variations of the rainfall, discharge rate, and groundwater levels of A1, SiO_2, and Mg^{2+} concentrations are shown in Table 6.2 and Figure 6.6. The rapid increase in the discharge rate during Event A99-2 coincided with a large increase in A1 groundwater levels. The SiO_2 concentrations were related inversely, and the Mg^{2+} concentrations directly, to the discharge rate. As discussed in earlier chapters, in this catchment the effects on the streamwater of bedrock flow are important. The contribution of the bedrock flow, probably with high SiO_2 and low Mg^{2+} concentrations, to the baseflow chemistry are especially important (**Chapters 4, 5**).

Thus, a runoff component that is low in SiO_2 and high in Mg^{2+} must also contribute to the stormflow. The hydrological pathways to the streamwater are throughfall as channel precipitation and the groundwater flow from SGW, in addition to the bedrock flow (**Chapter 3**). Based on the spatial distribution of solutes (Figure 4.1), the throughfall has lower SiO_2 and similar Mg^{2+} levels, and SGW has lower SiO_2 and higher Mg^{2+} levels, than those of the streamflow.

Table 6.2 Rainstorm characteristics of the Akakabe catchment

		Event A99-1	Event A99-2
Observed period	(from)	Jun 17, 1999	Jun 22, 1999
	(to)	Jun 22, 1999	Jun 27, 1999
Total rainfall	(mm)	44.3	111.4
Max. rainfall intensity	(mm/hr)	5.5	10.7
Total discharge	(mm)	5.4	62.7
Max. discharge intensity	(mm/hr)	0.5	1.9
Antecedent precipitation (5 days)	(mm)	1.7	46.6
Antecedent precipitation (10 days)	(mm)	50.8	48.3

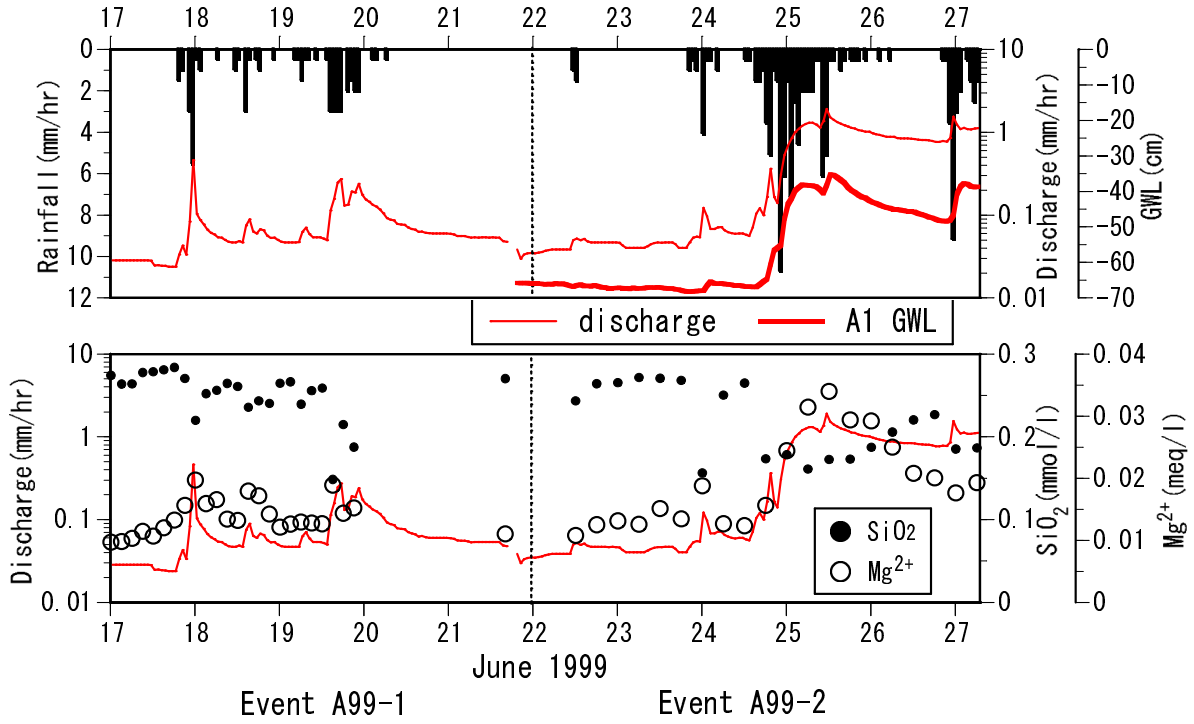

Figure 6.6 Temporal variations in rainfall, discharge rate, groundwater levels and SiO_2 and Mg^{2+} concentrations of the Akakabe catchment

A mixing diagram using SiO_2 and Mg^{2+} concentrations as the tracers is shown in Figure 6.7. The concentrations of solutes in the throughfall and in groundwater in A1-110 and A1-175 shown in Figure 6.7 are averaged values and their standard deviations were based on samples taken before the rainstorms. The bedrock groundwater was not sampled in this catchment, so the streamwater concentrations at August 10 2000, when conditions in the catchment were driest and the contribution of the bedrock groundwater was probably at its highest, are assumed to result from the bedrock groundwater as the missing end-member. In Event A99-1, the streamwater was formed by mixing with the missing end-member (the bedrock groundwater) and throughfall. In Event A99-2, in contrast, the effects of SGW with a higher Mg^{2+} concentration are seen. The separate contribution from each component cannot be quantified, because the bedrock groundwater concentrations were not determined; however, the SGW component contributed significantly during the periods of heavier rainfall. That is, the groundwater level in SGW rose with the onset of heavy rain, and the runoff from the groundwater body, strongly affected by the saturated throughflow occurring on the soil-bedrock interface during the rainstorm, rose considerably; thus, the stormflow chemistry is affected by the groundwater chemistry.

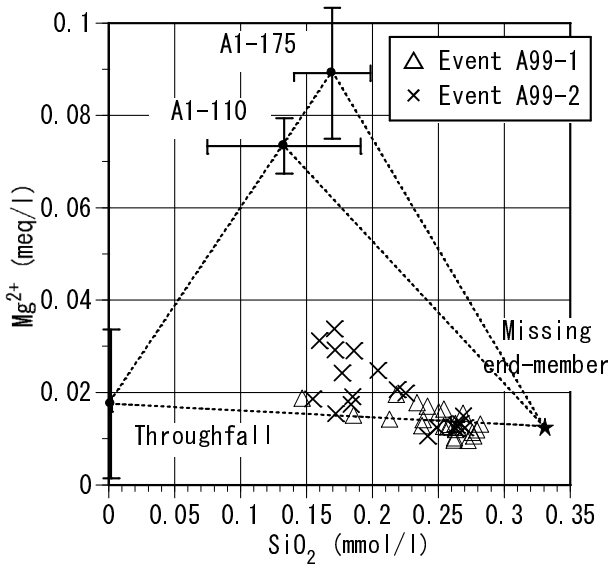

Figure 6.7 Mixing diagram of the Akakabe catchment

6.3.3 Hydrological Processes in the Rachidani and Toinotani Catchments

The saturated hydraulic conductivity of the soil in the Rachidani catchment is of the order of 10^{-1} cm/sec in the surface layer (a few cm from the soil surface) both in the upslope and downslope. Under the surface layer of the downslope, hydraulic conductivity is similar to that in the surface layer, but under the surface layer of the upslope it is much lower (of the order of 10^{-3} cm/sec), and the soil-bedrock border is clearly marked (Kimoto et al, 1999). These authors made intensive hydrometric observations, and showed that subsurface stormflow was generated in the upslope zone where soils are thin, and that saturated overland flow occurred in that part of the catchment during heavy rains. Based on *in situ* sprinkling experiments, Uchida et al. (1999) showed that during small rainstorms only subsurface stormflow occurs; in heavier storms, saturation overland flow is generated, but Horton-type overland flow is insignificant. As in the Matsuzawa catchment, preferential flow pathways were not detected and the dominant flow pathway apparent in this catchment was groundwater flow from the soil matrix.

In the Toinotani catchment, Uchida et al. (1998) demonstrated that pipe-flow rate increased with increasing rainfall intensity and regulated the discharge rate of the catchment. In addition, with the occurrence of pipe flow the transmissivity of the whole hillslope was enhanced, and the discharge from the spring increased more than the contribution of the pipe flow. Regarding the mechanisms of pipe-flow generation, when the throughfall infiltrated to the aquiclude layer, a saturated condition occurred and water entered the soil pipe and discharged (Uchida et al. 1996). During the rainstorm of this study, no discharge was detected from Pipe group B, so only discharge from Pipe A is discussed.

6.3.4 Comparison of Rainstorm Characteristics

The characteristics of the rainstorms in the Matsuzawa, Rachidani, and Toinotani catchments are summarized in Table 6.3. The season, observed period, total rainfall, and maximum rainfall intensity were similar in each catchment for all the rainstorms. Antecedent precipitation was also similar in the Matsuzawa and Rachidani catchments, since they are in close proximity to each other.

Table 6.3 Comparison of Rainstorm characteristics

		Matsuzawa	Rachidani	Toinotani
Observed Period	(from)	Sep 21, 1998	Sep 21, 1998	Sep 16, 1997
	(to)	Sep 23, 1998	Sep 23, 1998	Sep 18, 1997
Total rainfall	(mm)	92.5	89.0	75.5
Max. rainfall intensity	(mm/30min)	7.0	7.0	7.5
Total discharge	(mm)	28.6	38.7	5.5
Max. discharge intensity	(mm/30min)	0.5	2.9	0.3
Antecedent precipitation (5 days)	(mm)	47.0	48.5	25.5
Antecedent precipitation (10 days)	(mm)	65.0	62.5	90.5

6.3.5 Temporal Variations in Streamwater Chemistry

Figure 6.8 shows the temporal variations in the groundwater levels around the spring outflow points (G1 in the Matsuzawa and R1 in the Rachidani catchment) and the flow rate in Pipe A in the Toinotani catchment, in addition to the rainfall, discharge rate, and solute concentrations. The concentrations of Na^+, SO_4^{2-}, and SiO_2, which were higher in the deeper layer than in the surface layer, and of NO_3^- and NH_4^+, which were higher in the surface layer than in the deeper layer, are discussed in this study.

The groundwater levels in the Matsuzawa and Rachidani catchments varied considerably, and peaked sharply in the Rachidani catchment. The hydrographs were similar to the groundwater level variations in both catchments. The maximum discharge intensity was larger by one order of magnitude in the Rachidani catchment than in the Matsuzawa catchment.

The concentrations of Na^+, SO_4^{2-}, and SiO_2 were considerably lower at the peak discharge and decreased to some extent during the falling limb from the levels applying before the peak in the Matsuzawa catchment. The NO_3^- concentrations were slightly higher after the peak discharge and NH_4^+ was barely detected during the observation period.

The concentrations of Na^+, SO_4^{2-}, and SiO_2 were lower at the peak discharge in the Rachidani catchment. The NO_3^- concentrations were slightly higher after the rainfall stopped. The NH_4^+ concentrations were relatively higher before the peak discharge and not detected after it.

In the Toinotani catchment, all solute concentrations were affected by pipe flow. The concentrations of Na^+, SO_4^{2-}, and SiO_2 decreased when pipe flow occurred, and lower concentrations of Na^+ and SiO_2 were observed after the rainstorm. The NO_3^- concentrations increased when pipe flow occurred and NH_4^+ concentrations increased considerably after the pipe flow stopped.

In the Matsuzawa and Rachidani catchments, the variations of solute concentrations were relatively small, except at the peak discharge, when they varied for a short time. In contrast, the solute concentrations varied considerably with the occurrence of pipe flow, and even after pipe flow stopped, particularly in the case of NO_3^- concentrations, which did not return to the concentration recorded before pipe flow occurred in the Toinotani catchment.

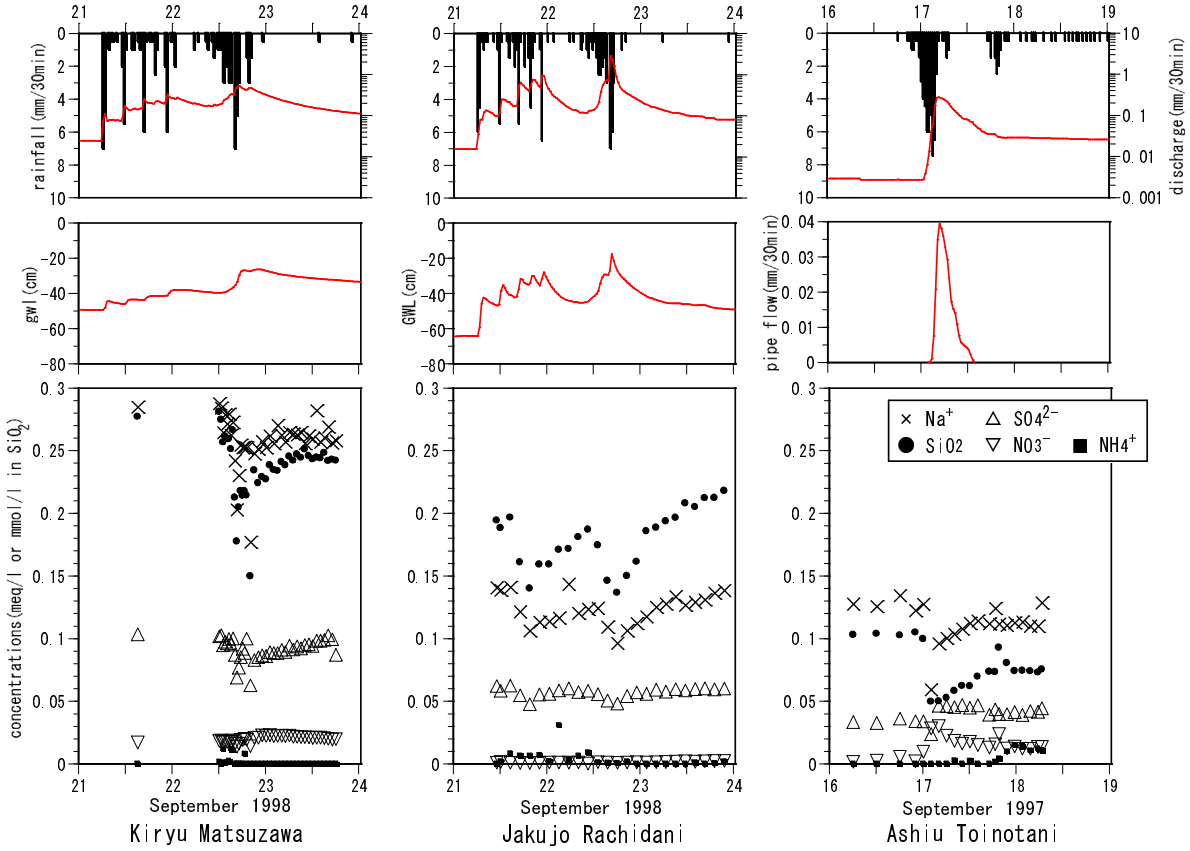

Figure 6.8 Temporal variations in rainfall, discharge rate and solute concentrations of each catchment

6.3.6 Analyses of Chemical Variations in Each Catchment with EMMA

EMMA was applied to each event, using Na^+ and SO_4^{2-} as tracers. The mixing diagrams are shown in Figure 6.9. The end-members in each catchment were as follows:

Matsuzawa: SGW and throughfall (two components)

Rachidani: SGW and rainfall (two components)

Toinotani: SGW, pipe flow, and throughfall (three components).

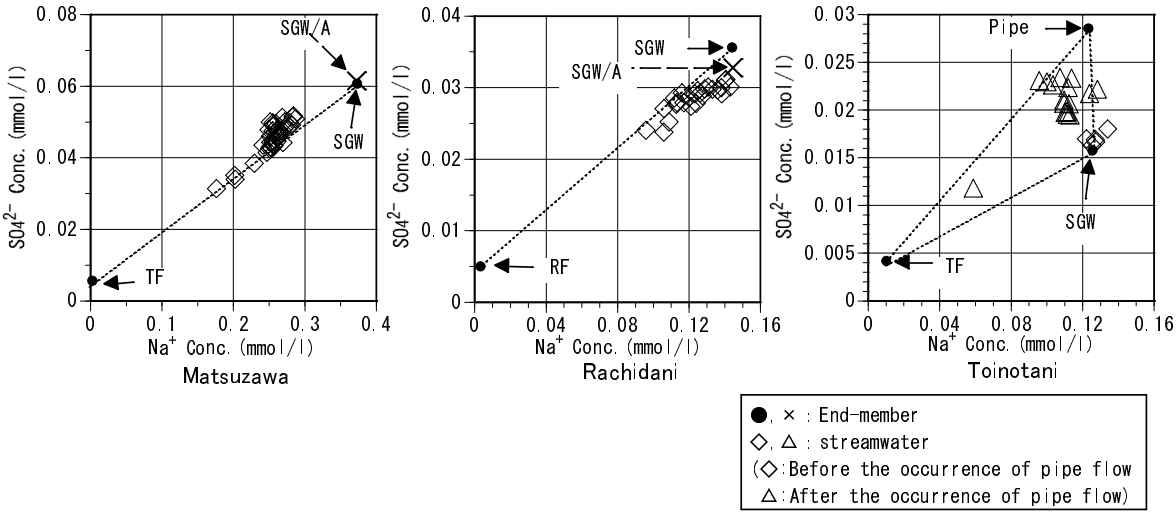

Figure 6.9 Mixing diagrams of each catchment

note: "RF", "TF", and "Pipe" denotes rainfall in Rachidani, throughfall in Matsuzawa and Toinotani, and the soilwater around the soil pipe, respectively. "SGW/A" denotes the groundwater of the saturated zone after the storm event.

In every catchment, throughfall or rainfall was one of the end-members, because they all had small stream channels and the channel precipitation mixed directly with the stormflow.

Baseflow chemistry is similar to perennial groundwater chemistry in the Rachidani catchment, and similar to that in the Matsuzawa catchment (Asano et al., 1998). Thus, the SGW groundwater was one of the end-members in both of these catchments. Groundwater flow from the perennial groundwater body to the stream was also observed in the Toinotani catchment, except in an extremely dry summer, so the SGW groundwater was one of the end-members. The groundwater concentrations in G2-177 in Matsuzawa and R1 in Rachidani were used in the analyses. The TGW component did not contribute to stormflow in the Matsuzawa catchment during this period of observation, as seen in Event M97-2, outlined above.

Pipe flow, the third end-member, could not be sampled directly; however, soilwater from around the soil pipe would have been discharged from the pipe (Uchida et al., 1997), so soilwater samples from around the soil pipe during the observation period were used in the analyses.

The contributions of each end-member were calculated by solving the mass balance equations. In the case of the Matsuzawa and the Rachidani catchments, the contributions were calculated using Na^+ and SO_4^{2-} concentrations in each and averaged over the two results. The results of the hydrograph separations are

shown in Figure 6.10. The SGW component was dominant during the period of observation, except during the peak discharge, when the contributions of the throughfall or rainfall component increased in both the Matsuzawa and Rachidani catchments. The pipe flow component was dominant when present and, even after pipe flow stopped, the contribution of this component was sizeable. In a comparison of the pipe-flow rates observed (Figure 6.8) with those calculated from EMMA, the calculated rate was the larger. For example, at the peak of pipe flow the observed rate was 0.039 mm/30 min in observed value, whereas the calculated value was 0.206 mm/30 min. The total pipe flow observed was 0.356 mm, whereas 2.377 mm was calculated. This indicates that some soilwater around the soil pipe discharged without passing through Pipe A during and after pipe flow occurred. That is, the observed pipe flow was one part of a component with the same source which discharged through different pathways. This corresponds with the results obtained by Uchida et al. (1998), who found that when the pipe flow occurred the transmissivity of the whole hillslope was enhanced and the discharge from the spring outflow was increased by contributions other than that from pipe flow.

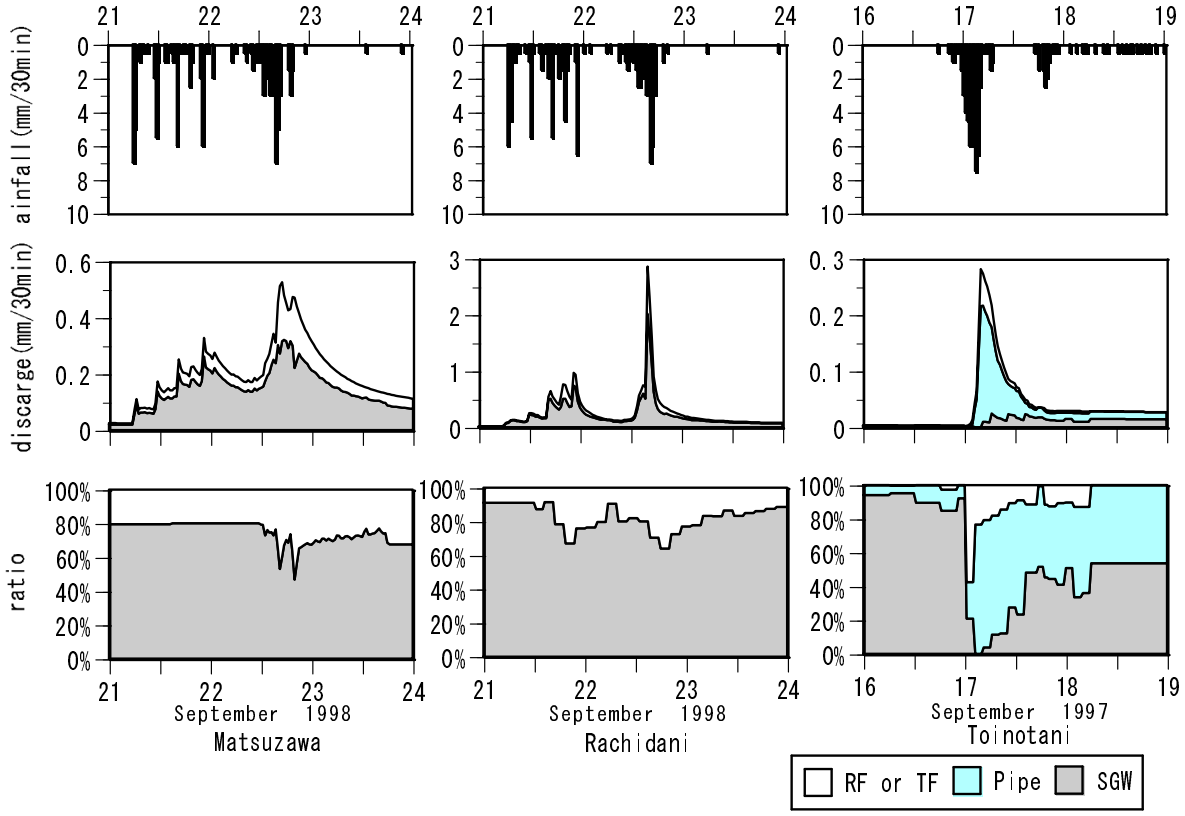

Figure 6.10 Hydrograph separations of each catchment

In the Matsuzawa and the Rachidani catchments, the stormflow chemistry comprised the mixing of the perennial groundwater and the throughfall or rainfall, and the perennial groundwater was dominant throughout the observation periods. Therefore, the groundwater, which had relatively constant chemistry, always came from the SGW in these catchments. As mentioned previously, saturated throughflow occurring in the upslope of the catchment during the rainstorm mixed with the perennial groundwater body; thus, it did not contribute directly to the stream during relatively small rainstorms. Therefore, the stormflow chemistry did not fluctuate appreciably, other than at the rainfall peak.

On the other hand, in the mixing diagram for the Toinotani catchment (Figure 6.9), the streamwater samples were plotted around the SGW component before the occurrence of pipe flow, and after pipe flow, the streamwater samples were plotted close to the Pipe component. This indicates that water from a source other than SGW was transported to the stream through the soil pipe. Based on the hydrograph separations (Figure 6.10), a water component with the same source as the pipe-flow component continued to contribute to streamflow after the pipe flow stopped. In this way, the streamwater chemistry was changed considerably when pipe flow discharged and, even after the pipe flow stopped, solute concentration levels did not return to pre-pipe-flow values. The saturated throughflow discharged through the soil pipe contributed directly to the streamwater, and strongly affected streamwater chemistry.

6.3.7 Effects of Hydrological Differences on the Stormflow Chemistry

To discuss the effects on streamwater chemistry of other factors besides conservative mixing (*e.g.*, biogeochemical factors), the SiO_2 and NO_3^- concentrations were simulated from the mixing ratio and observed concentrations in each end-member. The results of the simulations are shown in Figure 6.11. The SiO_2 concentrations were reproduced well in three catchments, but in the Rachidani catchment the simulated results did not fit as well, especially after the rainfall stopped. As discussed in **Chapter 4**, the chemistry in the SGW deep layer is constant in the Matsuzawa catchment, and it did not vary after the rainstorm (see SGW/A in Figure 6.9). However, in the Rachidani catchment the SO_4^{2-} concentrations decreased after the rainstorm, and the streamwater samples plotted were closer to SGW/A, than SGW. Using the concentrations in SGW/A and RF produced a better fit than that obtained by using SGW and RF (see Figure 6.11). This indicates that in the Rachidani catchment SGW chemistry is easily affected by

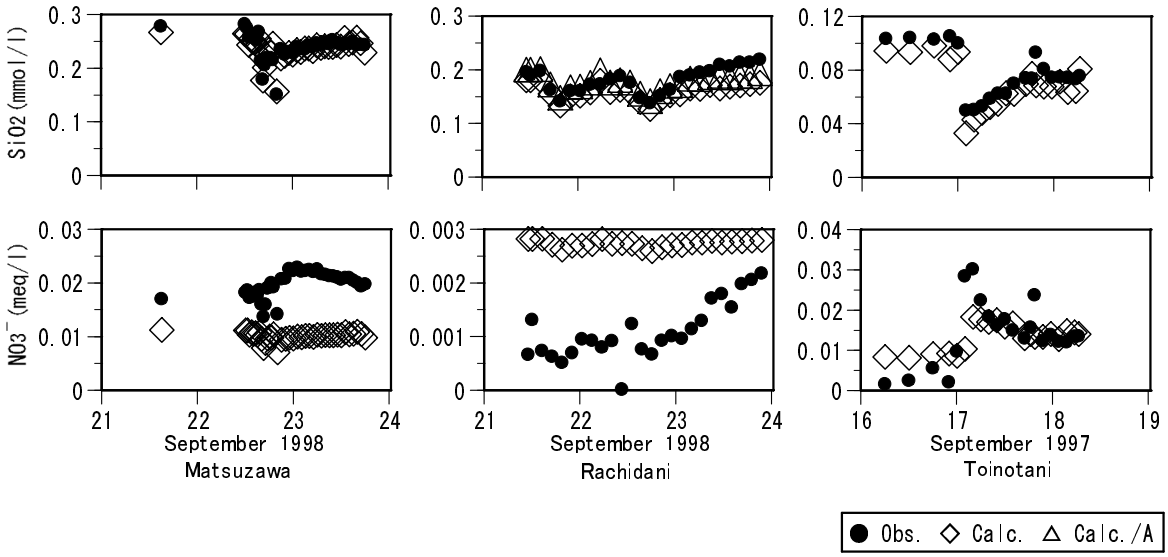

Figure 6.11 Calculated SiO_2 and NO_3^- concentrations of each catchment

note: "Calc./A" denotes the calculated values using the concentration of the groundwater of the saturated zone sampled after the rainfall stopped

rainstorms, because the groundwater body is smaller than in the Matsuzawa catchment. In catchments where matrix flow is the dominant pathway, stormflow chemistry is more easily affected when there is a smaller groundwater body, since the groundwater chemistry is relatively less stable in response to rainstorms.

The simulated NO_3^- concentrations fitted less well to the observed values in the Matsuzawa and Rachidani catchments. NO_3^- concentrations are easily affected by biological mechanisms and the effects are distributed unevenly within the soil profile; it is difficult to reproduce these effects using a conservative mixing model. In a catchment where matrix flow is dominant, the NO_3^- concentration in the source profiles can change within a short time, so it is difficult to reproduce the streamwater NO_3^- concentration by considering only the hydrological pathways.

In contrast to the cases of the Matsuzawa and the Rachidani catchments, the falling limb could be well-simulated in the Toinotani catchment. This implies that soilwater with high NO_3^- concentration was transported via the soil pipe, and the NO_3^- concentrations did not change in appearance after the occurrence of pipe flow. The increase of streamwater NH_4^+ concentration during the falling limb implies that biological activities like nitrification are inhibited or moderated by changes in environmental conditions as the soil-water contents change, and the NO_3^- concentrations were not changed within the end-members. In the catchment in which preferential flow was dominant, the surface soilwater with high NO_3^- concentrations was mixed directly into the streamwater, with a direct effect on the

streamwater chemistry.

To investigate the nitrogen dynamics of subsurface stormflow via preferential flow pathways on forested hillslopes that receive elevated levels of atmospheric N deposition, Hill et al. (1999) conducted observations in a subcatchment of the Plastic Lake Watershed, Canada. They demonstrated that more than 97% of subsurface stormflow occurred at the soil-bedrock interface, and a considerable fraction of this subsurface flow was event water that infiltrated by preferential flow paths to the bedrock surface; however, the NO_3^- losses were low, because the surface-soil horizon was a strong sink for inorganic N in throughfall. In contrast, surface soilwater discharges with high NO_3^- concentrations occur and streamwater NO_3^- concentrations increase during rainstorms in the catchments where lateral preferential flow paths exist within the surface soil layer, as in the Toinotani catchment. On the other hand, if matrix flow is dominant, NO_3^- concentrations can easily change within the end-members or during transport to the stream if biological activities such as denitrification (Koba et al., 1997) occur during the short time the water spends in the catchment, as in the Matsuzawa and Rachidani catchments.

The relationship between stormflow chemistry and the dominant hydrological pathways were investigated based on comparative studies of four catchments with different prevailing hydrological processes. In catchments where the groundwater flow from the perennial groundwater body is dominant, saturated throughflow is mixed with the groundwater body and does not contribute to the stormflow directly, so stormflow chemistry does not fluctuate much, except at rainfall peaks. In catchments where bedrock flow is dominant, the discharge from the groundwater body on top of the bedrock contributes when the groundwater level rises considerably during a heavy rainstorm, and thus streamwater chemistry is affected. In catchments where preferential flow such as pipe flow is dominant, stormflow chemistry depends absolutely on whether or not preferential flow occurs.

6.4 Estimation of the Contributing Area: Mixing Model Approach with a New Tracer- Fluorescence of Dissolved Organic Carbon

6.4.1 Introduction

This section describes the assessment of the spatial distributions of dissolved organic carbon (DOC) by the application of three-dimensional fluorescence spectrometry to waters sampled in the Matsuzawa catchment. Once the sources of streamflow components have been determined, riparian control of

stormflow quality can be introduced using the fluorescence properties as a tracer.

The mixing model approach has been used for many catchments using various tracers (*e.g.*, Hinton et al., 1994; Hensel and Elsenbeer, 1997; Ohrui and Mitchell, 1999). These studies showed that the sources of streamwater are groundwater, soilwater, and throughfall; in particular, the importance of soilwater has been emphasized in studies in recent decades (*e.g.*, DeWalle et al., 1988; Mulholland, 1993; Bazemore et al., 1994). The soilwater component corresponds to the TGW of this study, because it develops in response to rainstorms, and the soilwater, which was unsaturated before the rainstorms, contributes to the discharge (see Paragraph 6.2).

The use of DOC as a tracer for estimating runoff sources and to separate the contribution from soilwater has been validated. Brown et al. (1999) used DOC concentration and $d^{18}O$ in hydrograph separations and estimated the contribution from oxygen in the soil. Easthouse et al. (1992) used fractions of DOC, combined with inorganic tracers, to estimate the sources of runoff more accurately. In general, however, DOC is a complex mixture of organic materials of many differing molecular weights and structures; it is difficult to discriminate between two DOC components if they have the same concentrations and different compositions, and for this reason DOC is not always a satisfactory tracer.

In the fields of marine chemistry and limnology, three-dimensional fluorescence spectrometry is used to characterize the different components of dissolved organic carbon (*e.g.*, Coble et al., 1990; Mopper and Schultz, 1993). The method involves determining the intensity of fluorescence as a function of excitation and emission wavelengths, with results presented as a three-dimensional contour graph. The characteristic signatures of different humic or protein components from different water sources can then be determined (Coble, 1996). Application of this method might circumvent earlier problems in using DOC as a tracer. Generally, DOC is distributed in different amounts across a catchment, and it seems that three-dimensional fluorescence spectrometry may permit more precise estimation of source locations and amounts.

6.4.2 Rainstorm Characteristics

Rainstorm characteristics are summarized in Table 6.4 and temporal variations in rainfall, discharge rate, and groundwater levels at points GF and GD are shown in Figure 6.12. The origin for groundwater levels is the soil surface at each point. Points GF and GD are located at the upslope of SGW and TGW,

respectively. The groundwater level at GD rose rapidly, by a considerable amount, during storms, and fell more steeply relative to that at GF, which remained high even after a rainstorm ceased (see **Chapter 3**). Runoff as a proportion of total rainfall was very high (62%). The antecedent precipitation for the five previous days was 171.2 mm, and the groundwater level at points G1 and GA, located around the spring outflow, reached the soil surface.

Table 6.4 Rainstorm characteristics

Observed period	(from)	0:00 on Jun 28, 1999
	(to)	23:00 om Jul 1, 1999
Total rainfall	(mm)	108.9
Max. rainfall intensity	(mm/hr)	15.3
Total discharge	(mm)	67.5
Max. discharge intensity	(mm/hr)	2.0
Antecedent precipitation (5 days)	(mm)	171.2
Antecedent precipitation (10 days)	(mm)	208.5

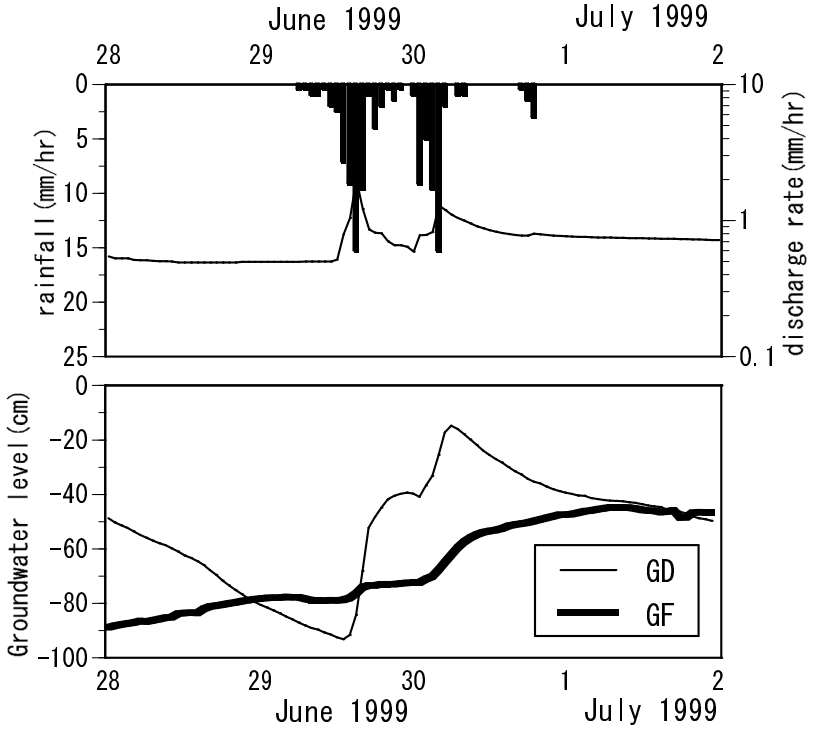

Figure 6.12 Temporal variation in rainfall, discharge rate, groundwater levels at points GF and GD

6.4.3 Sources of Stormflow Estimated from Fluorescence Properties

As mentioned previously, stormflow in the Matsuzawa catchment consists of three components, SGW, throughfall, and TGW, and the contribution of each component changes in response to the amount of rainfall.

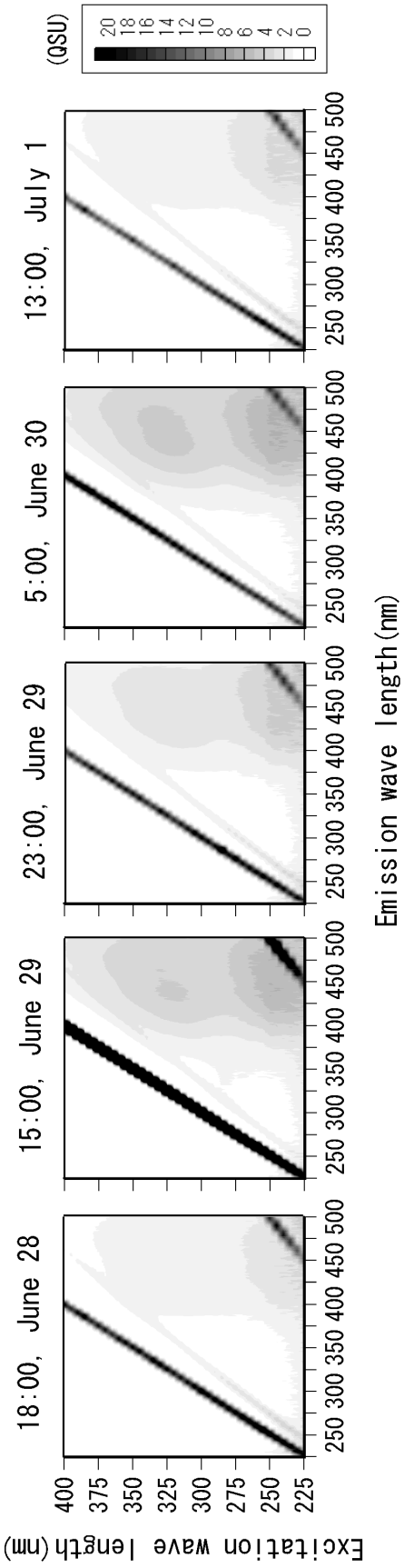

Figure 6.13 Temporal variation of Excitation-Emission Matrix of streamwater

Figure 6.13 shows the temporal variation of the Excitation-Emission Matrix (EEM) in streamwater. The two straight black lines seen in the EEM are due to Rayleigh scattering of the excitation, and Raman scattering in the water produces the gray line below one of these black lines. There is a fluorescence peak at excitation/emission (Ex/Em) = 320±10/435±10 nm in all the streamwater samples. Since the peak positions reflect the composition or structure of dissolved substances, it seems that all the streamwater samples contained similar DOC compounds. Suzuki et al. (1997) found that the peak positions of fulvic acid extracted from brown forest soil and from river water samples were almost the same as those found in this study. Similarly, the fulvic acid peak has been detected at almost the same position in many studies (*e.g.*, Coble et al., 1990; Senesi et al., 1990; Mopper and Schultz, 1993). Following these earlier studies, the fluorescence peak detected in this study can be identified as due to fulvic acid. Fulvic acid is one of the fractions of humic material, and is soluble under all pH conditions. More than 90% of humic substances in streamwater are fulvic acids

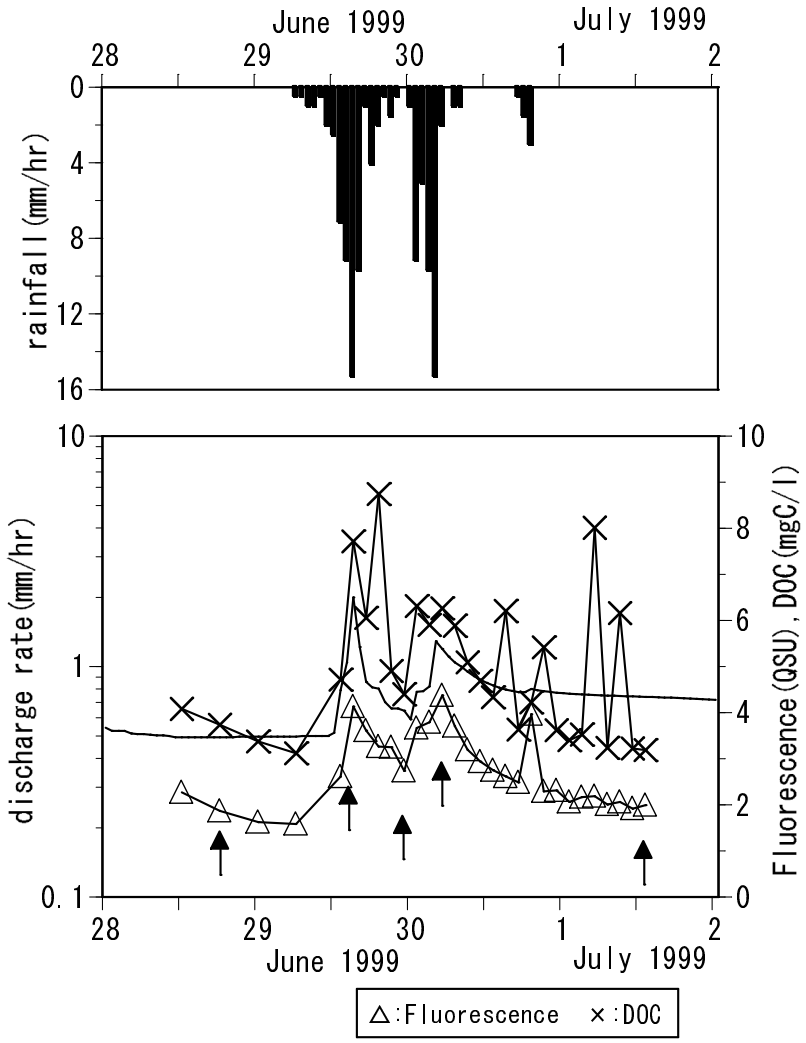

Figure 6.14 Temporal variation in the relative fluorescence intensity and DOC concentration of streamwater

(Malcolm, 1990). Figure 6.14 shows the temporal variations in the maximum fluorescence peak intensity around the Ex/Em = 320±10/435±10 nm point, rainfall, discharge, and DOC concentrations. The arrows in Figure 6.14 indicate the peak of EEM shown in Figure 6.13. A positive correlation between the fluorescence intensity and the discharge rate is seen in Figure 6.14. A positive correlation between fluorescence intensity and DOC concentration has been found in seawater (Chen et al., 1993) and in streamwater (Suzuki et al., 1997). From these results, it seems that the fluorescence intensity reflects the fulvic acid concentrations of streamwater in this catchment.

The EEM of SGW and TGW, sampled on June 29 1999 (before a rainstorm), and July 1 1999 (after the rainstorm), and that of rainfall and throughfall sampled on July 1, 1999, are shown in Figure 6.15. Two EEMs are shown in each

groundwater zone, sampled at the upslope sites (GF for SGW, GC for TGW) and in the downslope zone (G2-177 for SGW and GA for TGW), respectively. The characteristics of the observation wells and the variation in groundwater levels during the rainstorm gauged at each well are shown in Table 6.5. There was no clear fluorescence peak in the streamwater at 18:00 on June 28, before the rainstorm (Figure 6.13). Moreover, there were no clear fluorescence peaks in either the upslope or downslope SGW samples before the rainstorm (Figure 6.15 a, c). In the EEM of downslope SGW sampled after the rainstorm (Figure 6.15 b), there was a slight rise relative to the level seen before the rainstorm, but the intensity was weak and the peak was not well defined. The upslope SGW (Figure 6.15 d) showed no clear peak, even after the rainstorm.

There were clear fluorescence peaks in the downslope TGW at Ex/Em = 320±10/435±10 nm, the same position as that for the streamwater (Figure 6.13), sampled before and after the rainfall (Figure 6.15 e, f); this indicates that TGW contained fulvic acid. The upslope TGW also had the same fluorescence peak (Figure 6.15 g, h), and the peak intensity was higher after the rainfall than it was before the rainfall, showing that the organic carbon present in the surface soil layer dissolved in the groundwater as the groundwater level rose.

In the throughfall (Figure 6.15 i), there were fluorescence peaks at Ex/Em = 285/410 and 340/410 nm. These peak positions differ from the fulvic acid peak of streamwater, so the organic matter dissolved in throughfall is not fulvic acid. As the rainfall (Figure 6.15 j) did not have the same peak as the throughfall, the substance producing the fluorescence in the throughfall was probably washout or leached material from the trees.

Table 6.5 Characteristics of observation wells

		Point	Soil depth(cm) (N_4=100)	Well depth(cm)	Groundwater level from soil surface (cm)	
					before the storm	peak of the storm
SGW	Upslope	GF	356	200	−95	−70
	Downslope	G1	470	75	(overflow)	(overflow)
TGW	Upslope	GC	82	217	−67	0
	Downslope	GA	74	76	−11	−6

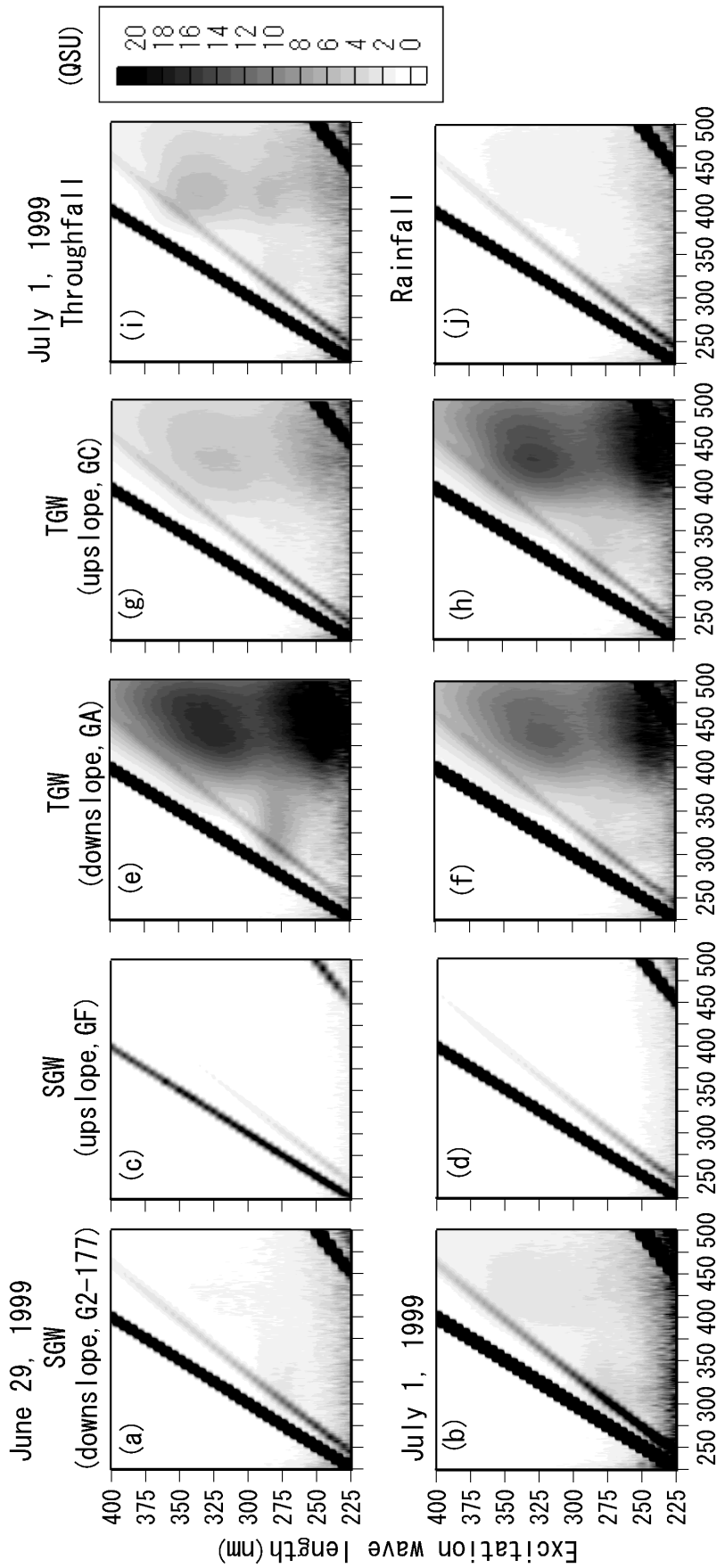

Figure 6.15 Excitation-Emission Matrix of groundwater, throughfall, and rainfall

These results show that the fulvic acids detected in the streamwater were supplied mainly from the TGW component, not from the SGW component or from throughfall, the other runoff components of this catchment (Paragraphs 6.2, 6.3; Katsuyama et al., 2000; Katsuyama et al., 2001). The fluorescence increased in upslope TGW when the groundwater level rose toward the soil surface and the fluorescent substances dissolved into the groundwater. In contrast, high fluorescence intensity was detected in the downslope TGW throughout the observed period. Therefore, downslope TGW was the major source of streamwater fulvic acids.

6.4.4 Contribution of Each Runoff Component

EMMA was applied to evaluate the contribution of each runoff component by using SiO_2 and DOC concentrations and the maximum fluorescence intensity at Ex/Em = 320±10/435±10 nm as tracers. The mixing diagrams plotted by the combinations of SiO_2 - DOC and SiO_2 - fluorescence intensity are shown in Figure 6.16. The concentrations and error bars of SGW and TGW represent the averages and standard deviations from samples taken before and after the rainstorm; those for throughfall are the weighted-mean values and standard deviations from four points (see Figure 2.4). The fluorescence intensity of throughfall is derived from the value obtained at only one point, and is the basis of the peak of Ex/Em = 340/410 nm, which is not a fulvic acid peak. The concentrations at G2-177 are used for SGW and those at GA are used for TGW in the analysis.

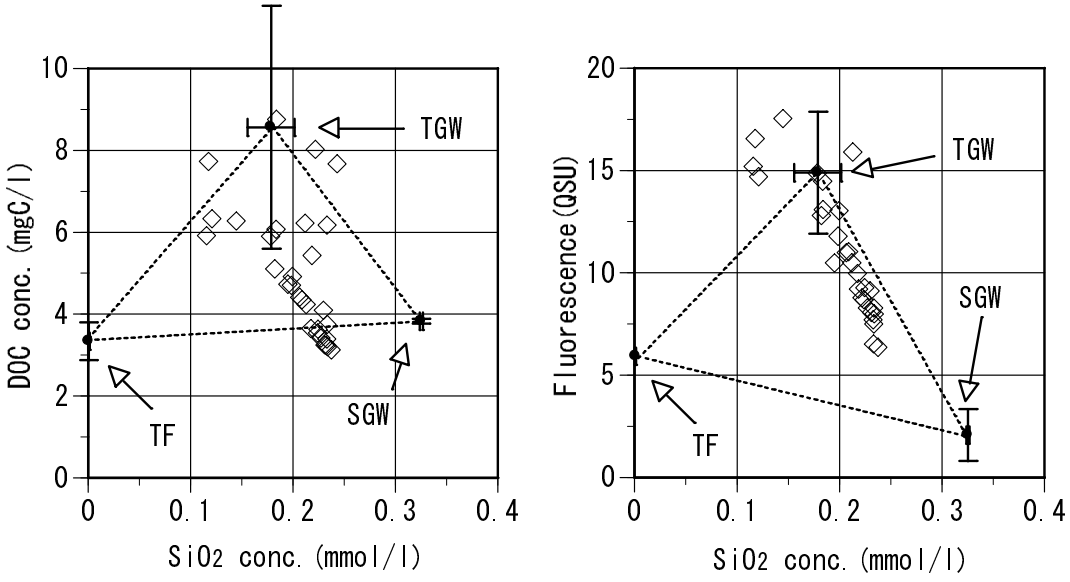

Figure 6.16 Mixing diagrams plotted by the combinations of SiO_2 - DOC and SiO_2 - fluorescence intensity

Both diagrams show that the streamwater is composed of a mixture of three runoff components: SGW, throughfall, and TGW. In the case of SiO_2 and fluorescence intensity, the streamwater plots around the SGW-TGW line and the contribution of TGW is larger than in the case of SiO_2 and DOC. DOC is a complex mixture of various organic materials of different molecular weights and structures, and the fulvic acid in streamwater is supplied mainly by the TGW component. The organic matter in throughfall is leached from trees, and is not fulvic acid. Therefore, for quantifying the contribution of the TGW component in this catchment, fluorescence intensity is more important than DOC as a tracer, after removing the effect of DOC from throughfall.

The contribution of each runoff component was calculated using SiO_2 concentration and fluorescence intensity. The contributions of the SGW, throughfall, and TGW components to the total discharge were 28.7%, 7.9%, and 63.4%, respectively; the contribution from TGW was clearly dominant. During the rainfall period, from 6:00 on June 29 to 19:00 on June 30, 1999, the contribution of TGW was even larger; the contributions of the SGW, throughfall, and TGW components were 7.9%, 6.6%, and 85.5%, respectively. This underlines the importance of the TGW component to the peak flow.

6.4.5 Source Area of the Transient Saturated Zone

The source area of TGW is calculated assuming that the saturated throughflow discharges as laminar flow from the transient saturated zone. The discharge rate of TGW is calculated from the total discharge rate and the contribution of the TGW component. This contribution was calculated by substituting the average SiO_2 concentrations and the fluorescence intensity in the mass-balance equations. At measuring point GA in the riparian zone, the groundwater level was reached and the soil became saturated to the surface; the water depth of the laminar flow of TGW was therefore assumed to be 74 cm, equal to the soil depth at this point. The saturated soilwater content was taken as 0.6 from the soil surface to a depth of 15 cm, and 0.5 at deeper than 15 cm (Ohte and Suzuki, 1990).

The temporal variations of the ratio of the TGW source area to the total catchment area are shown in Figure 6.17. The variation in the source-area ratio was less than 1% throughout the observation period and only 0.56% at the maximum. During the four-day observation period, the total TGW source area was 11.1% of the catchment area. According to Kim (1990), the groundwater body

enlarges to a maximum of 24% of the catchment area. Therefore, the TGW component of the groundwater increase drains from a small well-defined area within the riparian zone during storm runoff. Since 63.5% of the total discharge was supplied from this small area and fluorescence was barely detected in SGW even after the rainstorm, the downslope (riparian) TGW component must discharge directly to the stream through the highly permeable surface soil layer, with negligible mixing with SGW. Many studies (*e.g.*, Hooper et al., 1998; Tanaka and Ono, 1998) have demonstrated the importance of the contribution from groundwater, or soilwater, from the riparian zone, to storm runoff generation processes and their chemistry. It is evident from this study that the source area of these components is very small, less than 1% of the total catchment area at any one time.

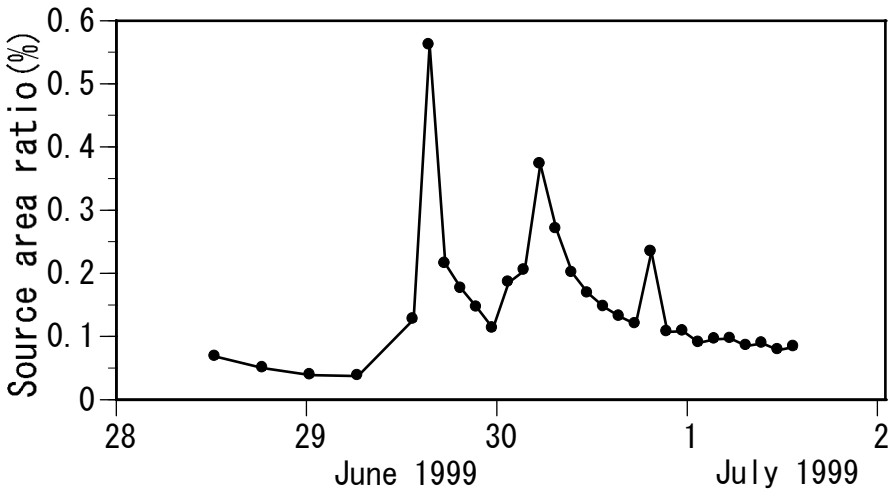

Figure 6.17 Temporal variations of the ratio of TGW source area to total catchment area

6.5 Conclusions

In recent studies, the fluorescence of DOC has been used estimate the sources of groundwater (Baker and Genty, 1999) and streamwater (Newson et al., 2001). The results of this study show that three-dimensional fluorescence spectroscopy is also a useful tool for estimating the sources and source area of stormflow, in combination with EMMA. The ratio of the source area of the transient saturated zone to the total catchment area was less than 1% during a storm event, so the increment in groundwater was drained quickly from a small area in the Matsuzawa catchment. The source area of the stormflow in this

catchment was very small, although the total rainfall was more than 100 mm. This small area seems important to streamwater chemistry as the source of biochemically-reactive substances (*e.g.*, NO_3^-), which could not be well simulated in the Matsuzawa and Rachidani catchments with the mixing model. In Event M97-2 (Paragraph 6.2), the total rainfall was 249.5 mm and the source area was enlarged to include the upslope of TGW, GC. In that case, the saturated zone was enlarged by the effects of saturated throughflow that was generated on the soil-bedrock interface during the rainstorm, and the end-member of the streamwater was changed. The results of comparative studies showed that differences in the dominant runoff processes of each catchment controlled the stormflow chemistry. The chemistry of the riparian groundwater end-members was more variable in the catchment with the smaller riparian zone, because of the effects of the saturated throughflow generated on the soil-bedrock interface during the rainstorm. The three factors—the spatial distribution of the sources of solutes, the hydrological pathways, and the time sequential variations in the contribution of the each flow component—were affected by the change of end-members; that is, the variation in the source area (Hewllet and Hibbert, 1967), and consequently the streamwater chemistry was changed.

In order to understand hydrochemical processes, it is generally considered important to collect information on the hydrological pathways of catchments (*e.g.*, Buttle, 1994). In earlier studies using EMMA (*e.g.*, Hooper et al. 1990), end-members were fixed and the contribution of each end-member during the rainstorm changed. The EMMA method is adaptable to hydrochemical analysis of streamwater in a catchment where end-members change incrementally, if combined with information on the hydrological processes.

References

Asano, Y., Ohte, N., Katsuyama, M. and Kobashi, S. (1998) Impacts of forest succession on the hydrogeochemistry of headwaters, Japan, *In* Headwaters: water resources and soil conservation (proceedings of Headwater '98, the fourth international conference on headwater control, Merano, Italy, April 1998), Haigh, M. J., Krecek, J., Rajwar, G. S., Kilmartin, M. P. (Eds.), A. A. Balkema Rotterdam, pp. 85-95.

Baker, A. and Genty, D. (1999) Fluorescence wavelength and intensity variations of cave waters, J. Hydrol., 217, pp. 19-34.

Bazemore, D. E., Eshleman, K. N. and Hollenbeck, K. J. (1994) The role of soil water in stormflow generation in a forested headwatar catchment: synthesis of natural tracer and hydrometric evidence, J. Hydrol., 162, pp. 47-75.

Brown, V. A., McDonnell, J. J., Burns, D. A. and Kendall, C. (1999) The role of event water, a rapid shallow flow component, and catchment size in summer stormflow, J. Hydrol., 217, pp. 171-190.

Buttle, J. M. (1994) Isotope hydrograph separations and rapid delivery of pre-event water from drainage basins, Prog. Phys. Geog., 18, pp. 16-41.

Chen, R. F., Bada, J. L. and Suzuki, Y. (1993) The relationship between dissolved organic carbon (DOC) and fluorescence in anoxic marine porewaters: Implications for estimating benthic DOC fluxes, Geochim. Cosmochim. Acta., 57, pp. 2149-2153.

Christophersen, N. and Neal, C. (1990) Linking hydrological, geochemical, and soil chemical processes on the catchment scale: An interplay between modeling and field work, Water Resour. Res., 26, pp. 3077-3086.

Coble, P. G., Green, S. A., Blough, N. V. and Gagosian, R. B. (1990) Characterization of dissolved organic carbon matter in the Black Sea by fluorescence spectroscopy, Nature, 348, pp. 432-435.

Coble, P.G. (1996) Characterization of marine and terrestrial DOM in seawater using excitation-emission matrix spectroscopy, Mar. Chem., 51, pp. 325-346.

DeWalle, D. R., Swistock, B. R. and Sharpe, W. E. (1988) Three-component tracer model for streamflow on a small Appalachian forested catchment, J. Hydrol., 104, pp. 301-310.

Easthouse, K. B., Mulder, J., Christopersen, N. and Seip, H. M. (1992) Dissolved organic carbon fractions in soil and stream water during variable hydrological conditions at Birkens, Southern Norway, Water Resour. Res., 28, pp. 1585-1596.

Genereux, D. P. and Hooper, R. P. (1998) Oxygen and hydrogen isotopes in rainfall-runoff studies, *In* Isotope tracers in catchment hydrology, Kendall, C. and McDonnell, J. J. (Eds.), Elsevier, Amsterdam, pp. 319-346.

Hensel, D., Elsenbeer, H., 1997. Streamflow generation in tropical rainforests: a hydrochemical approach, *In* Hydrochemistry (Proceedings of the Rabat Symposium), Peters, N. E., Coudrain-Ribstein, A. (Eds.), IAHS Publ. 244, Wallingford, pp. 227-234.

Hewlett, J. D. and Hibbert, A. R. (1967) Factors affecting the response of small watersheds to precipitation in humid areas, *In* International Symposium on

Forest Hydrology, Sopper, W. E. and Lull, H. W. (Eds.), Pergamon Press, Oxford, pp. 275-290.

Hill, A. R., Kemp, W. A., Buttle, J. M. and Goodyear, D. (1999) Nitrogen chemistry of subsurface storm runoff on forested Canadian Shield hillslopes, Water Resour. Res., 35, pp. 811-821.

Hinton, M. J., Schiff, S. L. and English, M. C. (1994) Examining the contributions of glacial till water to storm runoff using two- and three-component hydrograph separations, Water Resour. Res., 30, pp. 983-993.

Hooper, R. P., Christophersen, N. and Peters, N. E. (1990) Modelling streamwater chemistry as a mixture of soilwater end-members - an application to the Panola Mountain catchment, Georgia, U.S.A, J. Hydrol., 116, pp. 321-343.

Hooper, R. P., Aulenbach, B. T., Burns, D. A., McDonnell, J., Freer, J., Kendall, C. and Beven, K. (1998) Riparian control of stream-water chemistry: Implications for hydrochemical basin models, *In* Hydrology, Water resources and Ecology in Headwaters (Proceeding of the HeadWater '98 Conference held at Merano, Italy, April 1998), Kovar, K. Tappeiner, U. Peters, N. E., Craig, R. G. (Eds.), IAHS Publ. 248, Wallingford, pp. 451-458.

Katsuyama, M., Ohte, N., Uchida, T., Asano, Y., Kimoto, A. (2000) Effects of the differences of hydrological processes on the streamwater chemistry, J. Japan Soc. Hydrol. & Water Resour., 13, pp. 227-239 (in Japanese with English summary).

Katsuyama, M., Ohte, N. and Kobashi, S. (2001) A three-component end-member analysis of streamwater hydrochemistry in a small Japanese forested headwater catchment, Hydrol. Process., 15, pp. 249-260.

Kim J. S. (1990) Variations of soil moisture and groundwater table in a small catchment, Ph. D. thesis, Kyoto Univ., Kyoto, Japan, 87pp.

Kimoto, A., Uchida, T., Asano, Y., Mizuyama, T. and Li, C. (1999) Surface runoff generation of devastated weathered granite mountains -Comparison between Dahou experimental basin in the southern part of China and Jakujo Rachidani experimental basin in Tanakami mountains-, J. Jpn. Soc. Erosion. Control. Engng., 51, pp. 13-19 (in Japanese with English summary).

Koba, K., Tokuchi, N., Wada, E. Nakajima, T. and Iwatsubo, G. (1997) Intermittent denitrification: The application of a 15N natural abundance method to a forested ecosystem, Geochim. Cosmochim. Acta., 61, pp. 5043-5050.

Malcolm, R. L. (1990) Variations between humic substances isolated from soils, stream waters, and groundwaters as revealed by 13C-NMR spectroscopy, *In*

Humic Substances in Soil and Crop Sciences: Selected Readings, MacCarthy, P., Clapp, C. E., Malcolm, R. L. and Bloom, P. R. (Eds.), Amer. Soc. of Agron., Inc. Soil Sci. Soc. Amer., Inc. Wisconsin, pp. 13-35.

Mopper, K. and Schultz, C. A. (1993) Fluorescence as a possible tool for studying the nature and water column distribution of DOC components, Mar. Chem., 41, pp. 229-238.

Mulholland, P. J. (1993) Hydrometric and stream chemistry evidence of three storm flowpaths in Walker Branch Watershed, J. Hydrol., 151, pp. 291-316.

Newson, M., Baker, A. and Mounsey, S. (2001) The potential role of freshwater luminescence measurements in exploring runoff pathways in upland catchments, Hydrol. Process., 15, pp. 989-1002.

Ohrui, K. and Mitchell, M. J. (1999) Hydrological flow paths controlling stream chemistry in Japanese forested watersheds, Hydrol. Process., 13, pp. 877-888.

Ohte, N., Suzuki, S. (1990) Hydraulic properties of forest soils (2) Method of determining the volumetric water content-pressure head relationship by the saturated-unsaturated hydraulic conductivity test using large-size soil sample, J. Jpn. For. Soc., 72, pp. 468-477 (in Japanese with English summary).

Senesi, N. (1990) Molecular and quantitative aspects of the chemistry of fulvic acid and its interactions with metal ions and organic chemicals Part 2. The fluorescence spectroscopy approach, Anal. Chim. Acta, 232, pp. 77-106.

Shanley, J. B. and Peters, N. E. (1993) Variations in aqueous sulfate concentrations at Panola Mountain, Georgia, J. Hydrol., 146, pp. 361-382.

Sklash, M. G. (1990) Environmental isotope studies of storm and snowmelt runoff generation, *In* Process studies in hillslope hydrology, Anderson, M. G. and Burt, T. P. (Eds.), John Wiley and Sons, Chichester, pp. 401-436.

Suzuki, Y., Nagao, S., Nakaguchi, Y., Matsunaga, T., Muraoka, S., Hiraki, K. (1997) Spectroscopic properties of fluorescent substances in natural waters (1). Geochemistry, 31, pp. 171-180 (in Japanese with English summary).

Tanaka, T., Ono, T. (1998) Contribution of soil water and its flow path to stormflow generation in a forested headwater catchment in central Japan, *In* Hydrology, Water resources and Ecology in Headwaters (Proceeding of the HeadWater '98 Conference held at Merano, Italy, April 1998), Kovar, K. Tappeiner, U. Peters, N. E., Craig, R. G. (Eds.), IAHS Publ. 248, Wallingford, pp. 181-188.

Uchida, T., Kosugi, K., Ohte, N. and Mizuyama, T. (1996) The influence of pipe flow on slope stability, J. Japan Soc. Hydrol. & Water Resour., 9, pp. 330-339 (in Japanese with English summary).

Uchida, T., Kosugi, K. and Mizuyama, T. (1997) Analysis of the relationship between groundwater level and discharge rate of pipe flow at a valley head, J. Jpn. For. Soc., 79, pp. 202-210 (in Japanese with English summary).

Uchida, T., Kosugi, K. and Mizuyama, T. (1998) Effects of pipeflow on water discharge from mountainous watershed, J. Jpn. For. Soc., 80, pp. 89-97 (in Japanese with English summary).

Uchida, T, Kimoto, A., Ohte, N and Mizuyama, T. (1999) In-situ experiments for the sediment yield process at the devastated mountains, J. Jpn. Soc. Erosion. Control. Engng., 51, pp. 3-11 (in Japanese with English summary).

Chapter 7
Summary and Conclusions
- Hydrochemical dynamics of Groundwater and Streamwater in Forested Headwater Catchments -

7.1 Introduction

Intensive observations were conducted in small headwater catchments to elucidate the hydrochemical dynamics of groundwater and streamwater, and mixing-model approaches were applied to examine the hydrological pathways of the catchments and the sources of the streamwater. Comparative observations were conducted in two catchments (the Matsuzawa catchment and the Akakabe catchment, subcatchments of the Kiryu Experimental Watershed, Shiga prefecture, Japan) during baseflow conditions, and in four catchments (the Rachidani catchment and Toinotani catchment, together with the above two catchments) during stormflow conditions.

7.2 Hydrological Pathways of the Catchments

The discussion of hydrological pathways is based on the intensive groundwater level observations outlined in **Chapter 3** (see Figure 3.10). For the hillslope zone, the groundwater was divided into two flow components (ignoring the evapotranspiration component). Saturated throughflow occurred at the soil-bedrock interface during stormflow and bedrock flow, which infiltrated into the permeable bedrock and flowed downward. From the small hillslope-scale observations in the Akakabe catchment, the saturated throughflow runoff was less than 5% of each rainfall event, and the estimated bedrock infiltration was about 50%. Saturated throughflow and bedrock flow recharged the groundwater body above and below the bedrock, respectively, in the transient saturated zone where it connected with the hillslope zone. Subsequently, the groundwater in the saturated zone, which had very deep soil in the Matsuzawa catchment, was recharged by shallow saturated throughflow and by deep bedrock flow. Part of the bedrock flow in each catchment appeared to discharge directly to the stream without recharging the groundwater body. During rainstorms in the Matsuzawa catchment, subsurface or surface water flowed directly to the stream.

Comparing the annual hydrographs of the Akakabe and the Matsuzawa catchments (Figure 3.9) shows that variations in the discharge rate were smaller in the Matsuzawa catchment. In the Akakabe catchment, the discharge rate varied

considerably. These differences must be caused by differences in the groundwater storage or the volume of groundwater present. In the Matsuzawa catchment, deep soils are present in the depression of the bedrock, and a large volume of groundwater had accumulated there. In contrast, in the Akakabe catchment the area of the soil sedimentation zone is small; thus, the groundwater storage is small. The large volume of groundwater in the Matsuzawa catchment acts as a buffer and maintains a stable discharge rate during the dry seasons or rainstorms. The differences in the hydrological processes, whether groundwater pass through riparian zone or not in this case, must have an impact on the hydrochemical processes in the groundwater and the streamwater.

7.3 Geographic Sources of the Catchments and Their Hydrochemistry

The geographic sources of the catchments and their hydrochemistry were discussed in **Chapter 4**. The spatial and temporal distributions of the groundwater chemistry in the Matsuzawa and Akakabe catchments were observed. Spatial variability was generated by differences in the saturated throughflow and bedrock flow chemistry. The saturated throughflow had low concentrations of SiO_2, whereas SiO_2 concentrations were high in bedrock flow.

Bedrock flow persisted year round, and SiO_2 concentrations were always high in the deeper groundwater. On the other hand, SiO_2 concentrations in the saturated throughflow were seasonal, reaching a maximum in September (the wet season) and a minimum in March (the dry season). During rain, saturated throughflow occurred at the soil-bedrock interface, and vertical distribution patterns were generated by differences in the depth of groundwater. **Chapter 3** showed that there are two pathways that contribute to the perennial groundwater zone from the transient saturated zone, the soil-bedrock interface and the bedrock, and **Chapter 4** showed that the chemical signature of each flow was preserved with little intermixing, and that vertical variation patterns were generated. The different contribution levels of these flows at each point results in spatial variability among the sampling points. The groundwater chemistry in the riparian zone is heterogeneous. The mean residence time of the groundwaters estimated from the stable isotopes were also strongly correlated to the chemical spatial variability. In these processes, the seasonal variation in the saturated throughflow chemistry affected the groundwater, with some reduction in the range of variation, so seasonal variations in the groundwater chemistry were observed. This indicates the hydrochemical processes of groundwater are mainly controlled by the

hydrological processes in catchments, i.e., the geographic-source hydrograph separations with conservative chemical tracers are adequate here.

7.4 Hydrochemical Processes of the Streamwater: Mixing Model Approach

In **Chapter 5**, a two-component mixing model was applied to the baseflow chemistry of the Matsuzawa catchment. The seasonality of baseflow chemistry was generated by changes in the mixing ratio and by the seasonality of the groundwater chemistry in the shallow layer (see Figure 5.5). Following Hill (1990), this study sows that medium- or long-term phenomena, such as the seasonality of the baseflow chemistry, are largely affected by the spatial variability of the groundwater chemistry within the riparian zone. Thus, it is necessary to reevaluate the heterogeneities of groundwater chemistry when applying the mixing-model approach to the study of runoff generation and hydrochemical processes within the riparian zone.

In **Chapter 6**, two- or three-component mixing models were proposed to model the stormflow chemistry of the Matsuzawa, Akakabe, Rachidani, and Toinotani catchments. In the Matsuzawa catchment, groundwater in the transient saturated zone is the third end-member that contributes to stormflow, in addition to throughfall and the groundwater in the perennial saturated zone. The contributing area of the third end-member in the catchment extended upwards during heavy rainfall of long-duration, and became the dominant source. However, if the rainfall was about 100 mm or less, the contributing area of the third end-member was relatively small, less than 1% of the total catchment area at the discharge peak. In the Rachidani catchment, where the dominant source of baseflow is riparian groundwater, the stormflow hydrochemical processes are similar to those in the Matsuzawa catchment, but because the riparian groundwater body is small, the groundwater chemistry can change more readily and stormflow chemistry is affected. The dominant source of baseflow is bedrock flow in the Akakabe catchment, and riparian groundwater in the Toinotani catchment. During rainstorms, the contribution of the groundwater above the bedrock in the Akakabe catchment increases, while in the Toinotani catchment, pipe flow occurs and transports the solutes present in the surface soil. The three factors—the spatial distribution of the sources of solutes, the hydrological pathways, and the time sequential variations in the contribution of the each flow component—were affected by the change of end-members; that is, the variation in the source area (Hewllet and Hibbert, 1967), and consequently the streamwater

chemistry was changed. The EMMA method is adaptable to the hydrochemical analysis of streamwater in a catchment where end-members change incrementally, if combined with information on the hydrological processes.

7.5 General Conclusions

This study made intensive hydrological and hydrochemical observations have undertaken of small headwater catchments, and can respond to the challenges posed in a recent paper by Hooper (2001), in which present difficulties and future problems in catchment hydrochemical studies were outlined (see **Chapter 1**). The linkage of water flow between the hillslope — hillslope/riparian interface — riparian zones is dominated by two flows; saturated throughflow that occurs at the soil-bedrock interface during heavy rain, and bedrock flow, which probably occurs throughout the year, except during the driest season (Figure 7.1). These two flows are distinguishable hydrologically (through their flow rates and velocities) and hydrochemically (by their chemical characteristics and mean residence times). In the hillslope zone, the infiltrated rainwater divides into two components (omitting the evapotranspiration component): saturated throughflow, which occurs on the soil-bedrock interface during stormflow; and bedrock flow, which infiltrates into the permeable bedrock and flows downward. The bedrock flow rate is not negligible, and indeed is larger than the saturated throughflow. Most of the water that certainly contributes to the stream discharge infiltrates in the largest part of the catchment — the hillslope area. These flow components move downward, interact little with each other, and may collect in the groundwater body, where the chemical signature of each flow is conserved. There is little mixing between the components and vertical distribution patterns develop, depending on the bedrock-surface topography. The variation in stream chemistry in the catchments studied reflects the differing proportions of water coming from the relatively small area of the riparian zone. The baseflow chemistry reflects the differing proportions of water coming from the soil-bedrock interface and from the bedrock. During rainstorms, the flow source area varies and a third end-member, which does not contribute during baseflow conditions, occurs around the spring outflow point and flows along the specific pathways of the catchment; the stormflow chemistry reflects the contribution of this component.

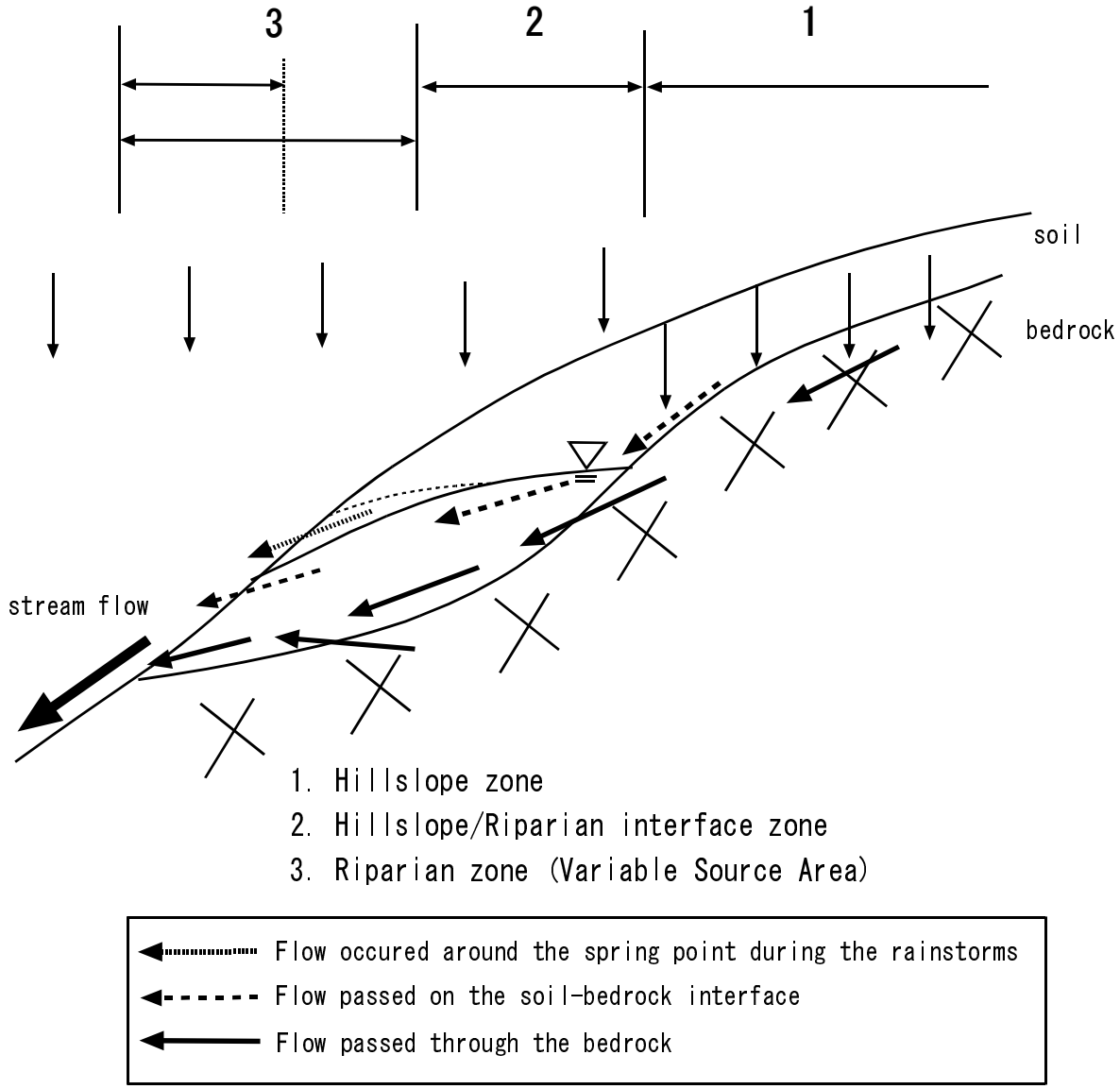

Figure 7.1 Schematic diagram of the linkage of water flow between the hillslope - hillslope/riparian interface - riparian zones and the streamwater

The relative importance of the riparian groundwater or the bedrock groundwater to runoff generation and streamwater chemistry varies for several reasons. Tsujimura et al. (2001) noted the significance of the relief ratio of catchments, and pointed out that the riparian zone is important in mountainous catchments with relatively low relief ratio (relief ratio less than 0.4, PMRW by Hooper et al., 1998; Kawakami by Tanaka and Ono, 1998; Sleepers River by McDonnell et al., 1998a), while bedrock flow is important in mountainous catchments with a relatively high relief ratio (relief ratio more than 0.8 at Koshibu;

Tsujimura et al., 2001). These differences are caused by the topography; in headwater basins with high relief ratio, a well-defined, wide riparian zone is generally not present, because the valley bottoms are very narrow. However, though the Rachidani and the Toinotani catchments in this study have high relief ratios (0.68 and 0.72, respectively), groundwater flow from the riparian zone and preferential flow through soil pipes are dominant in each catchment (see **Chapter 6**). There is a riparian zone in the Rachidani catchment in the soil sediment zone around the artificial dam. Additionally, although the Akakabe catchment in this study has a low relief ratio (0.40), bedrock flow is dominant (see **Chapters 3-6**). The Matsuzawa catchment has a low relief ratio (0.37) and the riparian zone is important to the streamwater chemistry. However, the bedrock groundwater exists in the deep riparian zone in this catchment, and the discharge of this component is controlled by riparian groundwater levels and bedrock topography (see **Chapters 3-6**). McDonnell et al. (1998b) also found that the bedrock topographic surface exerts the greatest control on spatial patterns of subsurface flow and Br tracer movement in the Maimai Watershed, New Zealand.

Recent research has indicated that the chemical signatures of hillslope runoff may not be apparent in stormflows in many catchments on an event time scale, such as at PMRW (Burns et al., 2001) or Sleepers River (McGlynn et al., 1999). McGlynn et al. (2002) pointed out that the volume of the riparian zone in relation to the volume of the hillslope zone might be an important factor in this phenomenon. In this study, hillslope signatures were apparent in the Toinotani catchment when transported through the soil pipe; as the transient saturated groundwater that was derived from the saturated throughflow generated on the soil-bedrock interface in the Matsuzawa catchment; and as saturation overland flow during particularly large rainstorms (see **Chapter 6**). Although the Matsuzawa catchment has a relatively large volume of water in the riparian zone, the runoff components are less intermixed within the riparian zone because of the topography of the bedrock and its permeability, and a runoff component that retains the chemical signature of the hillslope groundwater can contribute to the streamwater during large rainstorms. Therefore, bedrock topography is the most important factor controlling hydrochemical processes in this catchment.

From the results of this study, it was reconfirmed that the hydrochemical processes in the catchments were highly controlled by the specific hydrological processes of each catchment during both the baseflow and stormflow conditions. The chemical dynamics of groundwater and streamwater was clarified and the

baseline for more accurate determination of the hydrological structure in hydrochemical models was determined.

References

Burns, D. A., McDonnell, J. J., Hooper, R. P., Peters, N. E., Freer, J. E., Kendall, C. and Beven, K. (2001) Quantifying contributions to storm runoff through end-member mixing analysis and hydrologic measurements at the Panola Mountain Research Watershed (Georgia, USA), Hydrol. Process., 15, pp. 1903-1924.

Hewlett, J. D. and Hibbert, A. R. (1967) Factors affecting the response of small watersheds to precipitation in humid areas, *In* International Symposium on Forest Hydrology, Sopper, W. E. and Lull, H. W. (Eds.), Pergamon Press, Oxford, pp. 275-290.

Hill, A. R. (1990) Groundwater cation concentrations in the riparian zone of a forested headwater stream, Hydrol. Process., 4, pp. 121-130.

Hooper, R. P., Aulenbach, B. T., Burns, D. A., McDonnell, J., Freer, J., Kendall, C. and Beven, K. (1998) Riparian control of stream-water chemistry: implications for hydrochemical basin models, Hydrology, Water resources and Ecology in Headwaters (Proceeding of the HeadWater '98 Conference held at Merano, Italy, April 1998), Kovar, K. Tappeiner, U. Peters, N. E., Craig, R. G. (Eds.), IAHS Publ. 248, Wallingford, pp. 451-458.

Hooper, R. P. (2001) Applying the scientific methods to small catchment studies: A review of the Panola Mountain Experience, Hydrol. Process. 15. pp. 2039-2050.

McDonnell, J. J., McGlynn, B. L., Kendall, K. Shanley, J. and Kendall, C. (1998a) The role of near-stream riparian zones in the hydrology of steep upland catchments, Hydrology, Water resources and Ecology in Headwaters (Proceeding of the HeadWater '98 Conference, Merano, Italy, April 1998), Kovar, K. Tappeiner, U. Peters, N. E., Craig, R. G. (Eds.), IAHS Publ. 248, Wallingford, pp. 173-180.

McDonnell, J. J., Brammer, D., Kendall, C., Hjerdt, N., Rowe, L., Stewart, M. and Woods, R. (1998) Flow pathways on steep forested hillslopes: the tracer, tensiometer and trough approach, Environmental Forest Science (Proceedings of the IUFRO Division 8 Conference, Kyoto, Japan, October 1998), Sassa, K. (Ed.), Kluwer, Dordrecht, pp. 463-474.

McGlynn, B. L., McDonnell, J. J., Shanley, J. B. and Kendall, C. (1999) Riparian

zone flowpath dynamics during snowmelt in a small headwater catchment, J. Hydrol., 222, pp. 75-92.

McGlynn, B. L., McDonnell, J. J. and Brammer, D. D. (2002) A review of the evolving perceptual model of hillslope flowpaths at the Maimai catchments. New Zealand, J. Hydrol., 257, pp. 1-26.

Tanaka, T., Ono, T. (1998) Contribution of soil water and its flow path to stormflow generation in a forested headwater catchment in central Japan, *In* Hydrology, Water resources and Ecology in Headwaters (Proceeding of the HeadWater '98 Conference held at Merano, Italy, April 1998), Kovar, K. Tappeiner, U. Peters, N. E., Craig, R. G. (Eds.), IAHS Publ. 248, Wallingford, pp. 181-188.

Tsujimura, M., Onda, Y. and Ito, J. (2001) Stream water chemistry in a steep headwater basin with high relief, Hydrol. Process., 15, pp. 1847-1851.

Acknowledgement

謝辞

1996 年 4 月,研究室配属以来,数多くの方々に支えられ,この学位論文の完成を見ることができました.まず第一に興味深い研究テーマを設定し,野外における観測手法や解析の方針はもとより,研究に取り組む基本姿勢など,様々な局面でご指導いただくとともに,常に未熟な私を信頼し叱咤激励してくださった京都大学農学研究科 大手信人助教授に感謝いたします.また,日常の研究生活から論文作成に至る過程において,京都大学農学研究科 谷誠教授,小杉緑子助手,小杉賢一朗助手ならびに京都大学 小橋澄治名誉教授からは常に暖かいご指導･ご配慮をいただきました.京都大学農学研究科 水山高久教授,藤田正治助教授にはゼミ等の機会を通じて適切なご助言と激励とをいただきました. 京都大学農学研究科 三野徹教授ならびに小崎隆教授からは本学位論文の審査において,示唆に富むご意見をいただきました.また,福田路子さんには事務的な面でのご援助のみならず,常に細やかなご配慮をいただき,円滑で,充実した研究生活を送ることができました.

現地観測から化学分析,論文作成に至るまで,貴重な時間を割いて何もわからなかった私をここまで導いてくださった京都大学農学研究科 浅野友子さん,浜田美鈴さん(現アジア航測),京都大学農学研究科 徳地直子助教授,中西麻美助手,内田太郎さんらに深く感謝いたします.また,考察を深めるにあたり,京都大学情報学研究科 木庭啓介助手,総合地球環境学研究所 吉岡崇仁助教授,名古屋大学環境学研究科 木平英一さんら,多くの方々から多数の示唆に富むご意見をいただいたことに深謝いたします.西田顕郎さん(現筑波大学講師),田中克典さん(現 地球フロンティア研究システム),田中広樹さんら研究室の先輩方には常に先を行くお手本として,研究者としてのあり方を学ばせていただきました.特に戸田求さん(現 文部科学省特別研究員)とは同室だったこともあり,日々いろいろと語り合えたことが研究を続けていく上での大きな糧となっています.

本研究の観測の中心となっている桐生水文試験地の開設以来,維持管理に当たってこられた先人たちに敬意と謝意を表します.また,赤壁徹也君(現 中央出版),ヘンドラヤントさん(現 Institut Pertanian Bogor),保原達君,壁谷直記君(現 森林総合研究所),尾保手朋子さん,金秀珍さん,岡崎亮太君(現 国際航業),村上靖典君(現 王子木材工業),立花克朗君(現 日本 IBM),川崎雅俊君,矢野雅人君,高梨聡君,安藤宏幸君,片山辰弥君,伊藤雅之君

ら観測をともにした仲間たち,木本秋津さん,松尾奈緒子さんら研究室生活をともにした京都大学農学研究科森林水文学・山地保全学研究室の仲間たちを始め,多くの先輩・同輩・後輩の皆さんが示して下さった惜しみない協力,温かい励まし,そして忘れがたい友情に対して報いることは決して容易ではありません.壁谷直記君には 4.4 節に示した貴重な未公開データを利用することを快く承諾していただいたことも記しておかなければなりません.

この長いようで短かった 6 年間を経て,ようやく研究者としてのスタートラインに立つことができたように思います.ここから一歩一歩着実な歩みを重ねていくことが,これまで私を支えてくださった多くの方々と,これから先の人生で私と出会い,私を支えてくださることになるであろう多くの方々へのお返しになると信じ,前進していこうと思います.本当にありがとうございました.

2002 年 3 月

京都大学農学研究科 森林水文学研究室

勝山 正則